

ISNS
2019

International Symposium for

nano science

2019
NOV.
27·28
Wed Thu

Σ Hall,
Toyonaka campus,
Osaka University

Contents

Welcome Message	3
Organizing Committee	4
Acknowledgements	5
Practical Information	6
Agenda	9
Day 1 (27 th /Nov./2019)	10
Day 2 (28 th /Nov./2019)	12
Poster List	14
Invited Talks - CVs and Abstracts -	19
Contributed Talks	33
Poster Session	41
Venue	89
Sponsors	91

Welcome Message

On behalf of the organizing committee, we are pleased to announce the start of the International Symposium for Nano Science (ISNS) 2019, held at the Sigma Hall, Osaka University. This symposium centers around the theme of “Nano Science”, and mainly consists of lectures leading scientists who have made novel and creative by breakthroughs in nano science. This Symposium has been completely organized by graduate students under the support of the Interactive Materials Science Cadet (IMSC) Program, one of Osaka University’s Programs for Leading Graduate Schools. The IMSC Program is designed to apply the synergistic benefits of dialogic and interactive approaches to various facets of materials science education and research. In the context of the program, this symposium aims to promote communication and collaboration among researchers and students diverse in the fields of nano materials science and to advance their research activities. We truly hope that all participants can enjoy and benefit from this this symposium to the fullest.

Yours sincerely,

Student Chair of ISNS, Jinya Nomura

Chair of ISNS, Masaaki Ashida



Jinya Nomura



Masaaki Ashida

Organizing Committee

Chair

Masaaki Ashida (GS of Engineering Science)

Student Chair

Jinya Nomura (GS of Science)

Members of the Organizing Committee

Tatsuya Yamamoto (GS of Engineering)

Shingo Genchi (GS of Engineering Science)

Tomohiro Yamazaki (GS of Engineering Science)

Hiroki Oka (GS of Science)

Eisuke Watanabe (GS of Science)

Manato Fujimoto (GS of Science)

Advisory Committee

Kenji Iijima (Institute for Transdisciplinary Graduate Degree Programs)

Harushige Nakao (Institute for Transdisciplinary Graduate Degree Programs)

Kazushi Mashima (GS of Engineering Science)

Acknowledgements

The organizers would like to express our sincere gratitude to the following organizations for supporting this symposium.

Sponsors

Hitachi, Ltd.

KANEKA CORPORATION

NIPPON SHOKUBAI CO., LTD.

Noto Printing CO., Ltd.

Panasonic Corporation

Sumitomo Chemical Company, Limited

TDK Corporation

Micron Memory Japan, G.K.

Support

Institute for NanoScience Design, Osaka University

Endorsement

The Spectroscopical Society of Japan

The Optical Society of Japan

The Laser Society of Japan

The Society of Nano Science and Technology

The Japan Society of Applied Physics

Japan Society of Coordination Chemistry

The Society of Chemical Engineers, Japan

Practical Information

Registration desk

Opening hours

Wed., 27th, Nov., 9:00 -

Thu., 28th, Nov., 9:30 -

Banquet

Day, Date, Time: Wed., 27th, Nov., 17:30 - 19:00

Venue: Osaka Univ. Σ Hall (international Hall)

Contact

1-3 Machikaneyama-cho, Toyonaka, Osaka 560-8531, Japan

Tel&Fax: +81-6-6850-6403

Email: isns.cadet@gmail.com

mirai-jimu-dai3@office.osaka-u.ac.jp

Wi-Fi

Free Wi-Fi service is available for all participants in the Σ hall. Your ID and password for access to the Internet will be provided at the registration table.

Instructions for Oral Speakers

Please remember that the time assignments for presentations are as follows:

Invited Talk: 70 min (60 min talk + 10 min discussion)

Contributed Talk*: 15 min (12 min talk + 3 min discussion)

The bell will ring to let speakers know the remaining time.

1st bell: 5 min (*3 min) left until the end of the talk.

2nd bell: the end of the talk

3rd bell: the end of the discussion

Please ensure your presentation doesn't exceed the presentation time, otherwise you will be stopped by the session chair in order to keep conference schedule. We will prepare PCs including both Microsoft PowerPoint and Mac Keynote for your presentation. We will prepare VGA connector, you can also bring your own PCs and adapters (such as VGA- to-HDMI or VGA-to-Thunderbolt).

Instructions for Poster Presenters

Poster size: ISO A0 (W: 841 mm, H: 1,189 mm)

Location: Seminar Room 1 (1F)

Presentation time: 60 min.

Odd number: 11:15-12:15, Day1

Even number: 11:15-12:15, Day2

We don't provide printing service, please bring your printed poster to the meeting. Note that posters not retrieved by the end of the symposium will be discarded.

Awards for presentations

Contributed talk speakers were chosen based on their submitted abstracts. The organizing committee will award the all contributed talk speakers in recognition of their outstanding works.

The organizing committee will award the best poster presentations based on the voting from the audiences. Please vote your ballot by using a ballot box during the poster session. A voting paper will be distributed at the reception on the day. The detail will be announced in the symposium.

Agenda

Day 1 (27th/Nov./2019)

9:00-9:30 Registration

9:30-9:45 Opening Remarks

9:45-10:55 Invited Talk 1
Yusoo Kim (RIKEN)
Single-molecule Chemistry and Spectroscopy with a Scanning Tunneling
Microscope

10:55-11:10 Contributed Talk 1
Koki Sasaki
Novel synthesis method of nanosheets by using two-dimensional reactors
in amphiphilic phases

11:10-11:15 Short Break

11:15-12:15 Poster Session
(Odd Numbers)

12:15-13:45 Lunch Break

13:45-14:55 Invited Talk 2
Makoto Fujita (The University of Tokyo)
Self-assembly of Archimedean/Non-Archimedean Solids under
Mathematical Restriction

14:55-15:10 Contributed Talk 2
Yasutaka Kitagawa
Theoretical study on single molecule conductivity of extended metal
atom chains (EMACs) – Toward realization of single-molecule transistor
–

15:10-15:30 Coffee Break

-
- 15:30-16:40 Invited Talk 3
 Yoshiya Inokuchi (Hiroshima University)
 Supramolecular Chemistry Studied by Cold Gas-Phase Spectroscopy
- 16:40-16:55 Contributed Talk 3
 Satoshi Yamashita
 A study of distance dependence on vibrational energy flow in proteins
 taking advantage of the periodic character of α helices
-
- 16:55-17:30 Group Photo & Free Time
-
- 17:30- Banquet
-

Day 2 (28th/Nov./2019)

9:30-9:45 Registration

9:45-10:55 Invited Talk 4
Tongcang Li (Purdue University)
Laser-driven GHz Nanorotor and Ultrasensitive Torque Detection

10:55-11:10 Contributed Talk 4
Ryutaro Ohira
Phonon-number-resolving Detection of Multiple Local Phonon Modes in
a Trapped-ion Chain

11:10-11:15 Short Break

11:15-12:15 Poster Session
(Even Numbers)

12:15-13:45 Lunch Break

13:45-14:55 Invited Talk 5
Ken-ichi Uchida (National Institute for Materials Science)
Thermal Energy Engineering Based on Spin Caloritronics

14:55-15:10 Contributed Talk 5
Halimah Harfah
Understanding the Optimum Spin-Current Control by Induced Electric-
Polarization Reversal in hBN-based Magnetic Tunnel Junction

15:10-15:30 Coffee Break

-
- 15:30-16:40 Invited Talk 6
 Nobuyuki Matsuda (Tohoku University)
 Integrated photonics for quantum information science and technology
- 16:40-16:55 Contributed Talk 6
 Tomohiro Yamazaki
 Frequency Multiplexing of Polarization-Entangled Photon Pairs without
 External Filtering
-
- 16:55-17:10 Closing

Poster List

P1 Keita Miyagawa

Quantitative monitoring of internal electric field in solar cell with terahertz wave radiation

P2 Taikahiro Asada

Strategic Complexation between $\text{Al}(\text{C}_6\text{F}_5)_3$ and Phosphinoyl Substituent in N-Heterocyclic Carbenes

P3 Iat Wai Leong

Asymmetric ionic-voltage relation in low-aspect-ratio nanopore under salt gradients

P4 Manato Fujimoto

Topological pump induced by dynamics of moiré pattern

P5 Masahiro Ikeshita

Synthesis and Controlling Chiroptical Responses of Planar and Axially Chiral Vaulted Platinum(II) Complexes

P6 Ryo Izumi

Theoretical analysis on tip-ferromagnetic resonance force microscopy

P7 Hiroki Oka

Electric properties of hBN-graphene-hBN trilayer system

P8 Yuki Yagi

Toward site selective modification of pyrimidine base flipped out by naphthyridine carbamate dimer binding

P9 Daichi Kato

Many-variable variational Monte-Carlo studies of superconductivity in the bilayer Hubbard model

P10 Shohei Kishimoto

Single Particle Dynamics in Tandem Micropores

P11 Katsuki Nihongi

Optimization of circuit-coupling conditions for the magnetic-susceptibility measurement apparatus in pulsed high magnetic fields using a proximity detector oscillator

P12 Kazuki Kageyama

Construction of Polyacrylamide Gel Containing Engineered Hexameric Hemoprotein as a Cross-linker and Evaluation of its Mechanical Property

P13 Daijiro Okaue

The Reversible Interfacial Dynamics of Ionic Liquid Causing Operational Instability of Electric Double Layer Organic FET

P14 Tomomi Kawakami

Long-Range Ultrafast Electron Transfer Reaction of a Pyrene-Biphenyl System Driven by Multiphoton Absorption

P15 Tatsuya Yamamoto

The size and frequency dependence of permittivity of ZnO nanoparticles studied by electrostatic force microscopy

P16 Yuya Sawada

Magnetization and ESR of the Chiral Helimagnet CrNb_3S_6

P17 Mori Watanabe

Hall measurements in atomically thin CeTe_3 films

P18 Masaaki Geshi

Development of First-Principles Crystal Structure Search Method with High Precision and High Efficiency and Its Implementation

P19 Shintaro Kato

Selective hydrocarbon oxidation reactions by the gas diffusion electrode carrying Ru-modified covalent triazine frameworks

- P20 Tomoya Hosokawa
Metal-doped bipyridine linked covalent organic framework films for photoelectrochemical applications
- P21 Tomoharu Ohta
Spin transport measurements in atomic-layer materials with strong spin-orbit interaction
- P22 Kentaro Noi
Mechanism of affinity enhanced protein adsorption on bio-nanocapsules studied by viscoelasticity measurement with wireless QCM biosensor
- P23 Yuki Sakai
Machine Learning Approach to Analytic Continuation of Temperature Green's Function into Spectral Function
- P24 Eisuke Watanabe
Quantum Chemical Study on Nitrate complexes of Zr and Th for ^{104}Rf chemistry
- P25 Misato Funaoka
Study on Microscopic Phase-Separation in Multi-Component Polymer Solid by Single-Molecule Tracking Utilizing One-Color Fluorescence Switching
- P26 Mizuki Hayasaka
Detection of Micromechanical Motion Due to Excited-State Absorption Force
- P27 Jinya Nomura
Stepwise Creation of Supramolecular Structures of a Ball-like Au-Pd Nanomolecule with H_2SiF_6
- P28 Haruka Shinmen
Photophysical Properties of Fluorescent Diarylethene Derivatives Modulated by Molecular Aggregation
- P29 Hiro Tabata
Electrochemical oxidation of glycerol by Ru-modified covalent triazine frameworks

- P30 Colin K. Kitakawa
Development of New Semi-Empirical Method for Simulations of Reactive Oxygens Species and Antioxidants
- P31 Hitoshi Mori
Electronic Transport Properties of ZrS₂ with the Temperature Dependent Relaxation Time
- P32 Masaru Hitomi
Bulk Edge Correspondence of Monolayer Black Phosphorene
- P33 Kazuto Shimizu
Synthesis and Properties of Novel Anthracene Congested Systems: Radial Pi-Cluster Molecules
- P34 Shingo Genchi
Scaling effects in the resistance temperature characteristic of VO₂ on hBN
- P35 Kazuki Ikenaga
Theoretical Study on Intermolecular Magnetic Interaction between Double-Decker Phthalocyaninato Lanthanide(III) Complex
- P36 Yuto Takeuchi
Self-Sensing Cantilever Using Graphene Strain Sensor
- P37 Sho Tamaki
Light assisted synchronization of mechanical vibration in arrayed optomechanical system
- P38 Naoka Amamizu
Theoretical Study on Chain Length Dependence of Electron Conductivity of Polyenes
- P39 Hiromasa Sato
Theoretical Study on Substitution Effects on Frontier Orbital Energies of Ru(bpy)₃ by Multivariate Analysis
- P40 Kazuki Gen
Ultrafast electron diffraction using relativistic femtosecond electron pulses

P41 Yuki Hirota

Local Analysis of Interfacial Structure at Mg^{2+} -containing Ionic Liquid / Au(111) using Frequency Modulation Atomic Force Microscopy

P42 Yoshinobu Fujihira

Behavior of Solute Metal Ions at Ionic Liquid/Electrode Interface Studied by Electrochemical Impedance Spectroscopy

P43 Hiroki Ueda

Potential dependent compositional change of Mg^{2+} -containing ionic liquid solutions at the interface on Au(111) electrode for different Mg^{2+} concentrations analyzed by XPS

P44 Takahiro Koyake

Local Operational Mechanism of Electric Double Layer OFET at the Ionic liquid/Organic Semiconductor Interface revealed by Electrochemical Frequency Modulation AFM Analyses

P45 Kyoichiro Urano

Numerical estimation of the viscosity distribution in a gas-liquid interface

P46 Masaaki Geshi

Human Resource Development Program in Computational Science, Advanced Computational Science A & B

P47 Masaaki Geshi

Computational Materials Design (CMD[®]) workshop

P48 Zimeng Li

Temperature, Concentration and Solvent Dependence in Chromic Behaviors of Diflavinylenes Induced by Aggregation Based Control of π -Conjugated Platform

Invited Talks
- CVs and Abstracts -

Yousoo Kim

Surface and Interface Science Laboratory, RIKEN,
2-1 Hirosawa, Wako, Saitama 351-0198, Japan
E-mail: ykim@riken.jp
Tel +81-48-467-4073 Fax +81-48-467-1945



Research Interests:

single-molecule chemistry, metal or metal oxide thin film surfaces, self-assembled organic thin films, photon detection from a single molecule, energy conversion between electrons and photons of nano-scale materials

Employment:

1999-2002: Special Postdoctoral Researcher, RIKEN
2002-2006: Research Scientist, RIKEN
2006-2009: Senior Research Scientist, RIKEN
2010-2015: Associate Chief Scientist, RIKEN
2015-Present: Chief Scientist, RIKEN
2008-Present: Adjunct Professor, Dept. Electronic Chem., Tokyo Institute of Tech., Japan
2011-Present: Adjunct Professor, Div. of Materials Science, Saitama University, Japan
2017-Present: Adjunct Professor, Dept. Applied Chemistry, Kyusyu University, Japan
2018-Present: Adjunct Professor, College of Science, Univ. of the Philippines Diliman
2018-Present: Adjunct Professor, Dept. Chemistry, GIST, Korea
2019-Present: Adjunct Professor, Dept. Chemistry, Seoul National University, Korea

Education:

BSc Seoul National University (1991)
MSc Seoul National University (1993)
PhD University of Tokyo (1999)

Major Awards:

Sep. 2003: Publication Award (The Surface Science Society of Japan), Mar. 2008: Young Scientist Award (The Physical Society of Japan), Nov. 2009: Sir Martin Wood Prize (Millennium Science Forum), Sep. 2016: International Academic Prize (Japan Society of Molecular Science), Apr. 2018: Commendation for Science and Technology by the MEXT (MEXT), Jul. 2018: Nanoprobe Prize (Japan Science and Technology Agency), Mar. 2019: Academic Award, Chemical Society of Japan

Selected Significant Publications:

Selective triplet exciton formation in a single molecule, Kensuke Kimura, Kuniyuki Miwa, Hiroshi Imada*, Miyabi Imai-Imada, Shota Kawahara, Jun Takeya, Maki Kawai, Michael Galperin*, Yousoo Kim*, **Nature** 570 (2019) 210-213.

Real-space and real-time observation of a plasmon-induced chemical reaction of a single molecule, Emiko Kazuma, Jaehoon Jung, Hiromu Ueba, Michael Trenary, Yousoo Kim*, **Science** 360 (2018) 521-526.

Real-space investigation of energy transfer in heterogeneous molecular dimers, Hiroshi Imada, Kuniyuki Miwa, Miyabi Imai-Imada, Shota Kawahara, Kensuke Kimura and Yousoo Kim*, **Nature** 538 (2016) 364-367.

Single-molecule Chemistry and Spectroscopy with a Scanning Tunneling Microscope

Yonsoo Kim

*Surface and Interface Science Laboratory, RIKEN, Wako, Saitama 351-0198, Japan
ykim@riken.jp*

The study of single molecules provides deep insights into bonding nature and underlying quantum mechanics concerning about controlling chemical reaction. The scanning tunneling microscope (STM) is the most powerful tool for investigating and controlling chemistry of individual molecules on the solid surfaces. The coupling of tunneling electrons to the electronic and vibrational states of the target molecule allows us to realize mode-selective and state-selective chemistry of the individual molecules. Quantitative analysis of the controlled reactions enables us to understand how the electron energy can transport leading to various surface processes¹.

We have especially focused our recent STM studies on the excitation of a single molecule and the accompanied energetic processes, such as energy transfer, conversion and dissipation. Detailed understanding of the molecular excited states is crucial to develop organic energy conversion devices based on opto-electronic/opto-chemical processes. We developed an STM combined with optical systems both for photon detection and for optical illumination to achieve controlled excitation of the molecular quantum states either by tunneling electrons or by localized surface plasmon at the STM junction.

In this talk, I will share some issues concerning single-molecule chemistry and spectroscopy investigated by a photon STM. An explanation will be first given about construction of the photon STM by combining with optical systems, which will be followed by the detailed description of development of single-molecule luminescence and absorption spectroscopic techniques with the photon STM². The single-molecule luminescence spectroscopy was further utilized to detect both fluorescence and phosphorescence signals according to the recombination of singlet and triplet exciton states in a molecule, respectively³. I will also discuss how the molecular excitons are generated in a controlled manner at the STM junction and how we visualized the exciton formation/recombination processes playing in the energy transfer between a two different molecules on the solid surfaces⁴. Finally, if the time will be available, I will give a short introduction of quantum state control by localized surface plasmon (LSP)⁵. The LSP generated at the STM tip either by optical illumination or by applying bias voltage has recently been attracting great attention mainly as a novel light source to overcome diffraction limit of optical wavelength. In recent years, we have applied the LSP towards exploring novel chemical (catalytic) reaction and spectroscopy based on the interaction between the LSP and electronic/vibrational quantum states of a single molecule at the STM junction.

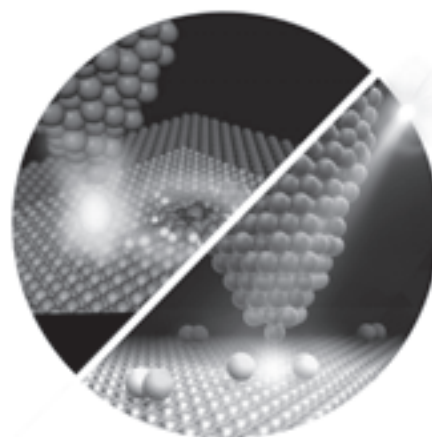


Figure 1. Conceptual images of single-molecule reaction and spectroscopy with a photon STM.

- (1) Y. Kim, K. Motobayashi, T. Frederiksen, H. Ueba and M. Kawai, *Prog. Surf. Sci.* **90** (2015) 85.
- (2) H. Imada, K. Miwa, M. Imai-Imada, S. Kawahara, K. Kimura and Y. Kim, *Phys. Rev. Lett.* **119** (2017) 013901.
- (3) K. Kimura, K. Miwa, H. Imada, M. Imai-Imada, S. Kawahara, J. Takeya, M. Kawai, M. Galperin and Y. Kim, *Nature* **570** (2019) 210.
- (4) H. Imada, K. Miwa, M. Imai-Imada, S. Kawahara, K. Kimura and Y. Kim, *Nature* **538** (2016) 364.
- (5) E. Kazuma, J. Jung, H. Ueba, M. Trenary, Y. Kim, *Science* **360** (2018) 521.

Makoto Fujita

Department of Applied Chemistry, The University of Tokyo
Bunkyo-ku, Tokyo 113-8656, Japan
E-mail: mfujita@appchem.t.u-tokyo.ac.jp
Tel +81-3-5841-7259 Fax +81-3-5841-7257



Research Interests:

Coordination Self-Assembly: Construction of nano-scale discrete frameworks, including MnL_2n Archimedian/non-Archimedian solids ($n = 6-48$), by self-assembly. Molecular Confinement Effects: Developing/creating new properties and new reactions in the confined cavities of self-assembled coordination cages. Crystalline Sponge Method: Single-crystal-to-single-crystal guest exchange in the pores of self-assembled coordination networks is applied to a new X-ray technique that does not require crystallization of target compounds.

Employment:

1982-1988. Researcher, Sagami Chemical Research Center.
1988 -1997 Assist. Prof. to Assoc. Prof., Chiba University.
1997- 1999 Assoc. Prof., Inst. for Molecular Science (IMS)
1999 – 2002 Professor, Nagoya University.
2002- current Professor, The University of Tokyo
2018- current Distinguished Professor, Institute for Molecular Science
2019- current University Distinguished Professor, The University of Tokyo

Education:

BSc Chiba University (1980)
MSc Chiba University (1982)
PhD Tokyo Institute of Technology (1987)

Major Awards:

Imperial Prize and the Japan Academy Prize, 2019; Wolf Prize in Chemistry, 2018; Naito Foundation Merit Award, 2017; Medal with Purple Ribbon, 2014; Fred Basolo Medal (ACS), 2014; Arthur C. Cope Scholar Award (ACS), 2013; The Chemical Society of Japan (CSJ) Award, 2013; Thomson Reuters Research Front Award, 2012; Reona Ezaki Award, 2010; Japan Society of Coordination Chemistry Award, 2010; The Commendation for Science and Technology by MEXT, 2009; International Izatt-Christensen Award in Macrocyclic Chemistry, 2004; Silver Medal of Nagoya Medal Seminar, 2003; Japan IBM Award, 2001; Gold Medal of Tokyo Techno Forum 21, 2001; The Divisional Award of the Chemical Society of Japan, 2000.

Selected Significant Publications:

“Self-Assembly of Tetravalent Goldberg Polyhedra from 144 Small Components”, D. Fujita, Y. Ueda, S. Sato, N. Mizuno, T. Kumasaka, M. Fujita, *Nature* **2016**, 540, 563.
“Self-Assembly of $M_{30}L_{60}$ Icosidodecahedron”, D. Fujita, Y. Ueda, S. Sato, H. Yokoyama, N. Mizuno, T. Kumasaka, M. Fujita, *Chem* **2016**, 1, 91.
”X-ray analysis on the nanogram to microgram scale using porous complexes”
Y. Inokuma, S. Yoshioka, J. Ariyoshi, T. Arai, Y. Hitora, K. Takada, S. Matsunaga, K. Rissanen, M. Fujita, *Nature* **2013**, 495, 461.

Self-assembly of Archimedean/Non-Archimedean Solids under Mathematical Restriction

Makoto Fujita^{1,2}

¹*Department of Applied Chemistry, The University of Tokyo and*

²*Division of Advanced Molecular Science Institute for Molecular Science (IMS)*

E-mail: mfujita@appchem.t.u-tokyo.ac.jp

We and others have been intensively studying the self-assembly of coordination polyhedra whose framework topologies are described by Platonic or Archimedean solids.^[1] The largest structure we have synthesized is $M_{30}L_{60}$ icosidodecahedron, one of the Archimedean solids.^[2] Here, we unexpectedly obtained another $M_{30}L_{60}$ polyhedron that is NOT depicted in any elementary geometry textbook. Triggered by this observation, we mathematically rationalized the unexpected polyhedron based on a theory seldom discussed: the tetravalent Goldberg polyhedra. The common Goldberg polyhedra are made up of hexagons and pentagons with three edges meeting at every node of the polyhedron; well-known real-life examples include footballs and fullerenes. We simply extend this “trivalent” form to generate a new family of “tetravalent” Goldberg polyhedra, made up of squares and triangles.^[3] These extended tetravalent Goldberg polyhedra are not described in the literature, presumably because nothing like them has ever been discovered in the real world. However, the square planar geometry of palladium(II) ions has the potential to direct the self-assembly of these unnatural polyhedra, allowing us to synthesize them in the laboratory. We further demonstrate the self-assembly of $M_{48}L_{96}$ (Figure 1), an extended Goldberg polyhedron, which was predicted by the theory.

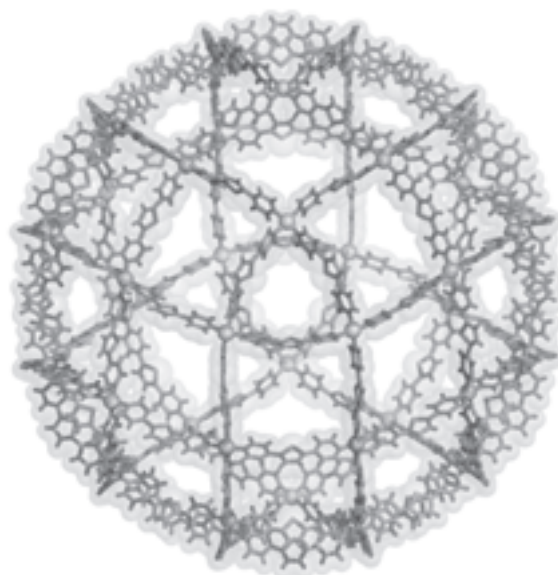


Fig. 1. X-ray structure of $M_{48}L_{96}$ complex

References:

- [1] M. Tominaga, K. Suzuki, M. Kawano, T. Kusukawa, T. Ozeki, S. Sakamoto, K. Yamaguchi, M. Fujita, *Angew. Chem. Int. Ed.* **2004**, *43*, 5621-5625.
- [2] D. Fujita, Y. Ueda, S. Sato, H. Yokoyama, N. Mizuno, T. Kumasaka, M. Fujita, *Chem* **2016**, *1*, 91.
- [3] D. Fujita, Y. Ueda, S. Sato, N. Mizuno, T. Kumasaka, M. Fujita, *Nature* **2016**, 540, 563.

Yoshiya Inokuchi

Professor

Hiroshima University

Kagamiyama 1-3-1, Higashi-Hiroshima, Hiroshima 739-8526, Japan

y-inokuchi@hiroshima-u.ac.jp

Tel +81-82-424-7407



Research Interests:

molecular spectroscopy, ion complexes, supramolecular systems

Employment:

- 1996 –1998 Research Fellow (DC2), Japan Society for the Promotion of Science, Institute for Molecular Science, Okazaki, Japan
- 1998 –2004 Assistant Professor, Institute for Molecular Science, Okazaki, Japan
- 2004 –2006 Assistant Professor, Graduate School of Arts of Sciences, The University of Tokyo, Tokyo, Japan
- 2006 –2019 Associate Professor, Graduate School of Science, Hiroshima University, Higashi-Hiroshima, Japan
- 2010 –2014 Visiting Scientist, Laboratoire de Chimie Physique Moléculaire, École Polytechnique Fédérale de Lausanne, Lausanne, Switzerland
- 2019 – present Professor, Graduate School of Science, Hiroshima University, Higashi-Hiroshima, Japan

Education:

- March, 1998 Ph. D. in Science (Department of Chemistry, Kyushu University)
- March, 1995 M. S. in Science (Department of Chemistry, Kyushu University)
- March, 1993 B. S. in Science (Department of Chemistry, Tohoku University)

Major Awards:

- 1996 Research Fellow (DC2), Japan Society for the Promotion of Science
- 2010 Research Fellow, JSPS Excellent Young Researcher Overseas Visit Program, Japan Society for the Promotion of Science
- 2012 Research Fellow, JSPS Strategic Young Researcher Overseas Visits Program for Accelerating Brain Circulation, Japan Society for the Promotion of Science

Publications:

- 1) Y. Inokuchi*, T. Ebata, and T. R. Rizzo, *J. Phys. Chem. A*, in press (DOI: 10.1021/acs.jpca.9b05706) (2019).
- 2) K. Wada, M. Kida, S. Muramatsu, T. Ebata, and Y. Inokuchi*, *Phys. Chem. Chem. Phys.*, in press (DOI: 10.1039/C9CP03194D).
- 3) M. Kida, D. Shimoyama, T. Ikeda, R. Sekiya, T. Haino, T. Ebata, C. Jouvét, and Y. Inokuchi*, *Phys. Chem. Chem. Phys.*, **20**, 18678 (2018).
- 4) Y. Inokuchi*, T. Ebata, and T. R. Rizzo, *J. Phys. Chem. A*, **122**, 3754 (2018).
- 5) M. Kida, M. Kubo, T. Ujihira, T. Ebata, M. Abe, and Y. Inokuchi*, *ChemPhysChem*, **19**, 1331 (2018).
- 6) Y. Inokuchi*, K. Hirai, and T. Ebata, *Phys. Chem. Chem. Phys.*, **19**, 12857 (2017).
- 7) Y. Inokuchi*, M. Kida, and T. Ebata, *J. Phys. Chem. A*, **121**, 954 (2017).
- 8) Y. Inokuchi*, M. Kaneko, T. Honda, S. Nakashima, T. Ebata, and T. R. Rizzo, *Inorg. Chem.*, **56**, 277 (2017).
- 9) Y. Inokuchi*, M. Nakatsuma, M. Kida, and T. Ebata, *J. Phys. Chem. A*, **120**, 6394 (2016).

Supramolecular Chemistry Studied by Cold Gas-Phase Spectroscopy

Yoshiya Inokuchi

*Department of Chemistry, Graduate School of Science, Hiroshima University, Higashi-Hiroshima, Hiroshima 739-8526, Japan
y-inokuchi@hiroshima-u.ac.jp*

[Introduction]

Crown ethers (CEs) are ones of the most famous host molecules and have been extensively used as phase transfer catalysis and building blocks in organic and supramolecular chemistry.¹ We study CE complexes with ion guests by cold gas-phase spectroscopy; one of our goals is to understand the origin of functions characteristic of CEs from microscopic viewpoints.² In this talk, we will firstly describe basic ideas and technical aspects of cold gas-gas phase spectroscopy, and then present some results of our spectroscopy for CE complexes.

[Experimental Methods]

Cold gas-phase spectroscopy of supramolecular systems is performed by using a home-made mass spectrometer equipped with a cryogenically cooled ion trap.³ Ion complexes are produced continuously at atmospheric pressure *via* electrospray of solutions containing host molecules and ion guests. Ion complexes of interest are introduced into a quadruple ion trap (QIT) cooled by a He cryostat (~4 K). Trapped ions in the QIT are cooled down to ~10 K. Cold ions in the QIT are irradiated by a UV laser and resulting fragment ions are mass-analyzed by a time-of-flight mass spectrometer. Ultraviolet photodissociation (UVPD) spectra of ion complexes can be obtained by plotting the yield of photofragment ions as a function of UV wavenumber. In addition, conformer-specific UV and IR spectra can be obtained *via* double-resonance schemes with another UV or IR laser. By analyzing UV and IR spectra observed under cold gas-phase conditions, one can determine the conformation and the number of conformers in the experiment, which will reveal the relation between the structure and the function for supramolecular systems.

[Results and Discussion]

Figure 1 displays UV photodissociation (UVPD) spectra of K^+ (dibenzo-18-crown-6) complex in the gas phase at room temperature and at ~10 K.² The UVPD spectrum at room temperature shows only structureless, broad absorption even in the gas phase (Fig. 1a). In sharp contrast, the cold complex shows a number of well-resolved, sharp bands in the same UV region (Fig. 1b). Analysis of sharp spectral features provide information on the conformation of the ion complexes. In this talk, we will present spectroscopic results of metal ion–CE complexes and pseudo-rotaxanes having a CE molecule as a ring part.⁴

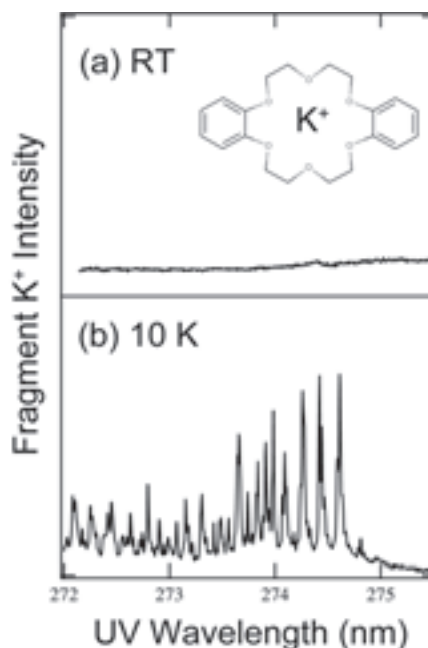


Fig. 1. UVPD spectra of K^+ (dibenzo-18-crown-6) at room temperature and 10 K.

(1) C. J. Pedersen, *J. Am. Chem. Soc.* **89** (1967) 7017.

(2) Y. Inokuchi et al., *J. Am. Chem. Soc.* **133** (2011) 12256.

(3) Y. Inokuchi et al., *J. Phys. Chem. A.* **119** (2015) 8512.

(4) M. Kida et al., *Phys. Chem. Chem. Phys.* **20** (2018) 17678.

Tongcang Li

Assistant Professor of Physics and Astronomy,
Assistant Professor of Electrical and Computer Engineering
Purdue University
525 Northwestern Ave, West Lafayette, IN 47907, USA
(765)-496-0072
tcli@purdue.edu



Research Interests:

Quantum optomechanics, Quantum sensing, Optical trapping

Employment:

August, 2014 –	Assistant Professor of Physics and Astronomy
August, 2014 –	Assistant Professor of Electrical and Computer Engineering
August, 2011 – July, 2014	Postdoctoral Scholar, University of California, Berkeley

Education:

May, 2011	Ph. D. in Physics (Department of Physics, The Univ. of Texas at Austin, USA)
July, 2004	B. S. in Physics (Department of Physics, Univ. of Sci. and Tech. of China)

Major Awards:

2018	APS Physics Top 10 Highlights of the Year, American Physical Society
2016	National Science Foundation CAREER Award,
2012	Springer Theses Prize

Publications:

- 1) J. Ahn, Z. Xu, J. Bang, ..., T. Li. *Phys. Rev. Lett.*, **121**, 033603 (2018).
- 2) T. M. Hoang, R. Pan, J. Ahn, ..., T. Li. *Phys. Rev. Lett.*, **120**, 080602 (2018)
- 3) T. M. Hoang, Y. Ma, J. Ahn, ..., T. Li. *Phys. Rev. Lett.* **117**, 123604 (2016).
- 4) T. M. Hoang, J. Ahn, J. Bang, T. Li. *Nature Communications*, **7**, 12550 (2016).
- 5) P. Zhang, T. Li, J. Zhu, ..., X. Zhang. *Nature Communications*, **5**, 4316 (2014).
- 6) S. Kheifets, A. Simha, K. Melin, T. Li, M. G. Raizen. *Science*, **343**, 1493 (2014).
- 7) T. Li, Z.-X. Gong, Z.-Q. Yin, ..., X. Zhang. *Phys. Rev. Lett.*, **109**, 163001 (2012).
- 8) T. Li, S. Kheifets, M. G. Raizen. *Nature Physics*, **7**, 527 (2011).
- 9) T. Li, S. Kheifets, D. Medellin, M. G. Raizen. *Science*, **328**, 1673 (2010)

Laser-driven GHz Nanorotor and Ultrasensitive Torque Detection

Tongcang Li^{1,2,3,4}

¹*Department of Physics and Astronomy, Purdue University, West Lafayette, Indiana 47907, USA;* ²*School of Electrical and Computer Engineering, Purdue University, West Lafayette, Indiana 47907, US;* ³*Purdue Quantum Science and Engineering Institute, Purdue University, West Lafayette, Indiana 47907, USA;* ⁴*Birck Nanotechnology Center, Purdue University, West Lafayette, Indiana 47907, USA*
tcli@purdue.edu

Optically levitated nanoparticles in vacuum have great potentials in precision measurements, quantum sensing, thermodynamics, and macroscopic quantum mechanics. We have assembled and levitated silica nanodumbbells in high vacuum. With a circularly polarized laser, we have driven them to rotate beyond 5 GHz, which is the fastest human-made rotor in the world^{1,2}. With a linearly polarized laser, we observed the torsional vibration of an optically levitated nanodumbbell^{1,3}. This levitated nanodumbbell torsion balance is a novel analog of the Cavendish torsion balance. Recently, we measured a torque as small as 10^{-27} Nm at room temperature. This system is several orders of magnitudes more sensitive than the former state-of-the-art torque sensor. Our calculations show that this system will be able to detect the long-sought vacuum friction under realistic conditions. The optically levitated nanorotor will also have applications in studying nanoscale magnetism and quantum geometric phase. With a levitated nanoparticle under drive, we also tested the differential fluctuation theorem and a generalized Jarzynski equality that is valid for arbitrary initial states⁴. This work deepens our understanding of nonequilibrium processes of small systems which are ubiquitous in biology, chemistry, and physics.

-
- (1) J. Ahn, Z. Xu, J. Bang, Y.-H. Deng, T. M. Hoang, Q. Han, R.-M. Ma, T. Li. *Phys. Rev. Lett.* **121** (2018) 033603.
(2) J. Ahn, Z. Xu, J. Bang, P. Ju, X. Gao, T. Li. *arXiv:1908.03453* (2019).
(3) T. M. Hoang, Y. Ma, J. Ahn, J. Bang, F. Robicheaux, Z.-Q. Yin, T. Li. *Phys. Rev. Lett.* **117** (2016) 123604
(4) T. M. Hoang, R. Pan, J. Ahn, J. Bang, H. T. Quan, T. Li. *Phys. Rev. Lett.* **120** (2018) 080602.

Ken-ichi Uchida

Position: Group Leader

Affiliation: National Institute for Materials Science

Address: 1-2-1 Sengen, Tsukuba, Ibaraki, 305-0047 JAPAN

Telephone: +81-29-859-2062

E-mail: UCHIDA.Kenichi@nims.go.jp



Research Interests:

Spintronics, Spin caloritronics, Thermoelectric conversion

Employment:

- Oct. 2016 - present Group Leader, Spin Caloritronics Group,
Research Center for Magnetic and Spintronic Materials,
National Institute for Materials Science
- Apr. 2014 - Sep. 2016 Associate Professor, Institute for Materials Research, Tohoku University
- Apr. 2012 - Mar. 2014 Assistant Professor, Institute for Materials Research, Tohoku University
[Cross appointment]
- May 2019 - present Professor, Institute for Materials Research, Tohoku University

Education:

- Mar. 2012 Doctor of Physics (Department of Physics, Tohoku University)
- Sep. 2009 Master of Science and Engineering
(Department of Applied Physics and Physico-Informatics, Keio University)
- Mar. 2008 Bachelor of Engineering
(Department of Applied Physics and Physico-Informatics, Keio University)

Major Awards:

- 2019 WCC Special Recognition (World Cultural Council)
- 2019 Marubun Research Encouragement Award (Marubun Research Promotion Foundation)
- 2015 NISTEP Award (National Institute of Science and Technology Policy)
- 2014 Nagase Prize (Frontier Salon Foundation)
- 2014 Gottfried Wagener Prize (German Innovation Award)
- 2013 Young Scientists' Prize, Commendation for Science and Technology (MEXT)
- 2011 JSPS Ikushi Prize (Japan Society for the Promotion of Science)

Publications:

- 1) K. Uchida, S. Daimon, R. Iguchi, and E. Saitoh, *Nature* **558**, 95-99 (2018).
- 2) S. Daimon, R. Iguchi, T. Hioki, E. Saitoh, and K. Uchida, *Nature Commun.* **7**, 13754 (2016).
- 3) K. Uchida, H. Adachi, D. Kikuchi, S. Ito, Z. Qiu, S. Maekawa, and E. Saitoh, *Nature Commun.* **6**, 5910 (2015).
- 4) K. Uchida, H. Adachi, T. An, T. Ota, M. Toda, B. Hillebrands, S. Maekawa, and E. Saitoh, *Nature Materials* **10**, 737-741 (2011).
- 5) K. Uchida, J. Xiao, H. Adachi, J. Ohe, S. Takahashi, J. Ieda, T. Ota, Y. Kajiwara, H. Umezawa, H. Kawai, G. E. W. Bauer, S. Maekawa, and E. Saitoh, *Nature Materials* **9**, 894-897 (2010).
- 6) K. Uchida, S. Takahashi, K. Harii, J. Ieda, W. Koshibae, K. Ando, S. Maekawa, and E. Saitoh, *Nature* **455**, 778-781 (2008).

Thermal Energy Engineering Based on Spin Caloritronics

Ken-ichi Uchida,¹⁻⁴

¹National Institute for Materials Science, Tsukuba 305-0047, Japan

²Institute for Materials Research, Tohoku University, Sendai 980-8577, Japan

³Center for Spintronics Research Network, Tohoku University, Sendai 980-8577, Japan

⁴Department of Mechanical Engineering, The University of Tokyo, Tokyo 113-8656, Japan
UCHIDA.Kenichi@nims.go.jp

Interaction between spin and heat is actively studied in the field of spin caloritronics from the viewpoints of both fundamental physics and applications¹. Early studies on spin caloritronics mainly focused on phenomena that generate a spin current from a heat current, such as the spin Seebeck effect²⁻⁴, toward the development of versatile thermoelectric generators. In contrast, there are many heat-generation phenomena that use spin and charge currents as input, e.g., the spin Peltier effect⁵⁻⁷, which is the reciprocal of the spin Seebeck effect; the anisotropic magneto-Peltier effect⁸⁻¹¹, in which the charge-to-heat current conversion efficiency depends on the angle between the charge current and magnetization in a ferromagnet (Fig. 1); and the anomalous Ettingshausen effect¹², in which a heat current is generated in the direction perpendicular to both the applied charge current and magnetization. Recently, we successfully observed the thermal response from these phenomena by means of an active infrared emission microscopy called the lock-in thermography¹³, and demonstrated thermal control functionalities that cannot be actualized without using spins. In this talk, we review our recent experimental results by focusing particularly on the thermal imaging measurements of the spin-caloritronic phenomena.

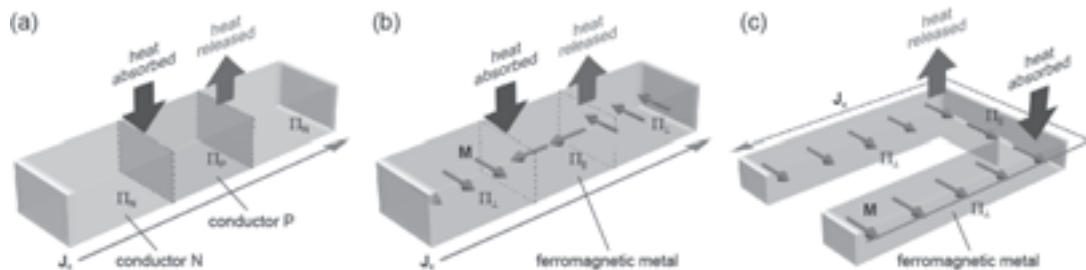


Figure 1 (a) Conventional Peltier effect. (b) Anisotropic magneto-Peltier effect. (c) Experimental configuration for measuring the anisotropic magneto-Peltier effect.

- (1) G. E. W. Bauer, E. Saitoh, and B. J. van Wees, *Nature Mater.* **11** (2012) 391.
- (2) K. Uchida *et al.*, *Nature* **455** (2008) 778.
- (3) K. Uchida *et al.*, *Nature Mater.* **9** (2010) 894.
- (4) K. Uchida *et al.*, *Proc. IEEE* **104** (2016) 1946.
- (5) J. Flipse *et al.*, *Phys. Rev. Lett.* **113** (2014) 027601.
- (6) S. Daimon, R. Iguchi, T. Hioki, E. Saitoh, and K. Uchida, *Nature Commun.* **7** (2016) 13754.
- (7) K. Uchida *et al.*, *Sci. Rep.* **8** (2018) 16067.
- (8) K. Uchida, S. Daimon, R. Iguchi, and E. Saitoh, *Nature* **558** (2018) 95.
- (9) R. Das and K. Uchida, *Appl. Phys. Lett.* **114** (2019) 082401.
- (10) K. Masuda, K. Uchida, R. Iguchi, and Y. Miura, *Phys. Rev. B* **99** (2019) 104406.
- (11) R. Das, R. Iguchi, and K. Uchida, *Phys. Rev. Applied* **11** (2019) 034022.
- (12) T. Seki, R. Iguchi, K. Takanashi, and K. Uchida, *Appl. Phys. Lett.* **112** (2018) 152403.
- (13) O. Breitenstein, W. Warta, and M. Langenkamp, *Lock-in Thermography: Basics and Use for Evaluating Electronic Devices and Materials* (Springer Science & Business Media, 2010).

Nobuyuki Matsuda

Associate Professor

Department of Communications Engineering, Graduate School of Engineering, Tohoku University

6-6-05 Aramaki Aza Aoba, Aoba-ku, Sendai 980-8579, Japan

E-mail: n.matsuda@ecei.tohoku.ac.jp

Tel +81-22-795-7102



Research Interests:

Quantum Optics, Photonics, Integrated photonics

Employment:

2009 – 2010 JSPS Research Fellow

2010 – 2018 Senior Research Scientist and Distinguished Researcher, NTT Basic Research Laboratories, NTT Corporation

2018 – Present Associate Professor, Tohoku University

Education:

2005 B. S. in Engineering (School of Engineering, Tohoku University)

2006 M. S. in Engineering (Graduate School of Engineering, Tohoku University)

2009 Ph. D. in Engineering (Graduate School of Engineering, Tohoku University)

Major Awards:

2009 Tohoku University Graduate School of Engineering Award

2012 JSAP Presentation Award

2018 RIEC Award

Publications:

- 1) C. Sparrow *et al.*, *Nature*, **557**, 660 (2018).
- 2) N. Matsuda *et al.*, *J. Opt.*, **19**, 124005 (2017).
- 3) A. Ishizawa *et al.*, *Sci. Rep.*, **5**, 45520 (2017).
- 4) N. Matsuda, H. Takesue, *Nanophotonics*, **5**, 440 (2016).
- 5) N. Matsuda, *Sci. Adv.*, **2**, e1501223 (2016).
- 6) J. Carolan *et al.*, *Science*, **349**, 711 (2015).
- 7) N. Matsuda *et al.*, *Sci. Rep.*, **2**, 817 (2012).
- 8) A. Peruzzo *et al.*, *Science*, **329**, 1500 (2010).
- 9) N. Matsuda *et al.*, *Nature Photon.*, **3**, 95 (2009).

Integrated photonics for quantum information science and technology

Nobuyuki Matsuda

Department of Communications Engineering, Graduate School of Engineering, Tohoku University, Sendai 980-8579, Japan
n.matsuda@ecei.tohoku.ac.jp

Smallness, stability, tunability and large optical nonlinearity of integrated optical waveguide circuitry have proven useful for their applications to quantum information processing (QIP) using photons. In this talk, I introduce our waveguide-based photonic QIP devices such as quantum entanglement sources, correlated photon sources¹, and universal linear optics² using silicon and silica-based planar lightwave circuits, as well as addressing the current status and prospects of integrated quantum photonics.

(1)N. Matsuda and H. Takesue, *Nanophotonics* **5** (2016) 440.

(2)J. Carolan *et al.*, *Science* **349** (2015) 711.

Contributed Talks

Novel synthesis method of nanosheets by using two-dimensional reactors in amphiphilic phases

Koki Sasaki, Tsuyoshi Okue, Yoshiaki Uchida, Norikazu Nishiyama

*Department of Chemical Science and Engineering, Graduate School of Engineering Science,
Osaka University, Toyonaka, Osaka 565- 8531, Japan
kokisasaki@cheng.es.osaka-u.ac.jp*

Recently, nanosheets (NSs) have been attracted attention owing to their various unique properties. The synthesis methods of NSs are divided into two categories: top-down and bottom-up methods. However, each of the methods has pros and cons. NSs of various layered materials have been fabricated by the top-down exfoliation methods; the thickness of the obtained NSs are a few nm, but this method can be applied only to layered materials. Meanwhile, the chemical vapor deposition as the bottom-up methods on a smooth substrate has recently been used to obtain NSs of nonlayered materials; this method can synthesize NSs of various materials, but the NSs are not so thin. Recently, it has been required to develop a new method to synthesize various kinds of thin NSs.

We focused on soft-template methods using surfactant, which enable us to easily control the shape of the product. We use hyperswollen lyotropic lamellar (HL) phase that is classified as one of lyotropic liquid crystalline phases. HL phases consist of amphiphilic bilayers separated by several hundreds of nm, and the thickness of the bilayers is several nm. We thought that we can use bilayers as a template for the synthesis of NSs. In fact, NSs of polystyrene were successfully synthesized in the thin hydrophobic reaction field inside the bilayers of aqueous amphiphilic solutions, and the calcination of the NSs gave carbon NSs as shown in Fig. 1 [1]. The thickness and horizontal width of the NSs are a few nm and several hundred nm, respectively. We named this method ‘two-dimensional reactors in amphiphilic phases (TRAP) method’.

Here, we present the synthesis of other NSs using TRAP method. We confirmed that TRAP method can be apply to the hydrophobic materials made from both hydrophilic and hydrophobic ingredients such as metal organic frameworks [2]. Furthermore, we found that it is possible to synthesize NSs in the thin hydrophilic reaction field inside the bilayers in HL phases of organic amphiphilic solutions.

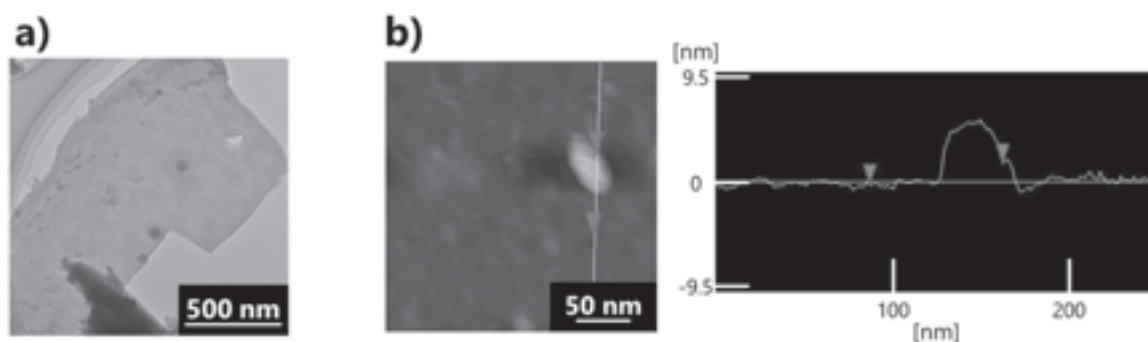


Fig.1 (a) TEM image of carbon NSs (b) AFM photograph and cross section of one of the synthesized carbon NSs

(1) Y. Uchida, *et al.*, *J. Am. Chem. Soc.*, **4**, 1103-1105 (2016).

(2) T. Omiya, *et al.*, *ACS Appl. Nano Mater.*, **1**, 3779-3784 (2018)

Theoretical study on single molecule conductivity of extended metal atom chains (EMACs) – Toward realization of single-molecule transistor –

Yasutaka Kitagawa,¹ Hayato Tada,¹ Naoka Amamizu,¹ Kazuki Ikenaga,¹
Hiromasa Sato,¹ Iori Era,¹ Takuya Fujii¹ and Masayoshi Nakano^{1,2}

¹*Division of Materials Engineering Science, Graduate School of Engineering Science, Osaka University, Toyonaka, Osaka 560-8531, Japan;*

²*Institute for Molecular Science, Okazaki, Aichi 444-8585
kitagawa@cheng.es.osaka-u.ac.jp*

A technology to manipulate the single-molecule has been developed to realize molecule-based devices. Linearly aligned polynuclear metal complexes, which are referred to as the extended metal atom chains (EMACs), are one of the most promising candidates for a molecular wire. Peng and co-workers have succeeded in synthesis of many novel EMACs by using oligo- α -pyridylamino ligands.¹ They have reported magnetic properties of those complexes in addition to the abilities of single molecule conductivity.²⁻³ From the viewpoint of the molecule-based device, however, it is crucial to control the conductivities by the external stimuli. In this context, our group has examined a relationship between electronic structures, magnetic properties and electron conductivities of one-dimensional nickel(II) complexes by density functional theory (DFT) calculations.⁴ Very recently, we found that the electron conductivities of tri- and penta-nickel(II) complexes depend on their intra-molecular spin coupling states.⁵⁻⁶ Figure 1 shows the molecular structure and I - V characteristics of $[\text{Ni}_5(\text{tripyridyldiamine})_4(\text{NCS})_2]$ (**1**). In this complex, only the terminal Ni(II) ions have spins, so that two spin coupling states, i.e., ferromagnetic (FM) and anti-ferromagnetic (AFM) states, must be considered. The calculated results indicate that the FM state exhibits higher conductivity than the AFM state, which demonstrates the potential of those EMACs for realizing a novel class of highly-efficient single molecule transistor controlled by the external magnetic field.

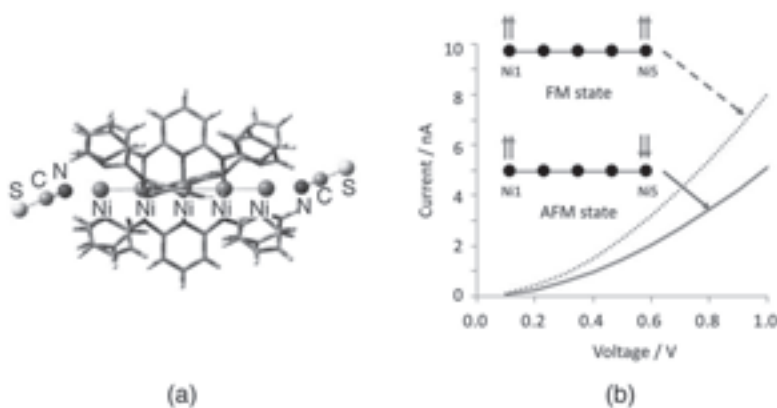


Figure 1. Molecular structure of complex **1** (a) and its simulated I - V characteristics (b).

- (1) C.C. Wang, W.C Lo, C.C. Chou, G.H. Lee, J.M. Chen, S.M. Peng, *Inorg. Chem.* **37** (1998) 4059.
- (2) S.M. Peng, C.C. Wang, Y.L. Jang, Y.H. Chen, F.Y. Li, C.Y. Mou, M.K. Leung, *J. Magn. Magn. Mat.* **209** (2000) 80.
- (2) S.-J. Shieh, C.C. Chou, G.H. Lee, C.C. Wang, S.M. Peng, *Angew. Chem. Int. Ed.* **36** (1997) 56.
- (3) T.W. Tsai, Q.R. Huang, S.M. Peng, B.Y. Jin, *J. Phys. Chem. C.* **114** (2010) 3641.
- (4) Y. Kitagawa, T. Matsui, Y. Nakanishi, Y. Shigeta, T. Kawakami, M. Okumura, K. Yamaguchi, *Dalton Trans.* **42** (2013) 16200.
- (5) Y. Kitagawa, M. Asaoka, Y. Natori, K. Miyagi, R. Teramoto, T. Matsui, Y. Shigeta, M. Okumura, M. Nakano, *Polyhedron.* **136** (2017) 125.
- (6) Y. Kitagawa, H. Tada, I. Era, T. Fujii, K. Ikenaga, M. Nakano, *Molecules.* **24** (2019) 1956.

A study of distance dependence on vibrational energy flow in proteins taking advantage of the periodic character of α helices

Satoshi Yamashita¹; Misao Mizuno¹; Yasuhisa Mizutani¹

¹Department of Chemistry, Graduate School of Science, Osaka University, Toyonaka, Osaka 565-08531, Japan
yamashitas16@chem.sci.osaka-u.ac.jp

We investigated vibrational energy transfer from heme in heme proteins by observing intensity changes of anti-Stokes Raman spectra of a tryptophan (Trp) residue [1-2]. In our previous study, we observed energy transfer using Trp residues at different distances from heme in globular proteins [1]. However, it is impossible to observe distance dependence without altering orientation between heme and Trp, because globular protein has complex folding structure. In this study, we systematically observed distance dependence on energy transfer in protein taking advantage of the periodic character of α helices.

Cytochrome b_{562} has four parallel helices (Figure 1a). Taking advantage of the periodic character of α helices, distance between heme and Trp can be changed with equal intervals by introducing a Trp residue to one-turn separated positions of the same helix. The schematic structures of the cytochrome b_{562} mutants are shown in Figure 1b. Anti-Stokes UV resonance Raman (UVRR) spectra were measured using 230 nm probe pulse light after photoexcitation of heme at 405 nm pump pulse.

In time-resolved anti-Stokes spectra of R98W, L94W and A91W, W18, W17, and W16 bands due to the introduced Trp residue were observed at 770, 877, and 1010 cm^{-1} , respectively. In the time-resolved difference spectra of R98W and L94W, positive bands were observed at the bands due to the excited Trp residue from 0 to 30 ps, resulting from the energy flow from heme to the Trp residue. We compared the temporal changes in the anti-Stokes W18 band intensities for cytochrome b_{562} mutants (Figure 1c). The intensity changes of W18 band decreased as the heme-Trp distance increased. The rise of W18 band intensity of L94W was slower than that of R98W. These results are consistent with the prediction from the classical thermal diffusion. However, intensity changes of W18 band of A91W is weaker than those calculated on the basis of a 1-dimensional classical diffusion model, which suggests more realistic diffusion model is required to describe the energy transfer in proteins.

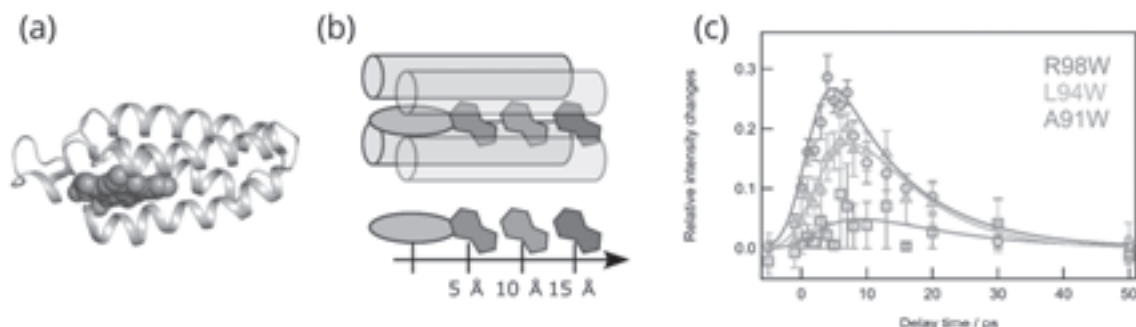


Figure 1. (a) Crystal structure of the cytochrome b_{562} . Orange spheres represent heme. (b) Schematic structure of the cytochrome b_{562} . Heme is shown as an orange ellipse, and Trp is represented by a polygon. The distance between heme and Trp for R98W (red), L94W (green) and A91W (blue) are about 5, 10, 15 Å, respectively. (c) Temporal changes of relative intensity in the W18 bands of R98W (red), L94W (green) and A91W (blue). Solid curves show the best fit using a bi-exponential function convoluted with the instrumental response function.

(1) N. Fujii, et al. J. Phys. Chem. Lett **5** (2014) 3269-3273.

(2) S. Yamashita, et al. J. Phys. Chem. B **122** (2018) 5877-5884.

Phonon-number-resolving Detection of Multiple Local Phonon Modes in a Trapped-ion Chain

Ryutaro Ohira,¹ Takashi Mukaiyama^{1,2}, Kenji Toyoda²

¹Graduate School of Engineering Science, Osaka University, 1-3 Machikaneyama, Toyonaka, Osaka, Japan

²Quantum Information and Quantum Biology Division, Institute for Open and Transdisciplinary Research Initiatives, Osaka University, 1-3 Machikaneyama, Toyonaka, Osaka, Japan
u696585a@ecs.osaka-u.ac.jp

Trapped-ion chains have been one of the best platforms to pursue quantum technologies because of its high controllability of the quantum state. There have been remarkable achievements especially in quantum information processing (QIT)¹⁻³ and quantum simulation^{4,5}. In trapped-ion experiments, the quantized oscillation of the ion, i.e. phonon, has been a major resource for these applications. There are two types of phonons, *collective phonons* and *local phonons*. Both types of phonons have different characteristics which are applicable to QIT and quantum simulation.

We are currently working on the experiments using the local phonon modes. One of the features of the local phonon mode is the phonon hopping^{6,7}. The localized phonons can hop between ions due to the Coulomb interactions in analogy with electron hopping between atoms in a solid state system. Thus, the local phonon modes are expected to provide the promising platforms to realize quantum simulation of the bosonic system⁸.

By simply increasing the number of ions and local phonon modes, it is possible to realize a large quantum system which can simulate many-body bosonic system^{9,10}. However, so far, almost all experiments using the local phonon modes are performed with only single phonon mode. One of the problems of the multiple phonon modes hopping is the projective measurement. The measurement time of the quantum state of the ion is usually longer than the period of the phonon hopping. Therefore, it is not straightforward to measure the time evolution of the multiple local phonon modes in a trapped-ion chain.

In the presentation, we will talk about our proposal of the projective measurement scheme to observe the dynamics of multi-phonon hopping, i.e. phonon-number-resolving detection. Using our phonon-number-resolving detection, we have successfully realized projective measurement of a Hong-Ou-Mandel interference of the local phonons¹¹. Our phonon-number-resolving detection is extendable in terms of both the number of the ions and the local phonon modes.

(1) F. Schmidt-Kaler et al., Nature **422** (2003) 408.

(2) T. Monz et al., Science **351** (2016) 1068

(3) C. Figgatt et al., Nature **572** (2019) 368.

(4) J. Zhang et al., Nature **551** (2017) 601.

(5) C. Kokail et al., Nature **569** (2019) 355.

(6) K. R. Brown et al., Nature **471**, (2011) 196.

(7) M. Harlander et al., Nature **471**, (2011) 200.

(8) K. Toyoda et al., Phys. rev. lett. **111**, (2013) 160501.

(9) S. Aaronson and A. Arkhipov, in Proceedings of the 43rd annual ACM symposium on Theory of computing (ACM, 2011) pp. 333.

(10) C. Shen et al., Phys. rev. lett. **112**, (2014) 050504.

(11) R. Ohira et al., arXiv:1909.08817 (2019).

Understanding the Optimum Spin-Current Control by Induced Electric-Polarization Reversal in hBN-based Magnetic Tunnel Junction

Halimah Harfah, Yusuf Wicaksono, Koichi Kusakabe

Division of Materials Engineering Science, Graduate School of Engineering Science, Osaka University, Toyonaka, Osaka 560-8531, Japan
 harfahhalimah@artemis.mp.es.osaka-u.ac.jp

Our recent study on hexagonal boron nitride (hBN) sandwiched by Ni(111) slabs reveals that the most stable stacking arrangement among 36 possible stacking arrangements shows the cross-correlation functionality coming from the bi-stable state of a rugged hBN plane and the controllable BN polarization [1]. The bistable state of the rugged hBN plane appears when the magnetic alignment of the upper and lower Ni(111) slabs is anti-parallel. The rugged hBN plane forms a unique pyramidal structure having two folding state, upward and downward pyramidal structure, which is interchangeable by controlling the BN polarization. The transmission probability calculations show a spin-filtering effect where the spin-polarized current is controlled by the electric field when a field-induced reversal of the polarization is realized. To achieve the optimum functionality of this spin-current control in hBN-based magnetic tunnel junction, different ferromagnetic slabs are considered to sandwiched the hBN layer. The investigation shows that the charge transfer mechanism from ferromagnetic slab to hBN layer affect the incline of pyramidal structure and the efficiency of spin-filtering effect.

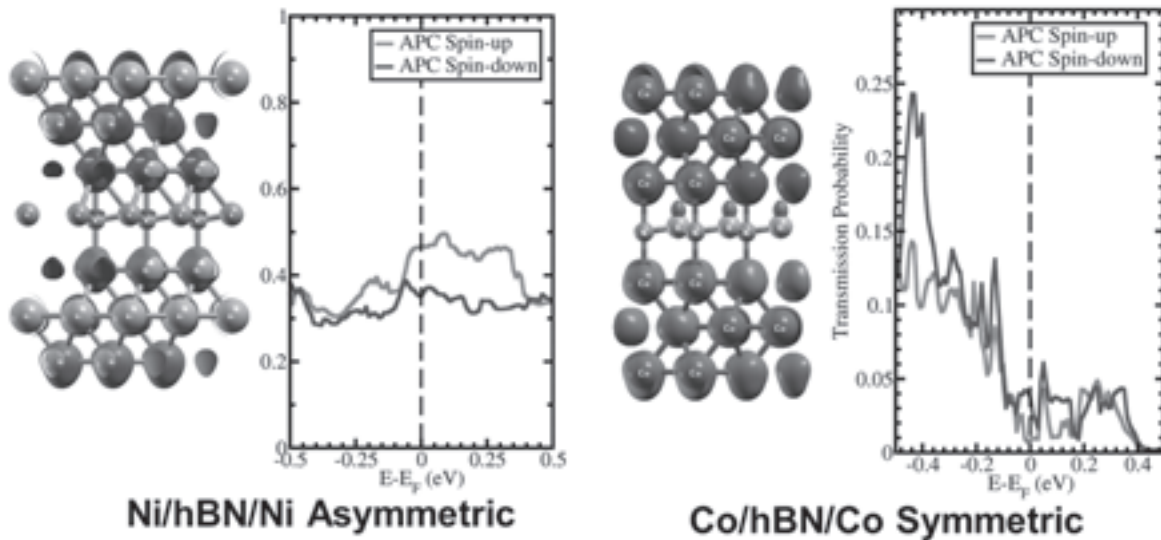


Figure 1. Spin-polarized current only occur for the case of Ni/hBN/Ni magnetic tunnel junction (left), but not for Co/hBN/Co magnetic tunnel junction (right)

(1) H. Harfah, Y. Wicaksono, M. A. Majidi, and K. Kusakabe, arXiv:1905.12252.

Frequency Multiplexing of Polarization-Entangled Photon Pairs without External Filtering

Tomohiro Yamazaki¹, Rikizo Ikuta^{1,2}, Toshiki Kobayashi^{1,2}, Shigehito Miki^{3,4},
Masahiro Yabuno³, Hiroataka Terai³, Nobuyuki Imoto², Takashi Yamamoto^{1,2}

¹Graduate School of Engineering Science, Osaka University, Toyonaka, Osaka 560-8531, Japan; ²Quantum Information and Quantum Biology Division, Institute for Open and Transdisciplinary Research Initiatives, Osaka University, Osaka 560-8531, Japan; ³Advanced ICT Research Institute, National Institute of Information and Communications Technology (NICT), Kobe 651-2492, Japan; ⁴Graduate School of Engineering Faculty of Engineering, Kobe University, Kobe 657-0013, Japan
yamazaki-t@qi.mp.es.osaka-u.ac.jp

Recently, quantum frequency combs are intensively researched¹, because they can easily generate high dimensional quantum states in the frequency domain. Especially, a generation of frequency-multiplexed polarization-entangled photon pairs enables to simultaneously prepare different frequency's polarization-entangled photon pairs and enhances the utility of quantum communication^{2,3}. So far, frequency-multiplexed polarization-entangled photon pairs have been prepared by external filtering. On the other hand, the use of cavity-enhanced spontaneous parametric down-conversion, that is, the generation of photon pairs by a nonlinear material placed inside an optical cavity, greatly improves the photon-pair generation rate.

In this presentation, we will show the first demonstration of the frequency-multiplexed polarization-entangled photon pairs generated by cavity-enhanced spontaneous parametric down-conversion. We used a monolithically-integrated periodically-poled lithium niobate (PPLN) waveguide resonator in a Sagnac interferometer for a polarization entangled photon-pair generation. In addition to the high efficiency, frequency-multiplexing extends over 1000 frequency modes, because of the resonance of only a higher frequency's photon. We verified the frequency multiplexing from the beat signals in the coincidence measurements, and the polarization entanglement from the quantum tomography of single mode and multimode photon pairs in each different frequency.

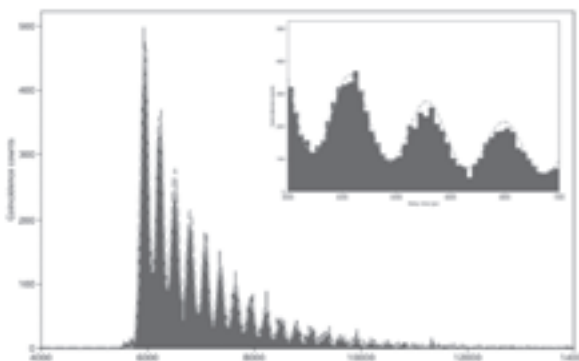


Fig. 1 Beat signal of about 100 frequency-modes around 1580 nm in the coincidence measurements

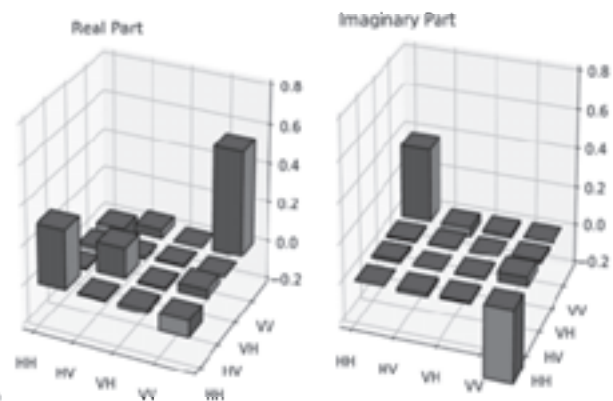


Fig. 2 Quantum tomography of polarization-entangled photon pair of single frequency-mode around 1580 nm

(1)M. Kues, *et al.*, Nat.Photonics **13** (2019) 170.

(2)H. C. Lim, A. Yoshizawa, H. Tsuchida, and K. Kikuchi, Opt. Fiber Technol. **16** (2010) 225.

(3)S. Wengerowsky, S. K. Joshi, F. Steinlechner, H. Hübel, and R. Ursin, Nature **564** (2018) 225.

Poster Session

Quantitative monitoring of internal electric field in solar cell with terahertz wave radiation

K. Miyagawa,¹ M. Nagai,¹ M. Ashida,¹ C. Kim,² H. Akiyama,² Y. Kanemitsu³

¹Graduate School of Engineering Science, Osaka University, Toyonaka, Japan;

²Institute for Solid State Physics, The University of Tokyo, Kashiwa, Japan;

³Institute for Chemical Research, Kyoto University, Uji, Japan
miyagawa@laser.mp.es.osaka-u.ac.jp

To maximize energy conversion efficiency of solar cell, it is important to elucidate ultrafast responses of electron-hole pair (carrier) generated by light irradiation. Evaluation of terahertz (THz) wave radiation from solar cell under an ultrashort optical pulse excitation is an effective method for characterizing them. This THz wave reflects a picosecond timescale drift current which carrier acceleration causes by an internal electric field in solar cell (1). Therefore, we can quantitatively evaluate the internal electric field with THz wave radiation. However, solar cells usually have a thin depletion layer for improving the energy conversion efficiency. It brings in strong internal electric field, and then drift current becomes saturated (2). Thus, evaluation of electric field amplitude for THz wave radiation may confuse us in characterization of solar cells. In this research, we focus on half-period time position (called zero-crossing time) for THz wave radiation. This time position corresponds to time when the drift current maximizes.

Figure shows bias-dependences of the (a) electric field amplitude and (b) zero-crossing time for THz wave generation under the ultrashort optical pulse excitation with power of 0.7 mW. This excitation power is close to solar power at ground level. Top axis is estimated from the depletion layer width and bias. (a) Electric field amplitude has constant below 0.5 V, and it indicates that the drift current saturated under strong internal electric field. On the other hand, (b) zero-crossing time has a significant bias-dependence during operating condition of solar cell. Therefore, we can quantitatively evaluate the internal electric field with zero-crossing time of THz wave radiation. In this presentation, we also report change of the internal electric field under simultaneous excitations with pulsed and continuous light for emulated solar cell operating condition, and discuss solar cell performance.

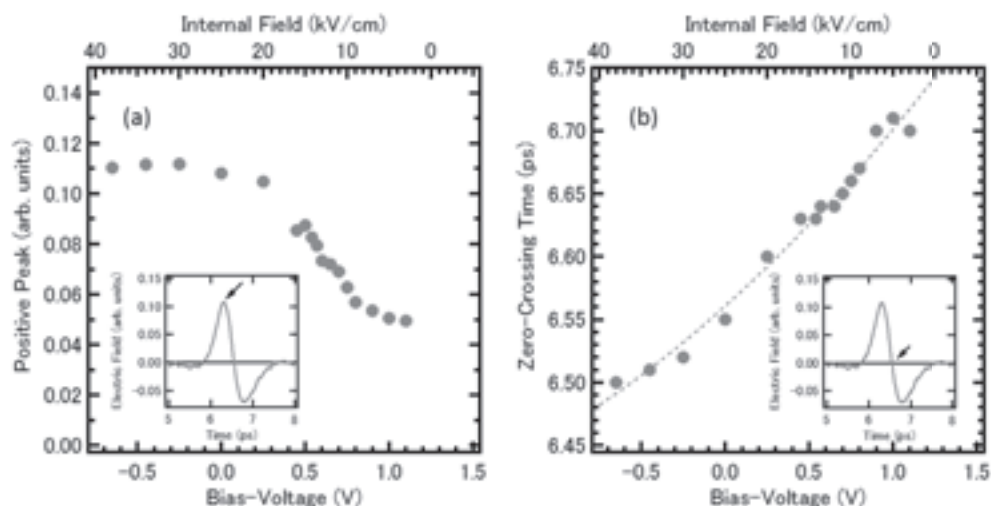


Figure: Bias-dependences of the (a) electric field amplitude and (b) zero-crossing time

(1)L. Xu, B. B. Hu, W. Xin, D. H. Auston and J. D. Morse, Applied Physics Letters. **62** (1993) 3507.

(2)M. Abe, S. Madhavi, Y. Shimada, Y. Otsuka, K. Hirakawa and K. Tomizawa, Applied Physics Letters. **81** (2002) 679.

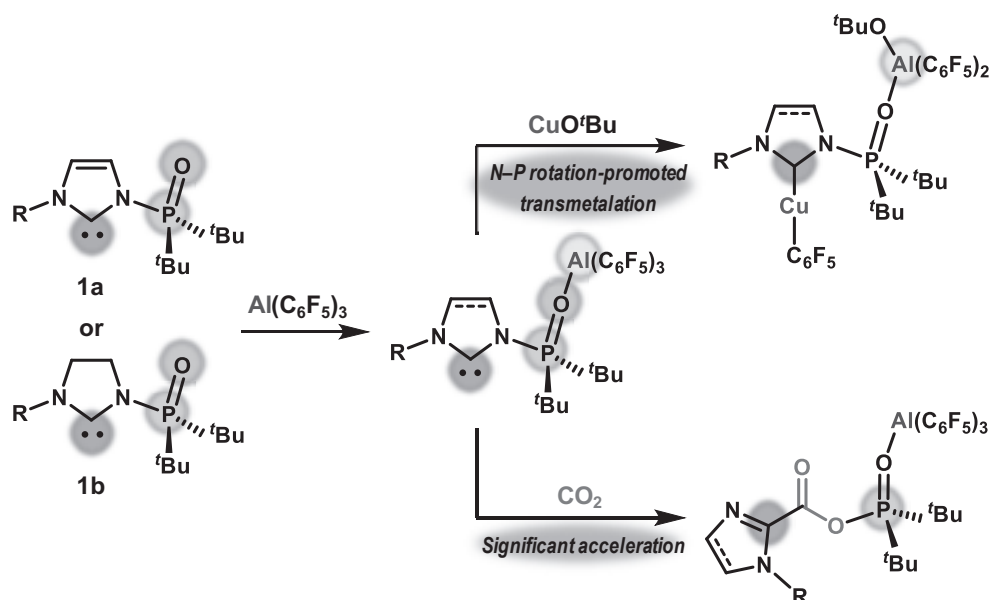
Strategic Complexation between $\text{Al}(\text{C}_6\text{F}_5)_3$ and Phosphinoyl Substituent in *N*-Heterocyclic Carbenes

Takahiro Asada,¹ Yoichi Hoshimoto¹, Sensuke Ogoshi¹

¹Department of Applied Chemistry, Faculty of Engineering, Graduate School of Engineering, Osaka University, Suita, Osaka 565-0871, Japan
hoshimoto@chem.eng.osaka-u.ac.jp, ogoshi@chem.eng.osaka-u.ac.jp

N-Heterocyclic carbenes (NHCs) have found a multitude of applications in diverse research areas in organic, inorganic, and organometallic chemistry.¹ Applications of NHCs have been significantly furthered by the advent of multifunctional NHCs by the introduction of substituents on either the nitrogen atom(s) or on the backbone of the NHCs.² Recently, we have developed *N*-phosphine oxide-substituted imidazolylidenes (PoxIm)s and the corresponding imidazolinylienes (SPoxIm)s through the direct introduction of the phosphinoyl group onto the nitrogen atom, which can work as a Lewis base and an electrophile showing multipurpose utility.^{3a-c}

Herein, we report the complexation between $\text{Al}(\text{C}_6\text{F}_5)_3$ and PoxIm **1a** as well as SPoxIm **1b** proceeded through dominant coordination of the *N*-phosphinoyl oxygen to the Al center, and the Lewis basic/nucleophilic carbene moieties are thus co-existed in the resultant molecules.⁴ A strategic use of these carbenes was demonstrated by treatment with CuO^tBu as well as CO_2 . The former reaction resulted into the rapid transfer of the C_6F_5 group from Al to Cu, quantitatively yielding a carbene-coordinated CuC_6F_5 complex in which the phosphinoyl oxygen in the (S)PoxIm units simultaneously coordinates to $\text{Al}(\text{O}^t\text{Bu})(\text{C}_6\text{F}_5)_2$. In the latter, phosphinoylation of CO_2 with SPoxIm was found to be significantly accelerated in the presence of 10 mol% $\text{Al}(\text{C}_6\text{F}_5)_3$, while $\text{B}(\text{C}_6\text{F}_5)_3$ did not show any catalytic activity.



(1) M. N. Hopkinson, C. Richter, M. Schedler, F. Glorius, *Nature* **510** (2014) 485.

(2) E. Peris, *Chem. Rev.* **118** (2018) 9988.

(3) a) Y. Hoshimoto, T. Kinoshita, M. Ohashi, S. Ogoshi, *Angew. Chem. Int. Ed.* **54** (2015) 11666; b) Y. Hoshimoto, T. Asada, S. Hazra, T. Kinoshita, P. Sombut, R. Kumar, M. Ohashi, S. Ogoshi, *Angew. Chem. Int. Ed.* **55** (2016) 16075; c) T. Kinoshita, M. Sakuraba, Y. Hoshimoto, S. Ogoshi, *Chem. Lett.* **48** (2019) 230.

(4) T. Asada, Y. Hoshimoto, S. Ogoshi, Submitted.

Asymmetric ionic-voltage relation in low-aspect-ratio nanopore under salt gradients

Iat Wai Leong¹, Makusu Tsutsui¹ and Masateru Taniguchi¹

¹ *The Institute of Scientific and Industrial Research, Osaka University, Osaka, Japan*
leong.iat.wai32@sanken.osaka-u.ac.jp

Using nanopore technology to measure the electric signals of single-particles has been broadly used in many research subjects because of its high sensitivity and simple mechanism. Most studies have been observed with nanopore sensor under the same electrolyte condition on both sides of a thin membrane. Nevertheless, salt concentration, pH and viscosity gradients across membranes truly exist in natural world such as neuron membrane ion channels in biological synapse. In fact, many researchers reported that heterogeneous solution conditions can be utilized to retard the particles' translocation speed and enhance the signal-to-noise ratio [1]. Many existing theories, can only explain the ion behavior of nanochannel-like system, will help us to build up an emulation of artificial nerve cell [2]. However, there is still lacks of mechanisms to support low-aspect-ratio nanopores more close to nature's biostructure. Hence, we attempt to first elucidate the behavior of ion transport in low-aspect-ratio nanopore under salt gradients.

A nanopore (as shown in Figure.1) formed in a 50nm-thick Si_3N_4 membrane with diameter 1000 nm and 300 nm was used as a model. We performed current-voltage and current-time measurements by sweeping bias voltage from -2 V to 2V through a pair of Ag/AgCl electrodes. We employed a series of combination of different concentration PBS solution in cis/trans cell. Furthermore, to investigate immiscible two-phase system created by water solution and room temperature ionic liquid(RTILs) was employed to study how the interface responds to the voltage bias and estimate the ionic current together with its influence on contact surface movements. Current-voltage characteristics through a single SiN_x pore as shown in Figure.2 will be discussed.

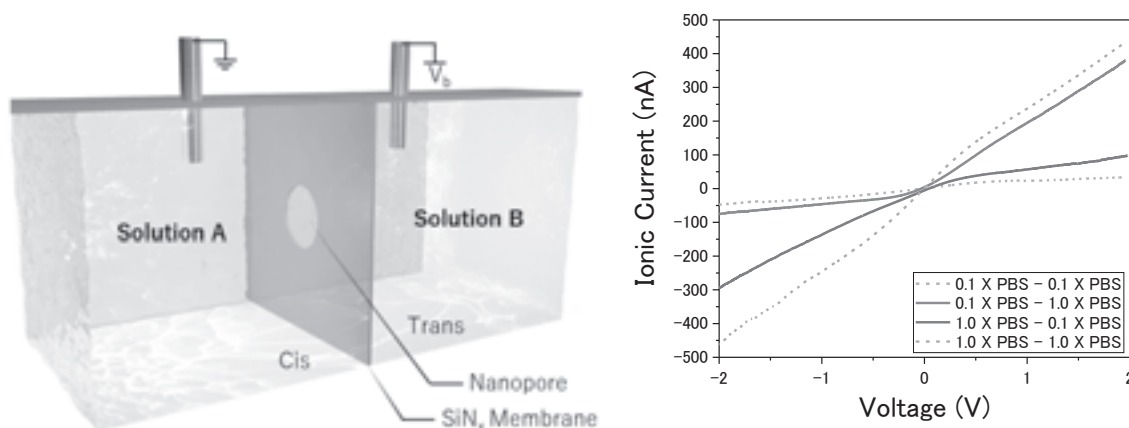


Figure.1 (a)Scheme of nanopore device assembling. (b) Asymmetric current were observed using 300-nm radius nanopore

(1) Y. Qiu et.al., *Anal. Chem.*, 2019, **91**, 1, 996-1004

(2) Y. He et.al., *Sci. Rep.*, 2017, **7**, 46661

Topological pump induced by dynamics of moiré pattern

Manato Fujimoto¹, Henri Koschke², Mikito Koshino¹

¹*Department of physics, Graduate School of Science, Osaka University, Toyonaka, Osaka 560-8531, Japan;* ²*Institut für Theoretische Physik, Universität zu Köln, 50937 Köln, Germany* *l of Engineering Science, Osaka University, Toyonaka, Osaka 560-8531, Japan*
m-fujimoto@qp.phys.sci.osaka-u.ac.jp

We theoretically study the charge transport induced by a motion of moiré pattern in a relative translation of overlapped crystals. In recent years, there have been remarkable advances in fabrication of atomically thin materials¹, and the technology enables us to stack different two-dimensional materials on top of each other in arbitrary twist angles. The interaction between the rotationally stacked layers have a crucial impact on the physical properties of the system, and even the superconductivity and correlated insulating states are realized in the twisted bilayer graphenes.¹ These emergent properties are actually caused by the existence of the moiré interference pattern, which is generated by the slight lattice mismatch of the stacked layers.

While so far most of theoretical and experimental studies on the twisted moiré superlattices are limited to the static systems, here we consider dynamical properties in *moving* moiré pattern. We consider a situation where one layer of the twist bilayer is slid with respect to the other layer [Fig. 1(a)]. Then a translation of an atom scale (\sim a few Å) leads to a shift of the moiré pattern with much larger length scale (\sim a few 10 nm), and it is known as “the moiré speed up”. We expect the moving of the moiré pattern should cause the electronic transport, and it should be explained in terms of the topological pumping in the time-periodic Hamiltonian².

In order to investigate the principle of the moiré pumping, First, we consider a simplified one-dimensional double chain model [Fig. 1(b)], where a pair of tight-binding chains with different periodicities are coupled by the inter-chain electron hopping. We calculate the charge pumping caused by a relative translation of the chains using the adiabatic formalism. We show that the electrons are actually conveyed by the moving moiré pattern, where the charge transfer can be described by the topological Chern number analogous to the quantum Hall effect.³ We also extend the analysis to the two-dimensional moiré superlattices.

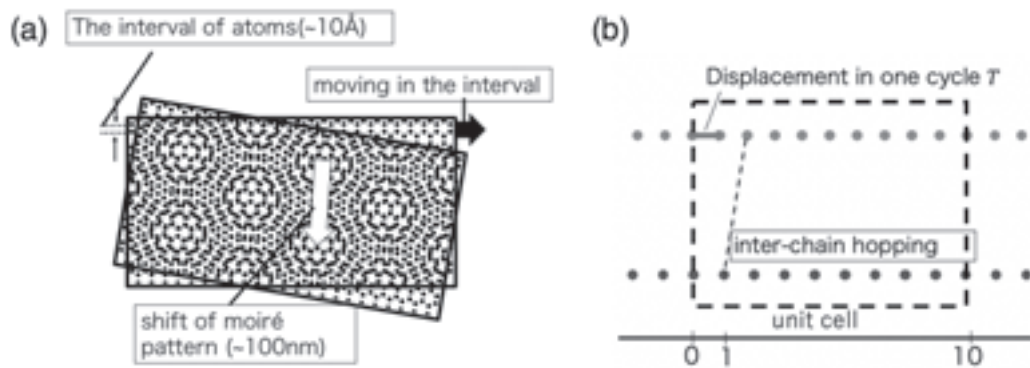


Fig 1(a) Schematic picture of the moiré pumping in relative sliding of the twisted bilayer. (b) One-dimensional double chain model.

1) Y. Cao. et al. Nature **556**, 80-84 (2018)

2) D. J. Thouless, Phys. Rev. B **27**, 6083 (1983)

3) D. J. Thouless, M. Kohmoto, M. P. Nightingale, and M. den Nijs, Phys. Rev. Lett. **49**, 405 (1982).

Synthesis and Controlling Chiroptical Responses of Planar and Axially Chiral Vaulted Platinum(II) Complexes

Masahiro Ikeshita, Takeshi Naota

Department of Chemistry, Graduate School of Engineering Science,
Osaka University, Toyonaka, Osaka 560-8531, Japan
ikeshita@soc.chem.es.osaka-u.ac.jp

Chiral molecules play important role for developing next-generation technologies such as 3D display, security device, CPL lasers, and biological probe. Recently, controlling chiroptical responses of organic or organometallic materials has attracted significant interest because of its wide potential for using novel functional materials. However, there are few guidelines for designing chiral molecules with desired chiroptical responses.

In this work, we focused on the chiroptical properties of planar chiral vaulted platinum complexes which have three-dimensional molecular structures. For this purpose, we designed and synthesized a series of planar chiral vaulted *trans*-bis[(β -iminomethyl)aryloxy]-platinum(II) complexes (S_p, R, R)-/ (R_p, S, S) -**1a-d** bearing axially chiral 1,1'-binaphthyl ligands (Figure 1). In these complexes, 1,1'-binaphthyl frameworks act as chirality-inducing building blocks and enantiopure Pt(II) complexes could be synthesized from commercially available (*R*)- or (*S*)-BINOL without optical resolution process. Interestingly, chiroptical responses such as specific rotation ($[\alpha]_D$), circular dichroism (CD) and circularly polarized luminescence (CPL) are gradually enhanced by shortening vaulting linker, whereas all complexes have similar absorption and emission properties in dilute 2-MeTHF solution state. The relation between the structure and chiroptical responses of these complexes has been clarified by density functional theory (DFT) calculations and ascribed to the distortion of coordination planes caused by restriction of vaulting linker.

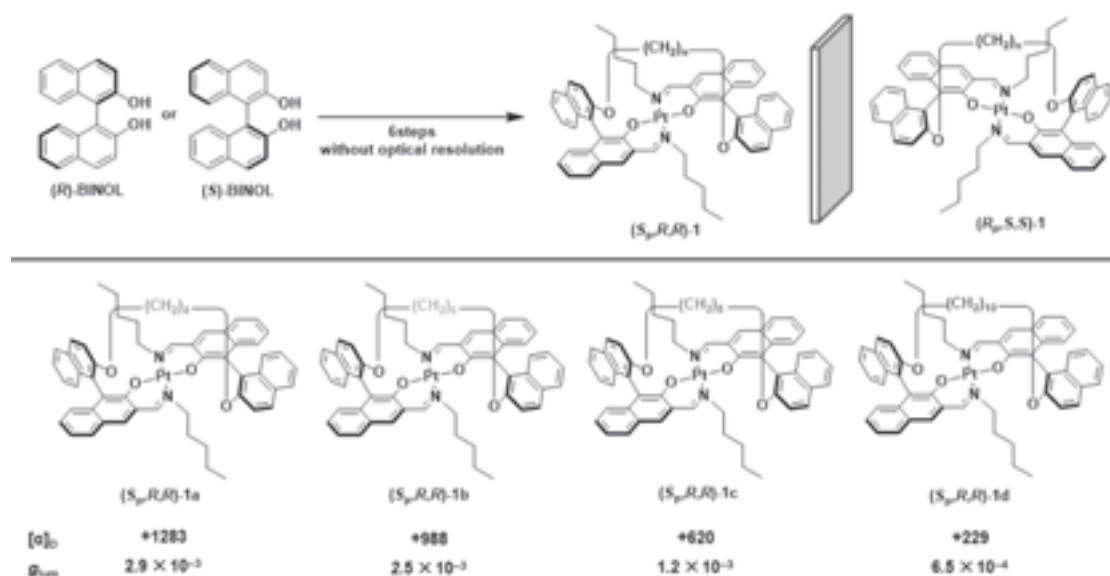


Figure 1. Chemical structures and chiroptical properties of vaulted *trans*-bis[(β -iminomethyl)aryloxy]Pt(II) complexes (S_p, R, R)-**1a-d**.

(1) N. Komiya, M. Okada, K. Fukumoto, D. Jomori, T. Naota, *J. Am. Chem. Soc.* **2011**, *133*, 6493–6496.

(2) N. Komiya, M. Okada, K. Fukumoto, K. Kaneta, A. Yoshida, T. Naota, *Chem. Eur. J.* **2013**, *19*, 4798–4811

Theoretical analysis on tip-ferromagnetic resonance force microscopy

Ryo Izumi¹

¹*Department of Applied Physics, Graduate School of Engineering, Osaka University, Suita, Osaka 565-0871, Japan
izumi@ap.eng.osaka-u.ac.jp*

Development of measurement tools capable of detecting magnetization of an individual magnetic nanostructure is an important issue because of the recent progress of spintronics. Magnetic resonance force microscopy (MRFM) [1] is a scanning probe technique which can observe magnetic resonance of a sample by detecting the deflection of a mechanical oscillator (cantilever). MRFM achieved ultrahigh sensitivity to detect single electron spin magnetic resonance [2].

However, the samples are not restricted to paramagnetic samples. Zhang et al. [3] used MRFM to investigate ferromagnetic resonance (FMR) of a YIG sample and, in the case of ferromagnetic samples, this method is referred to as ferromagnetic resonance force microscopy (FMRFM). Usually, FMRFM detects modulated magnetic force caused by ferromagnetic resonance of a sample by irradiating an amplitude-modulated microwave. This method is very useful to investigate the ferromagnetic resonance of an individual magnetic structure such as submicron-size permalloy samples [4]. On the other hand, another method which is based on utilizing tip-ferromagnetic resonance was proposed [5]. This method is based on using a high-coercive magnetic coated cantilever and modulating the magnetization of the ferromagnetic material of the tip. However, theoretical analysis about the method is not well discussed.

In this presentation, I will theoretically discuss about the tip-ferromagnetic resonance force and compare the efficiency of some microwave-irradiation methods.

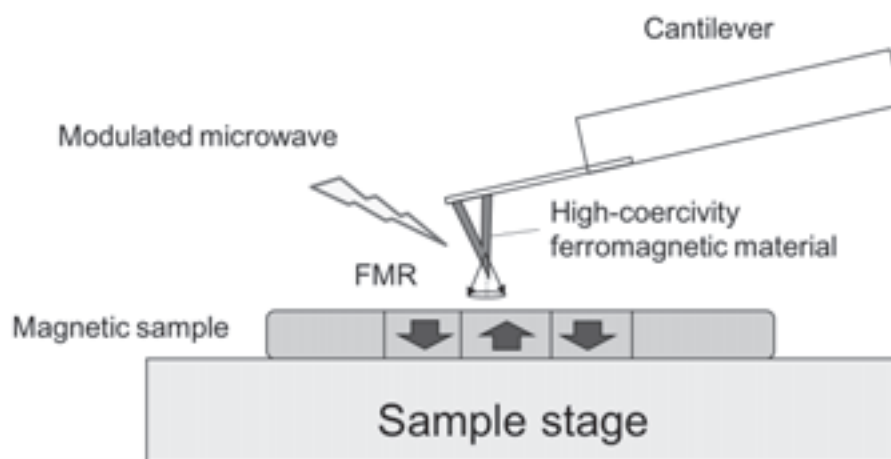


Fig.1 Schematics of tip-ferromagnetic resonance force microscopy.

- (1) J. A. Sidles et al., Rev. Mod. Phys. 67, 249 (1995).
- (2) D. Rugar et al., Nature (London) 430, 329 (2004).
- (3) Z. Zhang et al., Appl. Phys. Lett. 68, 2005 (1996).
- (4) O. Klein et al., Phys Rev B 78, 144410 (2008).
- (5) E. Arima et al., Nanotechnology 26, 125701 (2015).

Electric properties of hBN-graphene-hBN trilayer system

Hiroki Oka,¹ Mikito Koshino¹

¹*Department of Physics, Graduate School of Science, Osaka University, Toyonaka, Osaka 560-0043, Japan;*
h.oka@qp.phys.sci.osaka-u.ac.jp

Graphene and hexagonal boron nitride (h-BN) are two dimensional materials having honeycomb lattice structures with slightly different lattice periods. When graphene is stacked on h-BN, the moiré pattern induced by the lattice mismatch opens mini energy gaps in the graphene's Dirac cone (1,2). The energy band structure sensitively depends on the relative twist angle between the two materials, since the period of the moiré pattern is rule by the twist angle.

In this study, we theoretically study the electronic band structure of h-BN graphene h-BN trilayer systems, in which the top and bottom hBN layers are stacked with different twist angles to the middle graphene layer. We show that, unlike the single moiré system, the double moiré patterns having different periods give rise to a series of flat bands between the first-order mini gaps of the individual moiré patterns, as well as the higher-order mini gaps at very low energy near the graphene's Dirac point.

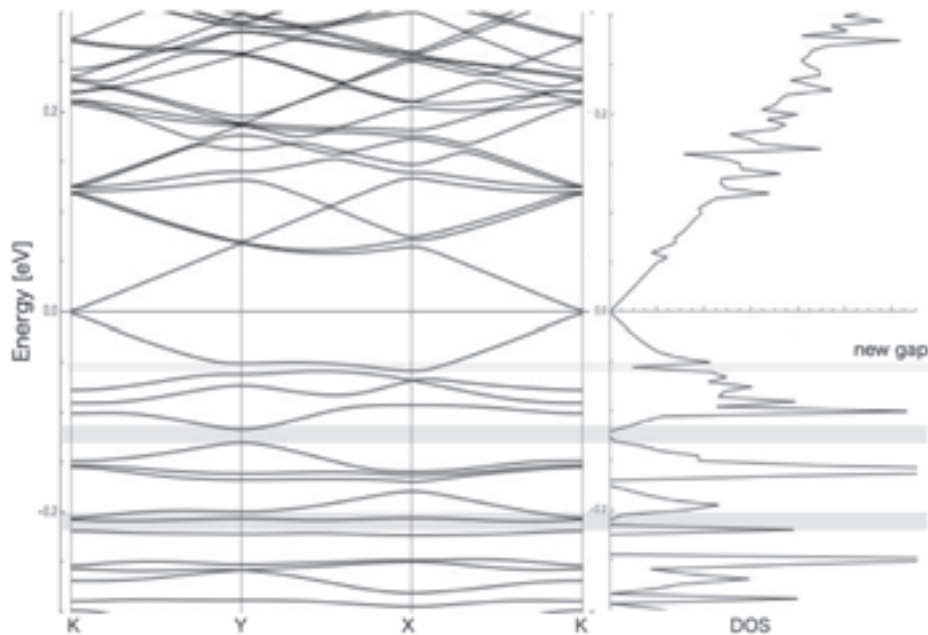


Fig. 1. Band structure of a h-BN graphene h-BN trilayer system

(1) G. Giovannetti et al., Phys. Rev. B **76**, 073103 (2007)
(2) B. Sachs et al., Phys. Rev. B **84**, 195414 (2010)

Toward site selective modification of pyrimidine base flipped out by naphthyridine carbamate dimer binding

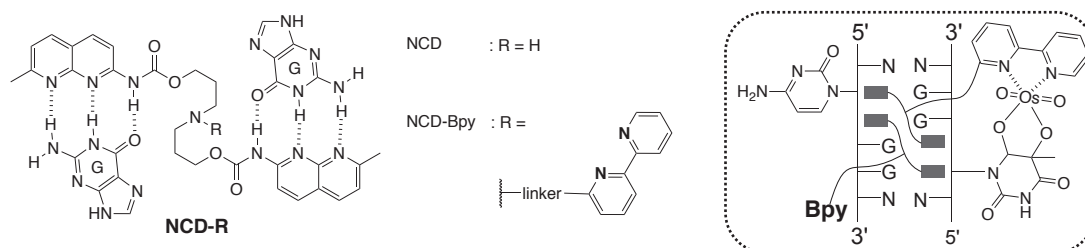
Yuki Yagi, Takeshi Yamada, Kazuhiko Nakatani

*The institute of scientific and industrial research, Osaka university, Ibaraki, Osaka, Japan
yagi26@sanken.osaka-u.ac.jp*

Abnormal expansion of CGG repeat in the FMR1 gene located on the X chromosome causes fragile X syndrome. We hypothesized that the interruptions in the CGG repeat tract by inducing mutation of base by some method may suppress the abnormal expansion of the CGG repeat.

Up to now, our laboratory has successfully synthesized the molecule (**NCD**), which binds to d(CG_n/CG_n) contained in the CGG repeat sequence and d(TGG/TGG) having 3 mismatch base pairs. In this study, we newly synthesized **NCD-Bpy**, where 2,2'-bipyridine was introduced in **NCD** and expected that carbon—carbon double bond in 5,6 position of thymine flipped out from DNA duplex could be oxidized by **NCD-Bpy** with osmium tetroxide.

The detail will be discussed in the poster presentation.



Many-variable variational Monte-Carlo studies of superconductivity in the bilayer Hubbard model

Daichi Kato, Kazuhiko Kuroki

*Department of Physics, Osaka University,
1-1 Machikaneyama, Toyonaka, Osaka 560-0043, Japan
d.kato@presto.phys.sci.osaka-u.ac.jp*

Superconductors exhibit zero resistivity and magnetic field shielding below the superconducting critical temperature T_c . Superconductors can be applied to electric wires and superconducting maglevs, power storage devices, and so on. However, industrial applications are restricted within narrow limits due to the low T_c compared with room temperature. For example, the cuprates have the highest T_c of 135 K at ambient pressure. Hence high-temperature superconductivity and its mechanism have been studied intensively for long years.

In the occurrence of superconductivity in general, there is a trade-off relation between strong pairing interactions and light electron mass: Strong pairing interaction, which itself enhances pairing, usually increases electron mass simultaneously. For instance, in the phonon mediated s-wave superconductivity, the strong electron-phonon coupling enhances the pairing interaction but increases the electron mass, giving rise to a reduction of T_c .

In a previous paper [1], one of the present authors and his coworkers proposed a possible way to circumvent this dilemma in specific multi-band systems with spin fluctuations. They considered systems where a wide band crosses the Fermi level and a narrow band sits close to, but does not intersect the Fermi level. In this case, the pairing instability may become very large because a large density of states of the narrow band leads to a huge number of inter-band pair scattering channels, and also because only the wide band crosses the Fermi level, so that electron mass is not so heavy as to strongly suppress superconductivity.

Recently, such a band which sits close to the Fermi level has come to be known as an “incipient band” [2,3]. The role of incipient bands has received much attention after observations of iron-based superconductors where hole-like bands are found to sink below the Fermi level, leaving only electron-like Fermi surfaces.

More recently, a fluctuation exchange (FLEX) approximation study suggested that in various systems with coexisting wide and narrow bands, superconductivity is optimized when a narrow band is incipient in the intermediate electron correlation regime [4]. However, the reliability of FLEX in the strongly correlated regime is questionable since it neglects vertex correlations. Here we apply a many-variable variational Monte-Carlo method [5], which can describe the strong correlation and various ordering fluctuations accurately, to the Hubbard model on the bilayer square lattice to study the effect of incipient bands on superconductivity.

[1] K. Kuroki, T. Higashida, and R. Arita, Phys. Rev. B **72**, 212509 (2005).

[2] P.J. Hirschfeld, M.M. Korshukov, and I.I. Mazin, Rep. Prog. Phys. **74**, 124508 (2011).

[3] H. Miao et al., Nat. Comm. **6**, 6056 (2015).

[4] K. Matsumoto, D. Ogura, and K. Kuroki, Phys. Rev. B **97**, 014516 (2018).

[5] <https://github.com/issp-center-dev/mVMC>

Single Particle Dynamics in Tandem Micropores

Shohei Kishimoto¹, Makusu Tsutsui¹, Masateru Taniguchi¹

¹ *The Institute of Scientific and Industrial Research (ISIR), Osaka University,
Suita, Osaka 565-0871, Japan;
shohei.kishimoto32@sanken.osaka-u.ac.jp*

1. Introduction

Coulter counter is known as a method for measuring size of particles¹. The principle is to create micro-sized pore, fill the electrolyte solution there, and apply voltage to measure the ionic current. As particles pass through the pore, the ionic current changes reflecting the size of the particles. This change in ionic current is affected by the translocation path of the particles causing variations in the ionic current signal patterns² whereby deteriorate the sensor accuracy for single-particle sizing.

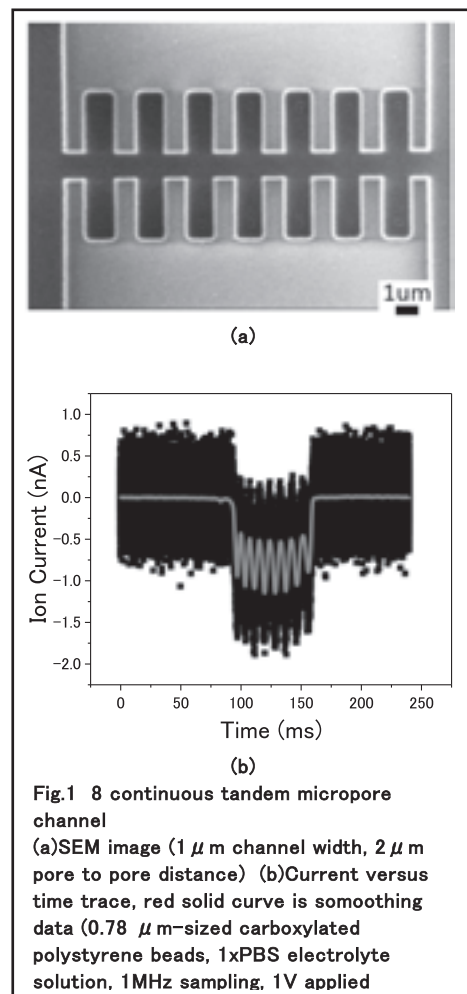
In the present work, we seek to develop a novel microchannel structure for multiple single-particle detections. The channel is constructed with multiple constrictions in series expected to provide several pulse signals by Coulter principle upon particle translocation. From a statistics point of view, the increased number of pulses per particle is expected to allow more reliable estimations of its physical properties.

2. Measurement / Experiment

A channel was made in a 1.5 μm thick SiO₂ thin film by electron beam lithography and reactive ion etching (Figs. 1 and 2). 1 \times PBS was used as the electrolyte solution. Ag / AgCl electrodes were placed at the inlet and outlet of the channel and a DC voltage was applied to one of the electrodes. A current amplifier and digitizer were used to record the cross-channel ionic current.

3. Result

When admitting 0.78 μm -sized carboxylated polystyrene beads into the fluidic channel, we observed resistive pulses suggesting electrophoretic translocation of the polymeric particles through the narrowest constrictions. Close inspection of each pulse signal pattern revealed characteristic sub-pulses reflecting the number of sensing zones in the channel (Fig. 1). As expected, the statistical variations of the sub-pulse width and height decreased with increasing the number of constrictions, which can lead to better accuracy for assessing the single-particle properties such as the size and the surface charge density.



(1)D. Marshall et al. JALA **8**(6) (2003) 72-81

(2)M. Tsutsui et al. ACS Nano **10**(1) (2016) 803-809

Optimization of circuit-coupling conditions for the magnetic-susceptibility measurement apparatus in pulsed high magnetic fields using a proximity detector oscillator

Katsuki Nihongi¹, Tame Tahara¹, Takanori Kida¹,
Yasuo Narumi¹, and Masayuki Hagiwara¹

¹Center for Advanced High Magnetic Field Science (AHMF), Graduate School of Science, Osaka University, Toyonaka, Osaka 560-0043, Japan
nihongi@mag.ahmf.sci.osaka-u.ac.jp

Radio frequency (rf) techniques utilizing a simple LCR circuit have been widely used in physical property measurements¹. For a magnetic insulator, the change of the inductance of the LCR circuit corresponds to its change of magnetic-susceptibility. The change of magnetic-susceptibility can be measured as the change of the resonant frequency. This technique is useful in magnetic measurements of tiny samples in high magnetic fields under high pressures due to the utilization of a compact searching coil and the extremely high sensitivity^{2,3}. In the present study, we have developed magnetic-susceptibility measurement apparatus in pulsed high magnetic fields using a proximity detector oscillator (PDO) and optimized circuit-coupling in the LCR circuit. We compared the signal of PDO method with the signal of conventional induction-method using a pick-up coil.

In Fig. 1, the PDO signal at 4.2 K is shown as a solid line, which is obtained by the time integral of the change in Δf against the applied magnetic field for the c -direction of MnF_2 . The sharp increase near 9T, which is also observed in the magnetization curve indicated by a dashed line in Fig. 1, corresponds to the spin flop transition of MnF_2 . These results show that the PDO method has enough to conduct magnetic-susceptibility measurements. We are going to perform magnetic measurements in high magnetic field under high pressures with a piston-cylinder type clamp cell (PCC). Since it is necessary to increase the outer diameter of the pressure cell in order to generate high pressure, the magnetization measurements by the induction method with high sensitivity must be impossible. Therefore, the PDO method possibly becomes an alternative to the magnetization measurements under such extreme conditions.

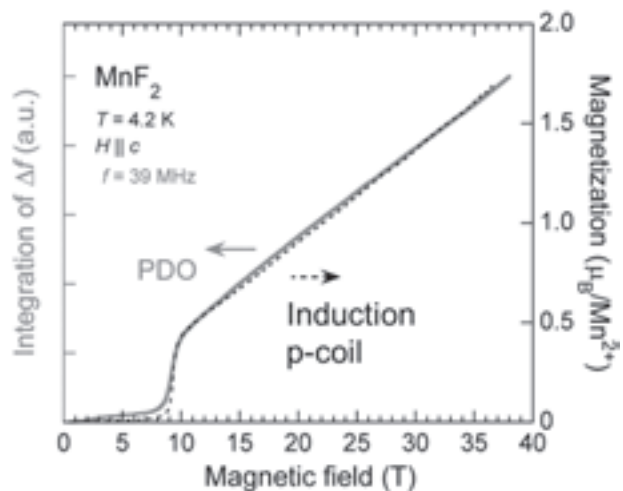


Fig. 1: Magnetization curves of MnF_2 ($H \parallel c$) at 4.2 K. The solid and dashed lines correspond to the results of the PDO method and the induction one, respectively. Both measurements use the same sample.

(1) M. M. Altarawneh *et al.*, Rev. Sci. Instrum. **80** (2009) 066104.
(2) S. Ghannadzadeh *et al.*, Phys. Rev. B **87** (2013) 241102(R).
(3) D. Graf *et al.*, Phys. Rev. B **85** (2012) 134503.

Construction of Polyacrylamide Gel Containing Engineered Hexameric Hemoprotein as a Cross-linker and Evaluation of its Mechanical Property

Kazuki KAGEYAMA¹, Koji OOHORA¹, Takashi HAYASHI¹

¹ Department of Applied Chemistry, Graduate School of Engineering, Osaka University, Suita, Osaka 565-0871, Japan

E-mail: k_kageyama@chem.eng.osaka-u.ac.jp

Hydrogels, unique materials containing water in polymer matrix, demonstrate soft physicochemical properties compared with other solid materials, and have been widely used as biomaterials such as cell scaffolds. However, the hydrogels are easily broken by mechanical damage. In this context, introduction of fragile components as sacrificial bonds into hydrogels is useful to enhance their mechanical property.¹ Recently, several researchers have focused on proteins as a building block of hydrogels.² Our group has employed hemoprotein as a building block, because reversible and strong heme–heme pocket interaction will be useful as a sacrificial bond. In this work, hexameric tyrosine-coordinated heme protein (HTHP) is chosen as a precursor of a cross-linker of a polyacrylamide gel. To introduce the reaction site in the protein, a heme derivative tethering an acrylamide group was designed and synthesized. Then, the reconstituted HTHP with the modified heme (rHTHP) was prepared by the replacement of heme with the synthesized heme derivative. Polymerization of acrylamide and rHTHP provided the hydrogel as shown in Figure 1. Control experiment using HTHP instead of rHTHP does not form the gel structure, indicating that rHTHP works as a cross-linker. We will report the stimuli-responsiveness toward reduction, and elastic properties, which were measured by atomic force microscopy.

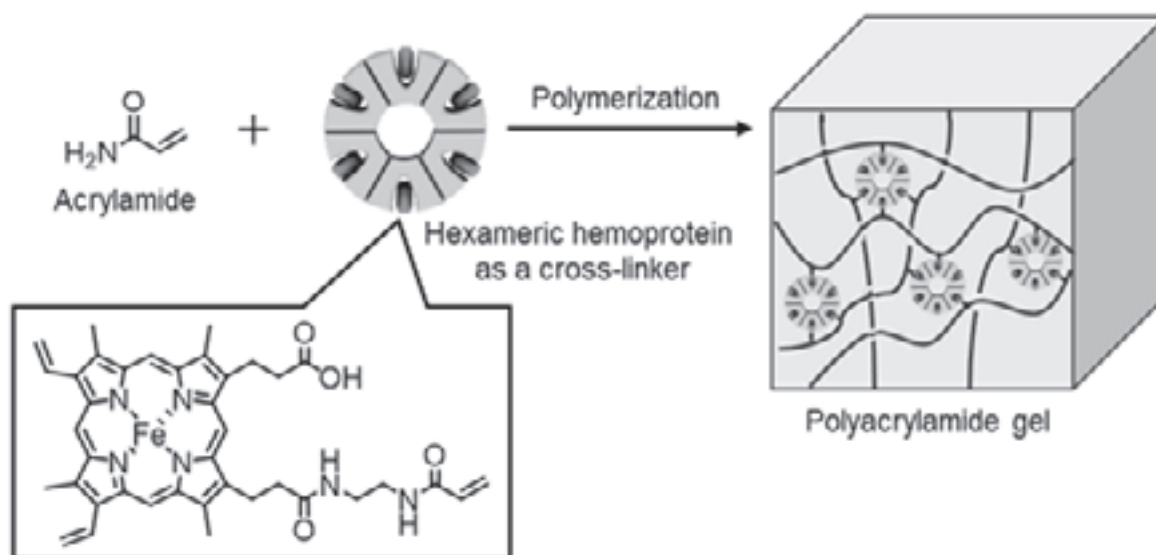


Figure 1. Schematic representation of the hydrogel containing rHTHP as a cross-linker.

(1) L. Sun, T. Kurokawa, S. Kuroda, A. Bin, T. Akasaki, K. Sato, A. Haque, T. Nakajima, J. P. Gong, *Nat. Mater.*, **12**, 932 (2013).

(2) H. Wang, Y. Shi, L. Wang, Z. Yang, *Chem. Soc. Rev.*, **42**, 891 (2013).

The Reversible Structring of Ionic-Liquid Monolayer in Electric Double Layer OFET Revealed by Operand Investigations

Daijiro Okaue,¹ Ichiro Tanabe,¹ Sakurako Ono¹, Kota Sakamoto¹, Taiki Sato¹, Akihito Imanishi,¹ Yoshitada Morikawa,^{2,3} Jun Takeya⁴ and Ken-ichi Fukui^{1,5}

¹Department of Materials Engineering Science, Graduate School of Engineering Science, Osaka University, Toyonaka, Osaka, Japan, ²Department of Precision Science and Technology, Graduate School of Engineering, Osaka University, Suita, Osaka, 565-0871, Japan, ³Research Centre for Ultra-Precision Science and Technology, Graduate School of Engineering, Osaka University, Suita, Osaka 565-0871, Japan, ⁴Department of Advanced Materials Science, Graduate School of Frontier Sciences, The University of Tokyo, Kashiwa, Chiba, 277-8561, Japan, ⁵Institute for Molecular Science (IMS), 38 Nishigo-Naka, Myodaiji, Okazaki 444-8585, Japan
okaue@surf.chem.es.osaka-u.ac.

Ionic liquids (ILs) gated electric double-layer organic FETs (EDL-OFETs) have attracted much attention owing to their ultralow operational voltage (~ 0.1 V)¹. However, ILs exhibit different behavior on the electrode from conventional electrolytes, resulting in operational instability of EDL-OFETs.

Fig. 1 shows the time course of the operational voltage of an IL-gated EDL-OFET with rubrene single crystal as the organic semiconductor and 1-ethyl-3-methylimidazolium bis(fluorosulfonyl)imide (EMIM-FSI) as the IL. Operational voltage of the EDL-OFET increased by twice in a few hours from initial operation. The increase in the operational voltage with time has been reported as bias stress, which causes severe degradation of FETs. Bias stress is generally caused by carrier trapping. We expected that adjacent FSI anions trap hole carriers in the rubrene single crystal by Coulomb force.

Operando electrochemical frequency modulation atomic force microscopy (operando EC-FM-AFM) revealed the formation of the IL monolayer on the rubrene surface by device operation at the same time scale as bias stress. IL monolayer took the checkerboard structure (**Fig. 2**) suggested by molecular dynamic (MD) simulations on the carrier injected rubrene surface. Moreover, the negative part in the FSI anions oriented to the rubrene surface (**Fig. 3**). Temperature dependence measurements elucidated that forming & deforming the IL monolayer took the activation energy by 0.23 and 0.53 eV, respectively.

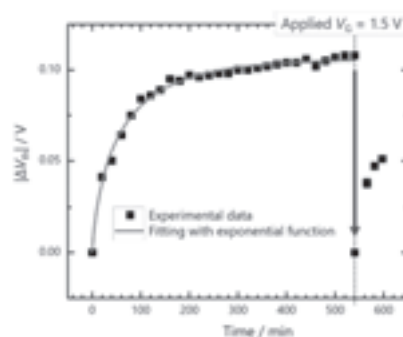


Fig. 1. Time course of operational voltage

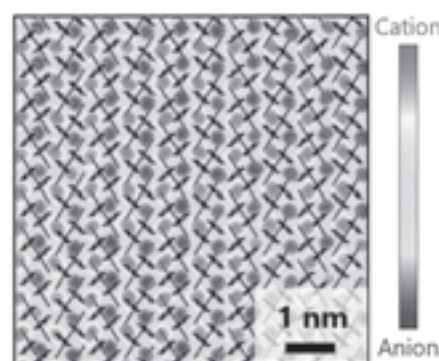


Fig. 2 Lateral distribution of the 1st interfacial IL at FET ON region.

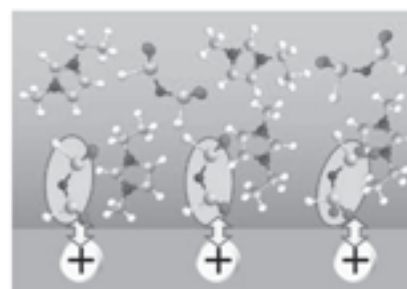


Fig. 3 Scheme of the carrier trapping derived from IL.

(1) S. Ono, S. Seki, R. Hirakawa, Y. Tomonori and J. Takeya, Appl. Phys. Lett., **92**, (2008) 103313.

Long-Range Ultrafast Electron Transfer Reaction of a Pyrene-Biphenyl System Driven by Multiphoton Absorption

Tomomi Kawakami, Masafumi Koga, Hikaru Sotome, Hiroshi Miyasaka

Department of Materials Engineering Science, Graduate School of Engineering Science,
Osaka University, Toyonaka, Osaka 560-8531, Japan
miyasaka@chem.es.osaka-u.ac.jp

For efficient light energy conversion in systems where photoinduced electron transfer reactions take place, rapid formation of charge separated states at high energy level and small rate of recombination are desirable in terms of energy and quantum yield. However, it is a difficult task to optimize the energy gap and the rate constant at the same time, as predicted by the Marcus theory¹. To overcome this problem, we focused on the multiphoton ionization reaction which can create long-lived charge separated states lying at the higher energy level. As a model of this approach, we have investigated a multiphoton-induced electron transfer reaction of pyrene as electron donor and biphenyl as acceptor (Figure 1a,b) using transient absorption spectroscopy. An intense femtosecond laser pulse induced multiphoton ionization of pyrene, leading to the formation of radical cation. In addition, absorption of radical anion of biphenyl was observed (Figure 1c,d). These results indicate that multiphoton ionization effectively induces the ultrafast electron transfer reaction.

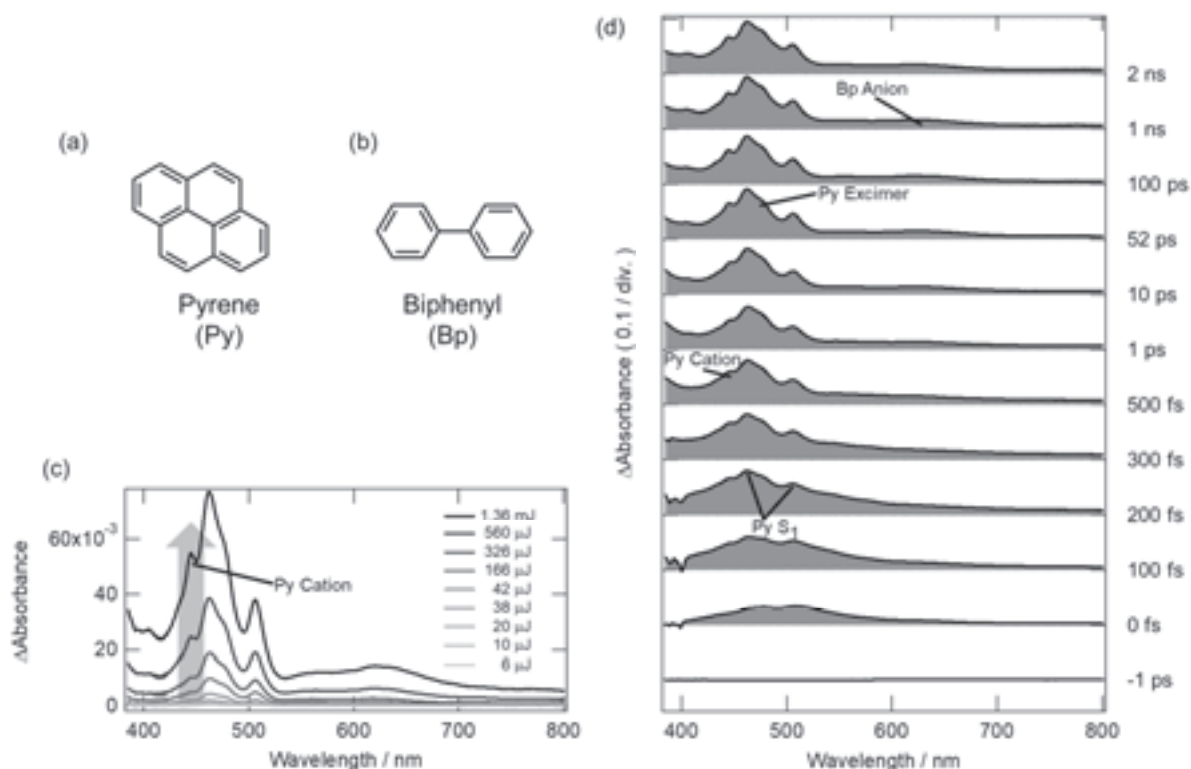


Figure 1. (a,b) Molecular structures of Py and Bp. (c) Excitation power dependence of transient absorption spectra of Py-Bp in acetonitrile solution at 100 ps after excitation. (d) Transient absorption spectra of Py-Bp in acetonitrile solution excited with a femtosecond laser pulse at 355 nm.

(1) R. A. Marcus and N. Sutin, *Biochim. Biophys. Acta* **811** (1985) 265.

The size and frequency dependence of permittivity of ZnO nanoparticles studied by electrostatic force microscopy

YamamotoTatsuya

*Department of Applied Physics, Osaka University, 2-1 Yamadaoka, Suita, Osaka 565-0871
Japan*

u054349j@ap.eng.osaka-u.ac.jp

When investigating the electrical characteristics of metal oxide nanoparticles, the relative permittivity is one of the important factors. The relative permittivity depends on the applied bias frequency and the particle size [1]. However, in the conventional dielectric constant measurement method (for example, measurement using an LCR meter), it is necessary to make the size of the nanoparticles to be produced uniform and to measure the overall value. On the other hand, the electrostatic force microscopy (EFM) can measure the dielectric constant of an insulator sample on the nanometer scale [2]. Therefore, it can be expected that the specific dielectric constant of the metal oxide nanoparticles can be individually measured by using EFM.

In this study, we measured the dielectric constant of ZnO nanoparticles dispersed on the substrate using EFM, and investigated the particle size dependence of the dielectric constant and the frequency dependence of the applied AC bias. Fig. 1 is a schematic diagram of EFM measurement on nanoparticles, and the magnitude of the force acting between the probe and a nanoparticle is expressed as

$$F = \frac{\pi \epsilon_0 R^2}{2 \left(z + \frac{t}{\epsilon_r} \right) \left(z + \frac{t}{\epsilon_r} + R \right)} V_{ac}^2 \quad \dots(1)$$

[3] Where t , ϵ_r , R , z , and V_{ac} are the size of the nanoparticle, the relative dielectric constant, the radius of the probe, the distance between the probe and the particle, and the amplitude of the applied AC bias, respectively. Figure 2 shows the relative dielectric constant calculated by the formula (1) from the force acting between the probe and the nanoparticle. The relative permittivity tended to increase as the particle size increased. In addition, when the frequency of the applied AC bias was changed between 10 kHz and 30 MHz, the relative permittivity at 10 kHz tended to be larger than that at 10 MHz.

[1] Y. P. Mao, et al. *J. Appl. Phys.* **108**, 014102 (2010).

[2] A. V. Valavade, et al. *Biomed. Phys. Eng. Express* **4** 055023 (2018).

[3] S. Hudlet et al. *Eur. Phys. J. B* **2**, 5 (1998).

Magnetization and ESR of the Chiral Helimagnet CrNb₃S₆

Yuya Sawada¹, Yusuke Shimamoto², Yusuke Kousaka^{3,3}, Yoshihiko Togawa^{2,3},
Takehito Nakano⁴, Daichi Yoshizawa⁵, Jun-ichiro Ohe⁶, Jun-ichiro Kishine^{3,7},
Katsuya Inoue^{3,8}, Yasuo Nozue⁹ and Masayuki Hagiwara^{1,3}

¹Center for Advanced High Magnetic Field Science, Graduate School of Science, Osaka University, Osaka 560-0043, Japan; ²Department of Physics and Electronics, Osaka Prefecture University, Osaka 599-8531, Japan; ³Center for Chiral Science, Hiroshima University, Hiroshima 739-8526, Japan; ⁴Graduate School of Science and Engineering, Ibaraki University, Ibaraki 310-8512, Japan; ⁵Institute for Molecular Science, Aichi 444-8585, Japan; ⁶Department of Physics, Toho University, Chiba 274-8510, Japan; ⁷Division of Natural and Environmental Science, The Open University of Japan, Chiba 261-8586, Japan; ⁸Graduate School of Science, Hiroshima University, Hiroshima 739-8526, Japan; ⁹Department of Physics, Graduate School of Science, Osaka University, Osaka 560-0043, Japan.
sawada@ahmf.sci.osaka-u.ac.jp

“Chirality”, which means left- or right-handedness, plays a crucial role in the symmetry properties of nano-scale phenomena in condensed matter physics. In materials science, chiral materials are frequently found in molecules or crystals with helical structures, and a chiral structure sometimes leads to the emergence of intriguing phenomena, such as chiral helicoidal order, skyrmion lattices, and topological Hall effect. One of the monoaxial chiral magnets CrNb₃S₆, which belongs to the non-centrosymmetric hexagonal space group $P6_322$, is known as the material that the helical magnetic order with a long period is realized along the c -axis below the long-range ordering temperature $T_c = 127$ K. As shown in Fig. 1, it is known that by applying a magnetic field perpendicular to the helical axis, an alternate helical magnetic and ferromagnetic order called the chiral soliton lattice (CSL) emerges. In 2012, Togawa et al. has succeeded the direct observation of the CSL evolution of CrNb₃S₆ by using Lorenz microscopy techniques for the first time¹. In this study, to investigate the CSL natures and dynamics in magnetic fields, we performed magnetization and electron spin resonance (ESR) measurements of CrNb₃S₆ single crystal under various conditions. In the presentation, we will discuss about the peculiar behavior of hysteresis of magnetization and observed novel spiked signals superposed on and ESR signal² due to the CSL dynamics. This work was supported by a Grant-in-Aid for Scientific Research (S) (No. 25220803) “Toward a New Class Magnetism by Chemically-controlled Chirality” and JSPS Core-to-Core Program, A. Advanced Research Networks.

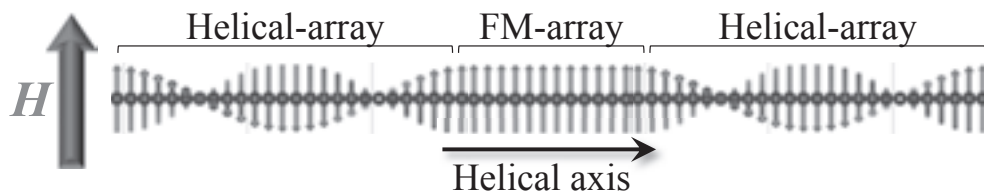


Fig. 1. Schematic of the chiral soliton lattice (CSL) in a magnetic field applied perpendicular to the helical axis.

(1) Y. Togawa, *et al.*, Physical Review Letter **108** (2012) 107202.

(2) D. Yoshizawa, YS, *et al.*, Physical Review B **100** (2019) 104413.

Hall measurements in atomically thin CeTe₃ films

Mori Watanabe¹, Takashi Ibe¹, Masashi Tokuda¹, Hiroki Taniguchi¹, Yoshinori Okada²,
Kensuke Kobayashi^{1,3}, and Yasuhiro Niimi^{1,4}

¹Graduate school of science, Osaka Univ., ²OIST,

³Institute for Physics of Intelligence, Univ. of Tokyo, ⁴CSRN, Osaka Univ.
watanabe@meso.phys.sci.osaka-u.ac.jp

CeTe₃ is an atomically layered material in the family of rare earth tritellurides. Its crystal structure consists of a CeTe slab which is responsible for its magnetic properties, separated by two Te sheets which are responsible for its highly two dimensional electric transport. CeTe₃ is known mainly for its formation of incommensurate charge density waves, which has been studied extensively (1). It also possesses interesting magnetic properties. According to heat capacity and magnetization measurements, the material shows two magnetic phase transitions at around $T_{N1} = 3$ K and $T_{N2} = 1.2$ K (2,3). These transitions are suggested to be antiferromagnetic, but the details of these magnetic structures are largely unknown. Moreover, despite its layered structure, most studies focus on bulk properties, and there are no reports on thin film measurements.

In order to gain a better understanding of its magnetic properties, we have performed transport measurements in 40 nm thick CeTe₃ films (see the inset of Fig. 1). Figure 1 shows Hall resistance R_{Hall} below and above T_{N1} ($= 3$ K). Although the R_{Hall} vs H_{\perp} curve is more or less similar above T_{N1} , the value of R_{Hall} is enhanced at $H_{\perp} > 0.5$ kOe below T_{N1} . In the presentation, we will discuss the detailed temperature dependence of this enhancement down to 0.3 K ($< T_{N2}$).

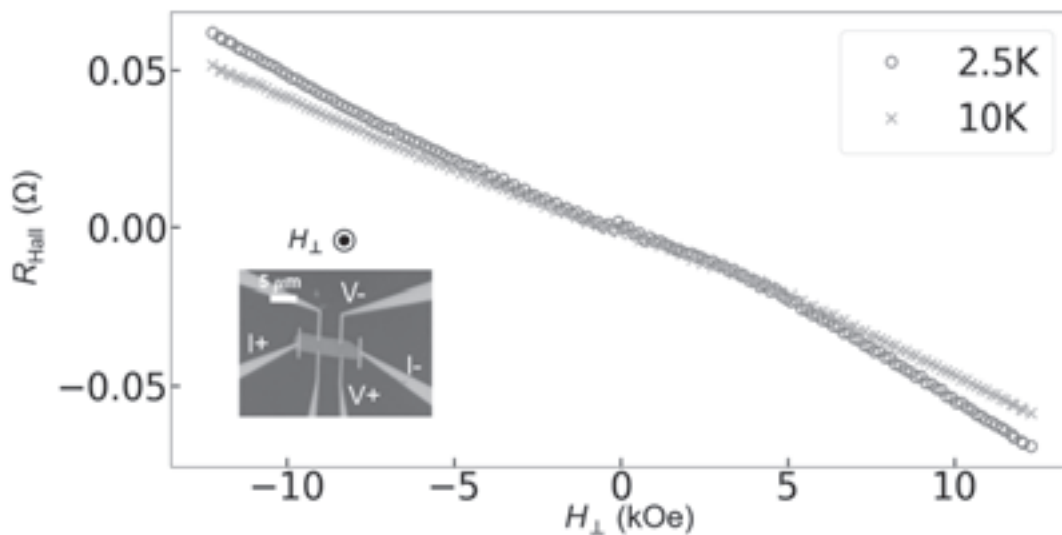


Figure 1: Hall measurements of a CeTe₃ thin film below and above T_{N1} ($= 3$ K). The Hall resistance is enhanced at $H > 0.5$ kOe below T_{N1} . The inset shows the optical microscope image of the device.

(1) V Brouet *et al.*, Phys. Rev. Lett. **93** (2004) 126405.

(2) Y Iyeiri *et al.*, Phys. Rev. B **67** (2003) 144417.

(3) K Deguchi *et al.*, J. Phys.: Conf. Ser. **150** (2009) 042023.

Development of First-Principles Crystal Structure Search Method with High Precision and High Efficiency and Its Implementation

Masaaki Geshi¹ and Hiroki Funashima

¹*Institute for NanoScience Design (INSD), Osaka University, Toyonaka, Osaka 560-0043*

²*School of Science, Kobe University, Kobe, Hyogo 657-8501, Japan*
geshi@insd.osaka-u.ac.jp

The crystal structure search method using the first-principles calculation becomes difficult to search effectively because the calculation time of the first-principles calculation becomes enormous with increasing the number of atoms. Moreover, none of the methods currently used can completely guarantee that the structure obtained is the most stable structure at the given element and composition ratio, and the correctness can only be confirmed by experimental data. One may consider impossible to cover the search space to be considered because of its large number. In this presentation, we show that it is possible to narrow down the candidate structure by checking all possibilities from 230 space groups. When examining interatomic distances taking into account physical quantities such as atomic radii, many crystal structures are physically impossible and the significant number of the crystal structures can be eliminated. Further refinement can be achieved by taking into account physical and chemical factors. By examining their enthalpies, the most stable structure with the given element and composition ratio is determined. Since the crystal structure is narrowed down, including the degree of freedom of internal coordinates, the time required for structure optimization in first-principles calculations can be greatly reduced. The most important thing is that the most stable structure of the given element and its composition ratio is definitely included in the refined structure.

Selective hydrocarbon oxidation reactions by the gas diffusion electrode carrying Ru-modified covalent triazine frameworks

Shintaro Kato¹, Takashi Harada², Kazuhide Kamiya^{1,2}, Shuji Nakanishi^{1,2}

¹Department of Materials Engineering Science, Graduate School of Engineering Science, Osaka University, Toyonaka, Osaka 560-8531, Japan; ²Research Center for Solar Energy Chemistry, Osaka University, Toyonaka, Osaka 560-8531, Japan
nakanishi@chem.es.osaka-u.ac.jp

The oxidative functionalization of organic substrates has attracted global interest from both fundamental and practical viewpoints. One of the promising approaches for the C-H oxidative functionalization is the aqueous electrochemical method because it can operate under mild conditions and in the absence of toxic or flammable chemicals. However, many organics are poorly soluble in aqueous media. Thus, in the present work, we attempt to realize electrochemical hydrocarbon oxidation reactions in aqueous solutions using gas diffusion electrodes (GDE), which allow us to supply gas substrate to electrodes.

Ru-doped covalent triazine frameworks (Ru-CTF) was employed as the electrocatalyst.¹ Ethylbenzene-saturated (1.2×10^3 Pa) argon gas was supplied from the back side of GDE as a model substrate. Reaction products in liquid phases after electrolysis were quantitatively analyzed using high-performance liquid chromatography. When the GDE electrode carrying Ru-CTF was applied at 1.5V vs RHE, acetophenone was generated as the product of ethylbenzene oxidation. The concentration of generated acetophenone reached up to 3.3 μ mol after 6h electrolysis. In contrast, the rate of acetophenone generation in ethylbenzene-saturated electrolyte without gaseous substrates was 4 times lower than that from gaseous substrate. These results clearly demonstrate the effectiveness of GDE for the partial oxidation of hydrophobic hydrocarbons.

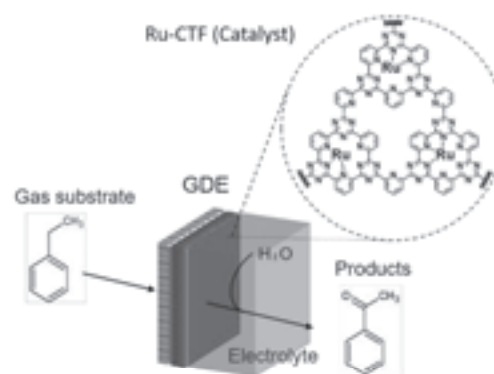


Figure 1. (left) Schematic illustration of GDE carrying Ru-CTF, (right) Molecular structure of Ru-CTF.

(1) S. Yamaguchi and K. Kamiya *et al.* Chem. Commun. **53** (2017) 10437.

Metal-doped bipyridine linked covalent organic framework films for photoelectrochemical applications

Tomoya Hosokawa,¹ Masaki Tsuji¹ Kazuhide Kamiya^{1,2} Takashi Harada² Shuji Nakanishi^{1,2}

¹Department of Engineering Science Graduate School of Engineering Science, Osaka University, Toyonaka, Osaka 560-8531, Japan; ²RCSEC, Osaka University, Toyonaka, Osaka 560-8531, Japan

nakanishi@chem.es.osaka-u.ac.jp

Covalent organic frameworks (COFs), which are crystalline porous polymers, have attracted much attention as novel platforms for catalysts, gas absorbents and optic materials because of their unique physiological properties, including their nano-porous structure, high design flexibility and visible light absorption. In addition, as COFs possess abundant hetero atoms with a lone electron pair, such as N, O and S, they can support metal atoms via coordination bonds and exhibit various functions originated from supported metals. For example, our group has demonstrated that copper (Cu)-doped COFs show the highest onset potential for the electrochemical oxygen reduction reaction (ORR) among synthetic Cu-based ORR catalysts reported to date [1]. In the present study, we synthesized a metal-doped COF film and investigated its photoelectrochemical properties by employing the ORR mediated by Cu sites as the model reaction.

Bipyridine-linked COF (bpy-COF) was synthesized by the polymerization of 5,5'-diamino-2,2'-bipyridine and triformylphloroglucinol as monomers [2]. Then, Cu²⁺ ions were doped by the impregnation of bpy-COF film in 5 mM CuCl₂ solution [Figure (A)]. The resulting Cu-bpy-COF films exhibited 5 times larger photocurrent under visible light irradiation than bpy-COF without the Cu modification. This indicates that the photoexcited electrons in the COF is transferred to the Cu sites and consumed by the O₂ reduction [Figure (B)]. At the poster presentation, the detail of structural characterizations and the photo-induced electron transfer properties will be explained.

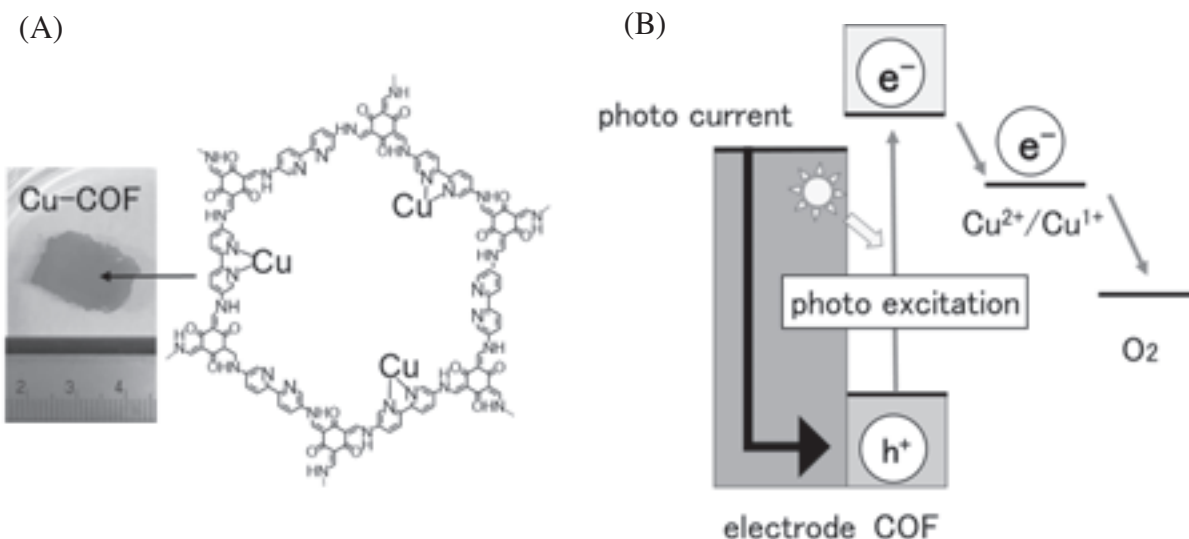


Figure (A) Cu-COF films and its molecular structure. (B) Proposed mechanism of photocathodic current generation

(1)K. Iwase and K. kamiya, *Angew. Chem. Int. Ed.* 54 (2015) 11068-11702.

(2)K. Dey and R. Banerjee, *J. Am. Chem. Soc.* **139** (2017) 13083-13091.

Spin transport measurements in atomic-layer materials with strong spin-orbit interaction

Tomoharu Ohta¹, Ryoma Kawahara¹, Shota Suzuki¹, Hiroki Taniguchi¹,
Kensuke Kobayashi^{1,2}, Yasuhiro Niimi^{1,3}

¹Department of Physics, Graduate School of Science, Osaka University, Toyonaka, Osaka 560-0043, Japan; ²Institute for Physics of Intelligence, University of Tokyo, Hongo, Bunkyo-ku, Tokyo 113-0033, Japan; ³Center for Spintronics Research Network, Osaka University, Toyonaka, Osaka 560-8531, Japan
ohta@meso.phys.sci.osaka-u.ac.jp

Since the discovery of graphene in 2004, there have been many studies on two-dimensional (2D) materials for manufacturing ultra-thin devices. Among 2D materials, transition metal dichalcogenides (TMDs) with phase transitions such as superconductors (1) and ferromagnets (2,3), have attracted much attention because the mechanism of the phase transitions is expected to be different from conventional 3D materials: that is known as the Berezinskii-Kosterlitz-Thouless transition. The motivation of the present study is to fabricate spintronic devices with such TMDs and investigate spin transport phenomena peculiar to the 2D system. One of the difficult points to realize 2D spintronic devices with TMDs is that most of the TMDs are easy to be degraded by O₂ or H₂O in atmosphere during the device fabrication.

In this work, we have fabricated under the Ar atmosphere a spintronic device with a ferromagnetic metal (Ni₈₁Fe₁₉: Py) and one of the TMDs, NbS₂, which shows the superconductivity below 5 K. Figure 1 shows a fabricated Hall cross device consisting of Py electrodes on a NbS₂ film. It has been demonstrated that the spin Hall effect in strong spin-orbit material can be observed with this device configuration (4). We then performed spin transport measurements near the superconducting transition temperature (T_C) of NbS₂. Above T_C , the Hall resistance R_{xy} is linear to the applied magnetic field H . Below T_C , on the other hand, we observe zero resistance up to the critical field (H_C) and peaks structures in addition to the normal Hall resistance above H_C (see Fig. 2). In this presentation, we will show our latest results and discuss the mechanism of the obtained Hall resistance.

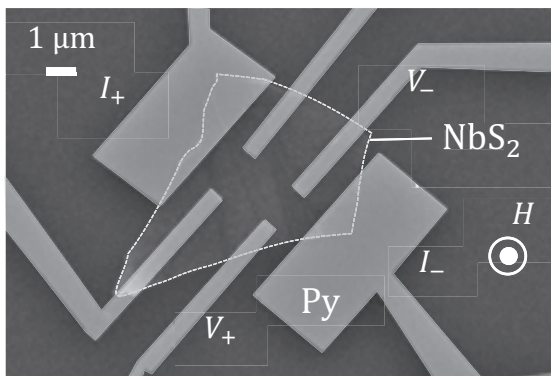


Figure 1. Scanning electron microscopy image of the Hall cross device.

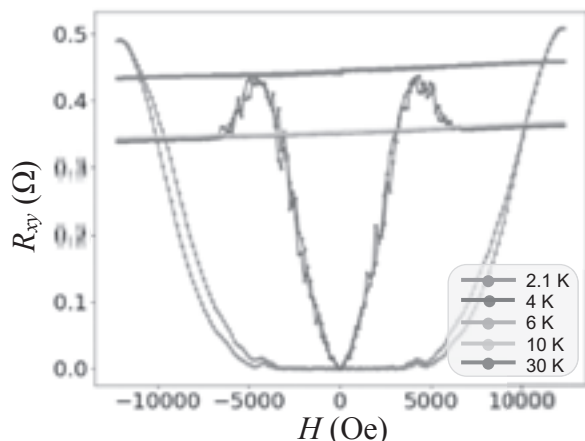


Figure 2. Temperature dependence of the Hall resistance measured with the Hall cross device.

- (1) Q. H. Wang *et al.*, Nat. Nanotechnol. **7** (2012) 699.
(2) B. Huang *et al.*, Nature, **546** (2017) 270.
(3) C. Gong *et al.*, Nature, **546** (2017) 265.
(4) V. T. Pham *et al.*, Nano Lett. **16** (2016) 6755.

Mechanism of affinity enhanced protein adsorption on bio-nanocapsules studied by viscoelasticity measurement with wireless QCM biosensor

Kentaro Noi¹, Masumi Iijima², Shun'ichi Kuroda³, and Hirotugu Ogi⁴

¹Institute for NanoScience Design, Osaka University, Toyonaka, Osaka 560-8531, Japan; ²Department of Nutritional Science and Food Safety, Faculty of Applied Bioscience, Tokyo University of Agriculture, Tokyo 156-8502, Japan; ³Department of Biomolecular Science and Reaction, The Institute of Scientific and Industrial Research, Osaka University, Suita, Osaka 565-0871, Japan; ⁴Graduate School of Engineering, Osaka University, Suita, Osaka, 565-0871, Japan
noi@insd.osaka-u.ac.jp

Bio-nanocapsules (BNC) are known as a useful tool in drug delivery system. Various BNCs have been developed and reported, and we focused on ZZ-BNC, which is BNC with the tandem-form IgG Fc-binding Z domain derived for *Staphylococcus aureus* protein A (1). It was reported that binding affinity between ZZ-BNC and IgG is higher than that between protein A and IgG by a conventional quartz crystal microbalance (QCM) measurement (1). However, mechanism of affinity enhanced IgG adsorption on ZZ-BNC remains unknown.

The QCM biosensor is a mass-sensitive label-free biosensor. It observes interaction between biochemical molecules through change in the resonance frequency of the quartz crystal oscillator. To compare with other biosensors such as surface plasmon resonance (SPR), the conventional QCM biosensor shows a lower sensitivity for targets with smaller molecular weight. One of the causes of the low sensitivity is the presence of gold electrodes and wires attached on the quartz surfaces. To improve the sensitivity, we have developed wireless-electrodeless QCM (WE-QCM) biosensors (2).

We propose to investigate mechanism of affinity enhanced IgG adsorption on ZZ-BNC by a viscoelasticity measurement using only frequency change. Unlike the existing method known as the QCM-D, our method can determine the viscoelastic properties of protein layers without the less-accurate dissipation measurement. This is made possible because with the high-frequency WE-QCM.

First, we measured the binding curves by injecting various concentration of human IgG solutions and determined the equilibrium dissociation (K_D) constants. The K_D value between human IgG and SPA is 5.0 ± 3.6 nM and that between human IgG and ZZ-BNC is 1.3 ± 0.6 nM, confirming higher affinity with ZZ-BNC.

Next, we performed simultaneous measurements of overtones up to 9th mode (522 MHz) for adsorption between ZZ-BNC and human IgG. We clearly observed the difference in the frequency change. We think that this difference may have the viscosity effect. We inversely evaluate viscosity using the Voight-Kelvin model under various conditions. We expect that the viscoelasticity measurement is made possible with the WE-QCM biosensor only from frequency information. If this viscoelasticity measurement method by WE-QCM biosensor can be established, it will reveal the mechanism of affinity enhanced protein adsorption on ZZ-BNC.

(1) M. Iijima, H. Kadoya, S. Hatahira, S. Hiramatsu, G. Jung, A. Martin, J. Quinn, J. Jung, S. Y. Jeong, E. K. Choi, T. Arakawa, F. Hinako, M. Kusunoki, N. Yoshimoto, T. Niimi, K. Tanizawa, and S. Kuroda: *Biomaterials*. **32** (2011) 1455-1464.

(2) H. Ogi, K. Motohisa, K. Hatanaka, T. Ohmori, M. Hirao, and M. Nishiyama, *Biosens. Bioelectron.*, **22** (2007) 3238.

Machine Learning Approach to Analytic Continuation of Temperature Green's Function into Spectral Function

Yuki Sakai,¹ Koichi Kusakabe¹

¹Department of Materials Engineering Science, Graduate School of Engineering Science,
Osaka University, Toyonaka, Osaka 560-8531, Japan
u898151i@ecs.osaka-u.ac.jp

In the condensed matter physics, *e.g.* many-body electron theory, spectral function is obtained by analytic continuation of the temperature Green's function. It represents a probability distribution of single-particle excitations with each energy as well as coherent collective excitations. However, this analytic continuation is practically ill-defined and currently no analytic transformation algorithm can produce an exact solution. As numerical method for analytic continuation, Maximum Entropy method¹ (MEM) and Stochastic Optimization method² (SOM) are widely used. Recently, a new method using Machine Learning approach (ML) is proposed. This method leverages Neural Network approach. Compared with above 2 methods, this method shows the same accuracy for low-noise input data as the others and even robustness against noisy input. But we found that ML as well as MEM and SOM has a problem where the accuracy is quite decreasing when the spectral function has more than 3 peaks. (Fig. 1) In this research, we found a method which improves Machine Learning approach to show more robustness for noisy input. Our new method increases accuracy for complex spectral functions.

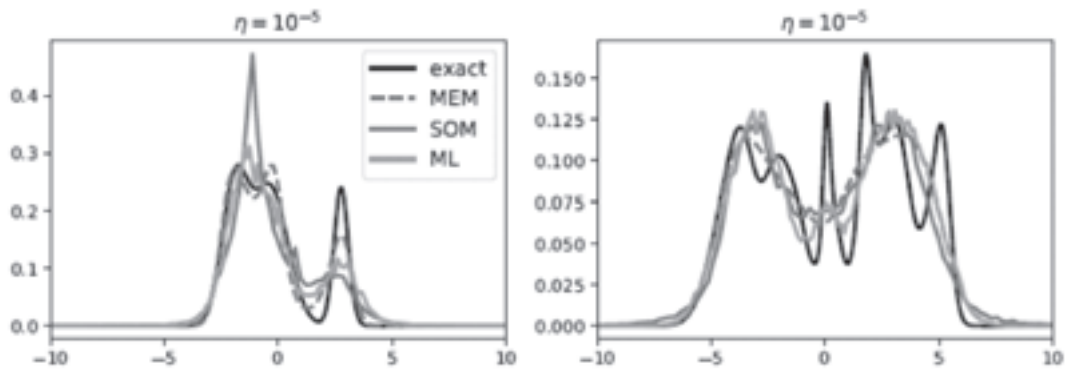


FIG. 1. Predicted functions by MEM, SOM, or ML, which is created from an exact spectral function. Labels are the same in both figures.

-
- (1) J. E. Gubernatis et al., Phys. Rev. B **44**, (1991) 6011.
(2) A. S. Mishchenko et al., Phys. Rev. B **62**, (2000) 6317.
(3) Romain Fournier et al., arXiv:1810.00913 (2018).

Quantum Chemical Study on Nitrate complexes of Zr and Th for $_{104}\text{Rf}$ chemistry

Eisuke Watanabe,¹ Yoshitaka Kasamatsu¹, Yasutaka Kitagawa², Masayoshi Nakano^{2,3}, Atsushi Shinohara¹

¹Department of Chemistry, Graduate School of Science, Osaka University, Toyonaka, Osaka 560-0043, Japan; ²Division of Materials Engineering Science, Graduate School of Engineering Science, Osaka University, Toyonaka, Osaka 560-8531, Japan; ³Institute for Molecular Science, Okazaki, Aichi 444-8585, Japan
watanabee17@chem.sci.osaka-u.ac.jp

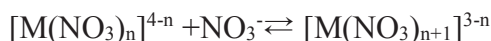
Introduction

Superheavy elements (SHEs) with $Z \geq 104$ are expected to have the curious chemical properties to deviate from the periodicity of their lighter homologues in the periodic table due to the strong relativistic effects on the orbital electrons. Several experimental studies of chemistry of element 104, rutherfordium (Rf) have been reported¹ but their results have not been systematically discussed combining with the theoretical study. Therefore, it is necessary to proceed with further Rf study from both experimental and theoretical aspects. Besides, it is important to investigate the more detail properties of the elements which are used to be compared with Rf: Zr, Hf (homologue elements), and Th (pseudo homologue element).

We are planning to investigate the formation of the nitrate complexes of Rf with both experimental and theoretical approaches. It is well-known that Th forms anion complexes having large coordination number such as 10 or 12 in nitric acid while Zr and Hf do not. Thus, the nitric acid is the interesting reaction system for investigating the chemical properties of Rf. However, the complex formation behavior between M^{4+} ion and nitric ion has not been investigated theoretically for not only Rf but also Zr, Hf and Th. In this study, we calculated some nitrate complexes of Zr and Th by quantum chemical calculation and discussed the stable species and their chemical bonds.

Method

All calculations were conducted by Gaussian 09. First, we compared the results obtained from some methods for various basis functions and functionals. For $[\text{Th}(\text{NO}_3)_6]^{2-}$ and $[\text{Zr}(\text{NO}_3)_5]^-$ which X-ray structural data are available^{2,3}, structural optimization calculations were performed and the results were compared with experimental values. Next, the Gibbs energy change was calculated for the sequential complex formation reaction as shown in the following equation:



Results and discussion

Since the calculated M-O bond length reproduced the experimental value well, we decided to use cam-B3LYP as the functional and Stuttgart-RSC-1997 (for Zr, Th) and 6-31G* (for N, O) as the basis sets. It was suggested that $[\text{M}(\text{NO}_3)_5]^-$ is formed more stably for Th but not for Zr from the Gibbs energy change of the complex formation reaction. Also, it was indicated that $[\text{M}(\text{NO}_3)_6]^{2-}$ is less stable than $[\text{M}(\text{NO}_3)_5]^-$ (M=Zr, Th). Natural bonding orbital analysis of $[\text{Th}(\text{NO}_3)_5]^-$ suggested that both 6d and 5f orbitals of Th participate in the bonding between Th^{4+} and NO_3^- ligand, and might contribute to higher coordination number of Th.

(1) Y. Nagame et al., EPJ Web of Conf. **131** (2016) 07007.

(2) G.B. Jin et al., J. Am. Chem. Soc. **139** (2017) 18003.

(3) I.V. Morozov et al., Russ. Chem. Bull. Int. Ed. **54** (2005) 93.

Study on Microscopic Phase-Separation in Multi-Component Polymer Solid by Single-Molecule Tracking Utilizing One-Color Fluorescence Switching

Misato Funaoka,¹ Syoji Ito,¹ Itsuo Hanasaki,² Satoshi Takei,³ Masakazu Morimoto,⁴ Masahiro Irie,⁴ Hiroshi Miyasaka¹

¹Graduate School of Engineering Science, Osaka University, Toyonaka, Osaka 560-8531, Japan;

²Graduate School of Engineering, Tokyo University of Agriculture and Technology, Koganei, Tokyo 184-0012, Japan; ³Graduate School of Engineering, Toyama Prefectural University, Imizu, Toyama 939-0398, Japan; ⁴Graduate School of Science, Rikkyo University, Toshima, Tokyo 171-8501, Japan

miyasaka@chem.es.osaka-u.ac.jp

Single molecule tracking (SMT) based on localization method with 2D gaussian fitting can determine the position of individual fluorescence molecules at *ca.* 10 nm accuracy. Since the lateral diffusions of guest molecules are affected by their surrounding environment, SMT is a powerful tool for evaluating microscopic properties of host materials. However, tracking a large number of single dye molecules for long time is still difficult task because of (1) the photobleaching of dyes and (2) the upper limit of dye concentration for ensuring 2D gaussian fitting. Recently we have overcome these problems by using one-color fluorescence switching^{1,2} of diarylethene derivatives (fDAEs). In the present study, we applied this technique to track guest molecules in blend polymer with microscopic phase-separation for evaluating its nanoscale structure and diffusivity of guest molecules depending on spatial position.

Blend polymer thin film was prepared from 1,4-dioxane solution containing poly(2-hydroxyethyl acrylate) (pHEA), hyper-branched silicon polymer (HBP), and fluorescence diarylethene derivative (fDAE) by spin-coating or drop-casting method. Fluorescent images of the fDAEs in the films are obtained by wide-field fluorescence microscopy with a 532 nm CW laser for excitation.

Figure 1(a) is the optical transmission image of a thin film of the blend polymer composed of pHEA and HBP, showing microscopic structures as a contrast. Such contrast is not observed neither in neat pHEA nor HBP films. Figure 1(b) and 1(c) respectively show the trajectories of fDAEs superimposed on (a) and the magnified image marked by the black square in (b), indicating that fDAEs did not enter the HBP areas but stay only in pHEA ones and hence the microstructure due to the phase separation was successfully visualized by accumulating the single-molecule trajectories. By further detailed analysis of the trajectories, we could also obtain detailed information on the distribution of diffusion coefficient in the blend polymer.

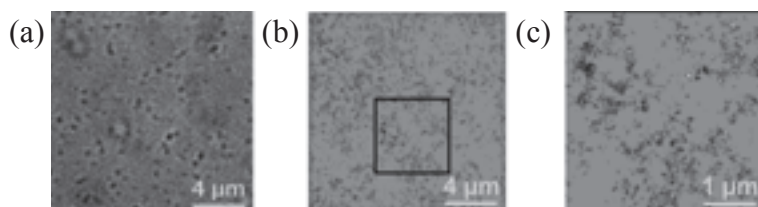


Figure 1. (a) The optical transmission image of blend polymer. (b) The trajectories of fDAEs superimposed on (a). (c) Magnified image marked by the square in (b).

[References]

- (1) Y. Arai, S. Ito, H. Fujita, Y. Yoneda, T. Kaji, S. Takei, R. Kashihara, M. Morimoto, M. Irie, H. Miyasaka, *Chem. Commun.* **53** (2017) 4066.
- (2) R. Kashihara, M. Morimoto, S. Ito, H. Miyasaka, M. Irie, *J. Am. Chem. Soc.* **139** (2017) 16498

Detection of Micromechanical Motion Due to Excited-State Absorption Force

Mizuki Hayasaka, Naoki Ide, Masafumi Koga, Hikaru Sotome,
Syoji Ito*, Hiroshi Miyasaka*

Osaka University, 1-3, Machikaneyama-cho, Toyonaka, Osaka 560-8531, Japan
e-mail: hayasaka@laser.chem.es.osaka-u.ac.jp

Via the allowed optical transition, the momentum of a photon is resonantly transferred to material. Therefore, strong absorption force is expected to exert on a target particle by tuning the wavelength of light to the peak absorption band of the target. This strong radiation force due to resonant absorption can be used for selective transport of nanomaterials¹. So far, resonant radiation force due to the ground state absorption has been ordinarily used for efficient optical manipulation, while the photon force due to the excited state (exciton) absorption has not been well studied. In general, the absorption band of the excited state is different from that of the ground state. Switching of the radiation force can therefore be expected by changing the population ratio between the ground state and the excited state. In this study, the modification of radiation force has been demonstrated by using short-lived excited state absorption of molecules.

As samples, we prepared aqueous colloid suspension of polymer particles containing dye molecules with an allowed absorption band at ca.400 nm and a transient absorption band at near-infrared (NIR) wavelength region. The polymer particle was photo-irradiated in water with a pair of successive light pulses (Fig. 1) with time-interval, Δt , under a tightly focused configuration. The repetition rate for each pulse was 80 MHz. One of the polymer particles was optically trapped with the 800-nm pulses and the trapped particle was additionally irradiated with the 400-nm pulses. At $\Delta t < 0$ (Fig. 1a), the 800-nm pulse arrived first and the 400-nm pulse followed, where the photo-irradiated particle experienced scattering and gradient forces of the 800-nm pulse and the absorption, scattering, and gradient forces of the 400-nm pulse. On the other hand, at $\tau_{ES} \gg \Delta t > 0$ (Fig. 1b, here τ_{ES} represents the lifetime of the excited state), the excited state of the dye produced by the 400-nm pulses efficiently absorbed the 800-nm pulses, leading to the generation of radiation force due to the excited state absorption, which resulted in the modification of the radiation pressure acting on the particle. The position of the trapped particle thus shifted along the optical (Z) axis by changing Δt . We have successfully tracked the reciprocal motion of the trapped particle synchronizing the change in Δt . We will discuss at the symposium the photo-mechanical motion due to the excited state absorption by showing detailed analysis.

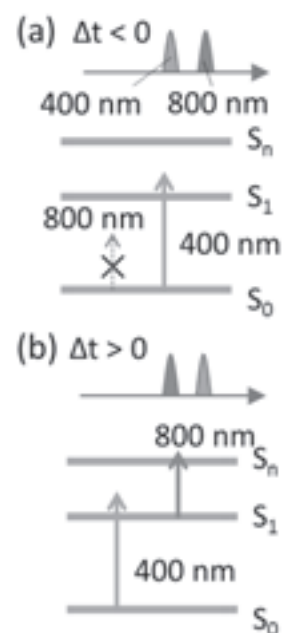


Fig. 1. Mutual timing of SHG and NIR pulses and corresponding resonant optical absorption.

Financial supports from JSPS KAKENHI Grant numbers JP16H06505, JP26107002, JP15H01096, and JP16H03827 are highly acknowledged.

* corresponding author e-mail: sito@chem.es.osaka-u.ac.jp
miyasaka@chem.es.osaka-u.ac.jp

(1) S. Ito *et al.* Sci. Rep., **3**, 3047, (2013).

Stepwise Creation of Supramolecular Structures of a Ball-like Au-Pd Nanomolecule with H₂SiF₆

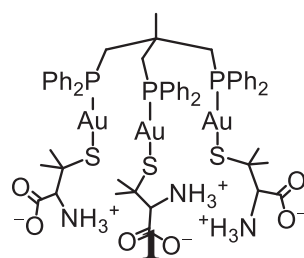
Jinya Nomura,^a Naoto Kuwamura,^a and Takumi Konno^{a,*}

^a Graduate School of Science, Osaka University, Osaka 560-0043 Japan

nomuraj17@chem.sci.osaka-u.ac.jp

Control of supramolecular structures with metal complexes is an important subject because their functionality is generally determined by the assembled structures. To control the supramolecular structure, a variety of molecular designs and synthetic approaches were studied. Acid-template is one of the good approaches to control the total supramolecular structure. For example, we have reported that the S-bridged Au₄Ni₂ complex with mixed hydrophobic diphosphine and hydrophilic D-penicillamine (D-H₂pen), [Ni₂{Au₄(*trans*-dppee)(D-pen)₂}] (*trans*-dppee = *trans*-1,2-bis(diphenylphosphinomethyl)ethylen), is cocrystallized with HClO₄ to form an unique metallosupramolecular architecture, in which ten ClO₄⁻ anions aggregated in an adamantane-like arrangement.¹ Recently, we have synthesized an S-bridged Au₆Co₃ nonanuclear complex, [Co₃{Au₆(tdme)(D-Hpen)₃}] (tdme = 1,1,1-tris(diphenylphosphinomethyl)ethane), bearing triphosphine and D-pen, from the reaction of a trigold(I) metalloligand, [Au₃(tdme)(D-Hpen)₃] (**1**), with Co^{II} ion. However, the Au₆Co₃ complex does not have free hydrogen-bonding groups supramolecular interacting sites, because all of functional groups coordinate to Co^{II} centers.²

In this work, we synthesized an S-bridged Au₆Pd₃ complex (**2**) with free carboxylate groups by the reaction of **1** with Pd^{II}. The supramolecular aggregation behavior of **2** with inorganic acids will also be reported.



1. Itai. T.; Yoshinari. N.; Kojima. T.; Konno. T. *Cryst. Growth Des.*, **2017**, *17*, 949-953
2. Hashimoto. Y.; Yoshinari. N.; Matsushita. N.; Konno. T. *Eur. J. Inorg. Chem.*, **2014**, 3474-3478.

Photophysical Properties of Fluorescent Diarylethene Derivatives Modulated by Molecular Aggregation

Haruka Shinmen,¹ Tatsuhiro Nagasaka,¹ Hikaru Sotome,¹ Masakazu Morimoto,²
Masahiro Irie,² Hiroshi Miyasaka¹

¹Division of Frontier Materials Science, Graduate School of Engineering Science, Osaka University, Toyonaka, Osaka 560-8531, Japan; ²Department of Chemistry, Rikkyo University, Toshima-ku, Tokyo 171-8501, Japan
miyasaka@chem.es.osaka-u.ac.jp

Diarylethene derivatives are one of photochromic molecules showing a reversible photoisomerization reaction between the open- and closed-ring isomers. Among them, fluorescent derivatives can be used for fluorescence switching materials for super-resolution microscopies such as PALM and RESOLFT.¹ However, fluorescent dyes often form aggregates in practical applications, resulting in self-quenching of fluorescence. In this context, photophysical properties specific to molecular aggregates are crucially important as well as those of individual molecules. In the present study, we have investigated photophysical properties of molecular aggregates

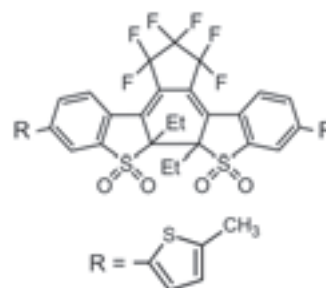


Figure 1. Structure of **fDAE**.

of a fluorescent diarylethene derivative (**fDAE**, Figure 1), in order to elucidate the effects of aggregation. As shown in Figure 2a, the absorption and fluorescence bands of **fDAE** shifted toward longer wavelengths with a decrease of temperature. This spectral change indicates formation of the J-aggregate, which was also confirmed by concentration dependence. Figure 2b shows fluorescence spectra of **fDAE** under various conditions. The fluorescence peak wavelength was further red-shifted in the nanoparticles and crystals, which indicates that size of the aggregate becomes larger. The degree of aggregation involved in emission was estimated by using exciton model.² Figure 2c shows relationship between the spectral shift and degree of aggregation (n). This quantitative analysis of spectral shift revealed that **fDAE** forms oligomer such as dimer and trimer, depending on morphology of the sample.

(1) Y. Arai et al., *Chem. Commun.* **53** (2017) 4066-4069.

(2) M. Kasha, *Radiat. Res.* **20** (1963) 55-71.

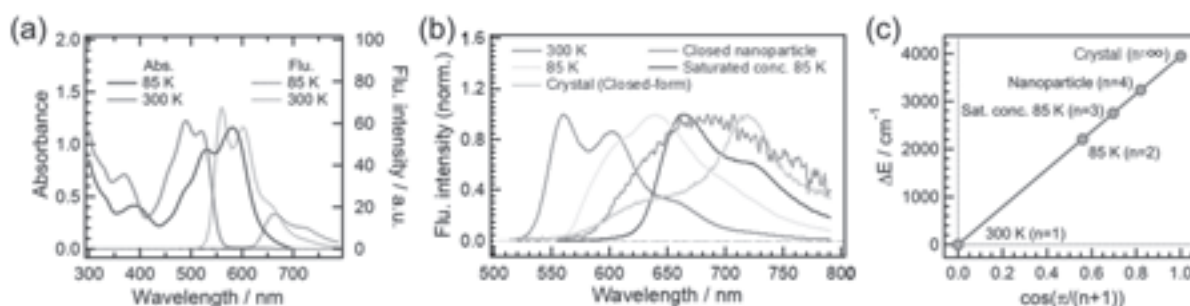


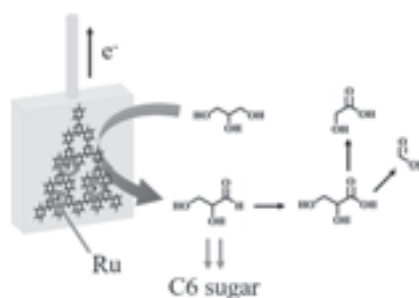
Figure 2. (a) Absorption (solid line) and fluorescence (dots) spectra of **fDAE** in isopentane and methylcyclohexane at 300 (red) and 85 K (blue). (b) Fluorescence spectra of **fDAE** under various conditions; solution at 300 K (red), at 85 K (light blue), in sat. conc. At 85 K (blue), nanoparticle (pink), crystal (yellow) (c) Spectral shift of the fluorescence maximum wavelength plotted as a function of degree of aggregation.

Electrochemical oxidation of glycerol by Ru-modified covalent triazine frameworks

Hiro Tabata¹, Shintaro Kato¹, Takashi Harada², Kazuhide Kamiya^{1,2}, Shuji Nakanishi^{1,2}

¹*Department of Materials Engineering Science, Graduate School of Engineering Science, Osaka University, Toyonaka, Osaka 560-8531, Japan;* ²*Research Center for Solar Energy Chemistry, Osaka University, Toyonaka, Osaka 560-8531, Japan*
nakanishi@chem.es.osaka-u.ac.jp

Biodiesel fuel (BDF) has received a lot of attentions as an alternative source of valuable chemicals in place of fossil fuel due to its renewability and biodegradability. However, when purifying BDF, waste liquid containing glycerol is obtained as a by-product. Therefore, it is strongly demanded to develop efficient methods for treating glycerol solutions. Electrochemical oxidative conversion of glycerol to other chemicals has been studied as one of the effective approaches.^[1] However, only bulk noble metals have been known to exhibit electrocatalytic activity for glycerol oxidation. In this study, aiming at drastically reducing the amount of noble metal and also at obtaining high reaction selectivity, we verified the electrocatalytic activity of Ru-doped covalent organic framework (Ru-CTF) having single Ru atoms as the electrocatalytic active sites.^[2]



scheme 1. C6 sugar production from glycerol
by Ru-CTF

When electrolysis was conducted at +1.1 V vs. RHE, oxidation current was confirmed to flow. HPLC analyses of the solution after the electrolysis revealed the formation of glyceraldehyde (GCA), glyceric acid, glycolic acid and formic acid. These results suggested that the glycerol oxidation on Ru-CTF proceeded based on the reaction scheme 1. Considering that some of glycerol oxidation products such as GCA give hexose by aldol reactions in the presence of appropriate catalysts, we're currently trying to combine glycerol electrooxidation with the aldol condensation reactions, toward the one-step synthesis of high value chemicals.

(1) Y. Kwon, *et al. ChemCatChem* **3** (2011) 1176-1185

(2) S.Yamaguchi and K. Kamiya *et al. Chem. Commun.* **53** (2017) 10437

Development of New Semi-Empirical Method for Simulations of Reactive Oxygens Species and Antioxidants

Colin K. Kitakawa,¹ Takashi Kawakami¹, Shusuke Yamanaka¹, Mitsutaka Okumura¹

¹Department of Chemistry, Graduate School of Science, Osaka University,
Toyonaka, Osaka, Japan
kitakawac15@chem.sci.osaka-u.ac.jp

Introduction Reactive oxygen species (ROS) have been studied in great depth for the past several decades, but their reaction mechanisms are still largely unknown, because *in vivo* experiments are faced with multiple difficulties. One approach to this problem is molecular simulation. Since both quantum effects and thermal fluctuations play important roles in radical reactions *in vivo*, molecular dynamics (MD) based on quantum mechanics/molecular mechanic (QM/MM) methods need to be utilized in order to explore the reaction mechanisms. Typical *ab initio* quantum mechanical methods are too time-consuming for this purpose and semi-empirical (SE) methods have attracted much attention¹. However, existing SE methods are optimized for closed shell systems, and thus cannot simulate radicals accurately. To overcome this problem, we have developed a new hybrid semi-empirical method.

Method and Theory Present SE methods can be divided into PM_x (x=3,6,7) and DFTB_x (x=1,2,3) series, which inherit traits, including weak points, from their base *ab initio* methods, Hartree-Fock (HF) and Density Functional Theory (DFT), respectively. A difference in stability between singlet and triplet states makes this shortcoming apparent, where DFTB_x and PM_x overestimates triplet and singlet stability each, like DFT and HF². Motivated by how the errors are in the opposite way, we have developed a new SE method by hybridization of current SE methods, with the aim to improve accuracy of open-shell molecules. The method can be summarized by the following equation,

$$[\alpha F^{PM6} + (1 - \alpha) F^{DFTB}] \psi_i = \varepsilon_i^{Hybrid} \psi_i, \quad 0 < \alpha < 1$$

where F^{PM6} and F^{DFTB} are orthogonalized Hamiltonian matrices of PM6 and DFTB respectively, and ε_i^{Hybrid} is the orbital energy of the hybridized Hamiltonian. We implemented this method on a QM program within the MD simulation package AmberTools17. *Ab initio* calculations for reference were done on Gaussian09 Rev. C.

Result and Discussion By one parameter (α) optimization, improvement was seen in singlet-triplet gap calculation (Fig. 1). RMSE for PM6 and DFTB2 were 13 kcal/mol and 7.2 kcal/mol respectively, while for our hybrid method it was reduced to 2.6 kcal/mol. A more extensive to test structure optimization were performed on the following nine molecules: H₂, OH radical, HO₂ radical, singlet and triplet oxygen, singlet and triplet methylene radical, O₂⁻ anion radical, water. For bond length, hybrid method outperformed DFTB2 and PM6 in 7/10 values, while for bond angle only 2/4 were better than DFTB2. Based on the current results, we are expecting further improvements by optimization of all parameters.

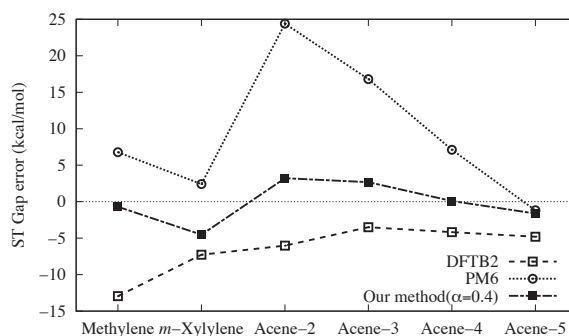


Fig. 1. Singlet-triplet gap error of current SE methods and our hybrid method for a set of radical molecules

(1) T. Saito, Y. Kitagawa, Y. Takano, *J. Phys. Chem. A*, **120** (2016) 8750.
(2) A. J. Cohen, P. Mori-Sánchez, W. Yang, *Science*, **321** (2008) 792.

Electronic Transport Properties of ZrS₂ with the Temperature Dependent Relaxation Time

Hitoshi Mori, Masayuki Ochi, and Kazuhiko Kuroki

Department of Physics, Osaka University, Toyonaka, Osaka, 560-0043, Japan
h-mori@presto.phys.sci.osaka-u.ac.jp

Multi-valley structure is one of the favorable band structures for enhancing thermoelectric efficiency, which is realized in several good thermoelectric materials such as PbTe and Bi₂Te₃. N-type TiS₂, whose crystal structure is shown in Fig. 1, also has electronic structure with multi-valley character, and its power factor is relatively high: $\sim 40 \mu\text{W}/\text{cmK}^2$ at room temperature [1]. In previous experimental studies, the electrical resistivity of TiS₂ has been found to exhibit strong temperature dependence of $\sim T^2$. One of the previous studies indicated that inter-valley scattering among conduction band valleys may be related to the peculiar temperature dependence of the electrical resistivity [2].

Since understanding the inter-valley scattering effect on the transport properties may provide a clue toward designing materials with higher thermoelectric efficiency, in the present study, we perform electronic and phonon band calculations based on DFT, and calculate the electronic transport properties by considering the electron-phonon scattering effect using the EPW code [3-6]. As a target material in this study, we consider not TiS₂, but instead its analogous compound ZrS₂. The calculated temperature dependence of the electrical resistivity is shown in Fig. 2. We will discuss the role of the inter-valley scattering played in the electronic transport properties of ZrS₂.

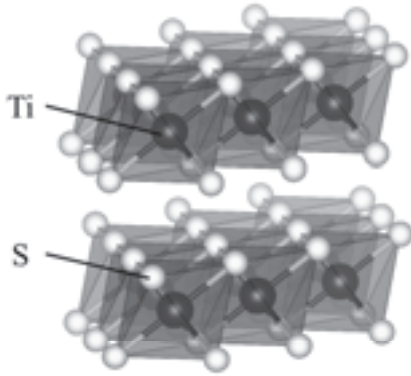


Fig. 1. Crystal structure of TiS₂

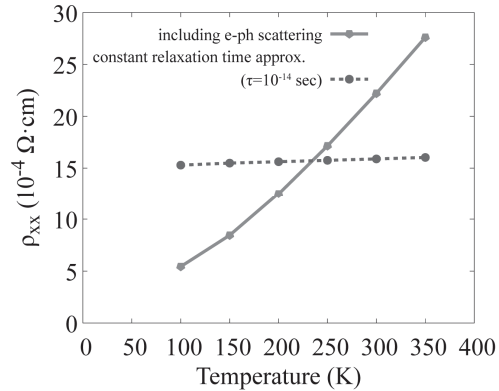


Fig. 2. Calculated electrical resistivity

-
- [1] H. Imai, Y. Shimakawa, and Y. Kubo, Phys. Rev. B **64**, 241104(R) (2001).
 [2] P. C. Klipstein *et al.*, J. Phys. C: Solid State Phys. **14**, 4067 (1981).
 [3] F. Giustino, M. L. Cohen, and S. G. Louie, Phys. Rev. B **76**, 165108 (2007).
 [4] S. Ponce *et al.*, Comput. Phys. Commun. **209**, 116 (2016).
 [5] S. Ponce, E. R. Margine and F. Giustino, Phys. Rev. B **97**, 121201 (2018).
 [6] A. A. Mostofi *et al.*, Comput. Phys. Commun. **185**, 2309 (2014).

Bulk Edge Correspondence of Monolayer Black Phosphorene

Masaru HITOMI¹ Mikito KOSHINO¹

¹*Department of Physics, Graduate School of Science,
Osaka University, Toyonaka, Osaka 560-8531, Japan
hitomi@qp.phys.sci.osaka-u.ac.jp*

We present a theoretical study on the edge state of monolayer black phosphorene (MBP) and its topological origin. The MBP, a single atomic layer of phosphorus, was recently realized by the mechanical exfoliation [1]. The MBP has the buckled honeycomb lattice as shown in Fig. 1, and it has a semiconducting band structure with a finite band gap. It was theoretically shown that the nanoribbon of MBP has edge states for both zigzag edge and armchair edge [2](Fig. 2), in contrast to graphene which has edge states only for zigzag direction[3].

Here we investigate the edge states of MBP from the topological point of view. The study is based on the bulk-edge correspondence [4] between the electric polarization, which is defined by Berry phase, and the existence of localized states at the boundary of the MBP ribbon. We find that the zigzag and armchair edge states originate from the different atomic orbitals, and they have the different center positions in the electric polarization. We actually calculate the Berry phase and Wannier orbitals of MBP, and associate the existence of the edge states with nontrivial topological numbers.

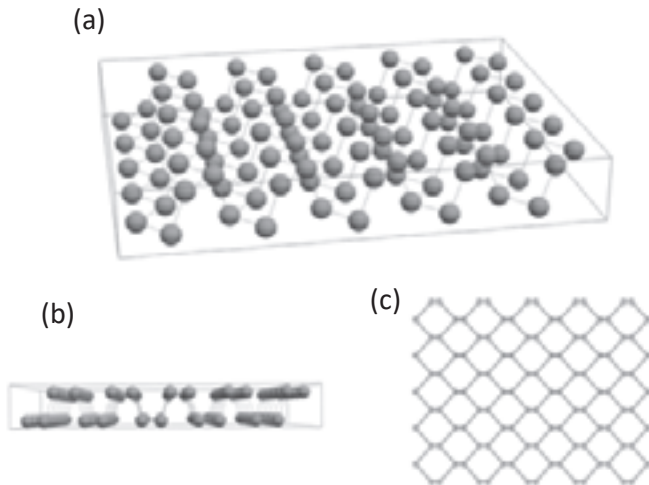


Fig. 1 monolayer black phosphorene

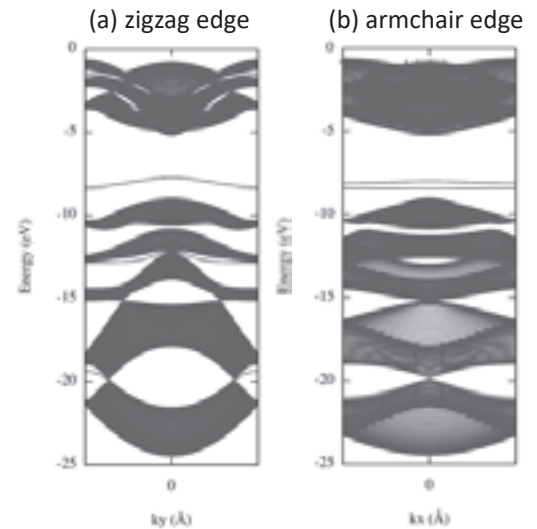


Fig. 2 The band structure

- [1] H. Liu, A. T. Neal, Z. Zhu, Z. Luo, X. Xu, D. Tomanek, and P. D. Ye, ACS Nano 8, 4033 (2014).
 [2] T. Osada, J. Phys. Soc. Jpn. 84, 013703 (2015).
 [3] K. Nakada, M. Fujita, G. Dresselhaus, and M. S. Dresselhaus, Phys. Rev. B 54, 17 954 (1996).
 [4] S. Coh, D. Vanderbilt, phys. Rev. Lett. 102, 107603 (2009)

Synthesis and Properties of Novel Anthracene Congested Systems: Radial Pi-Cluster Molecules

Kazuto Shimizu, Tomohiko Nishiuchi, Yasukazu Hirao,
and Takashi Kubo

Department of Chemistry, Graduate School of Science, Osaka University
shimizuk14@chem.sci.osaka-u.ac.jp

By closing multiple aromatic units tightly, their π -orbitals are overlapped and exhibit distinct properties caused by through-space interaction. We have designed novel π -electron congested systems having closely aligned multiple anthracene units, that is π -cluster molecules, and reported its intramolecular isomerization as well as physical properties derived from through-space π conjugation by employing 1,2-di(9-anthryl)benzene derivatives **1a** as a fundamental moiety of π -cluster molecules.

In this study, efficient synthetic methodology has been developed to synthesize 1,2,3-tris(9-anthryl)benzene derivatives **2a**. Due to having radially arranged three anthracene units, **2a** showed several properties different from **1a** in both solid and solution state. We also confirmed the enhanced stability of oxidized species derived from **2b** bearing n Bu groups on their anthryl moieties. In this presentation, spectroscopic measurements of oxidized species will be mainly discussed.

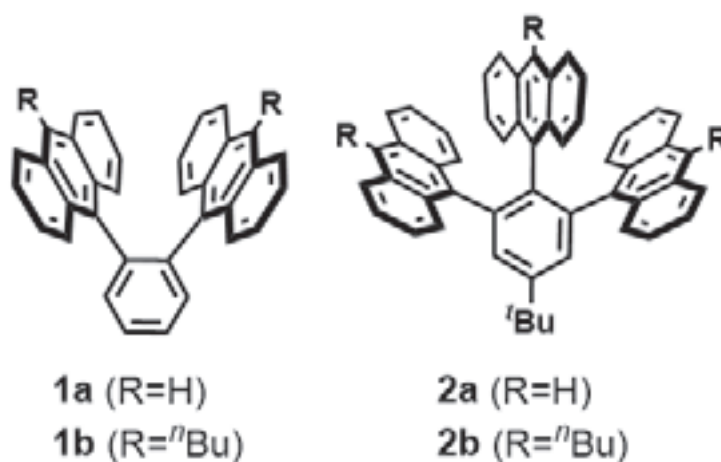


Figure 1. Radial π -cluster molecules

Scaling effects in the resistance temperature characteristic of VO₂ on hBN

Shingo Genchi¹, Mahito Yamamoto^{1*}, Teruo Kanki¹, Kenji Watanabe², Takashi Taniguchi², Hidekazu Tanaka^{1*}

¹*Institute of Scientific and Industrial Research, Osaka University, Ibaraki, Osaka, Japan*

²*National Institute for Materials Science, Tsukuba, Ibaraki, Japan*

genchi77@sanken.osaka-u.ac.jp

Correlated oxide thin films often show spatial inhomogeneity in the phase states in the vicinity of the critical temperature, and consequently, the phase transitions become rather gradual. To extract the intrinsic phase transition properties of correlated oxides in device structures, therefore, spatial characterization of the phase domain sizes and the device scaling down to the domain size are necessary. Vanadium dioxide (VO₂) is an archetypal correlated oxide that shows a metal-insulator transition (MIT) around 340 K and of great interest for electronic device applications because the resistance changes by up-to 5 orders of magnitude across the MIT. Some studies have shown that VO₂ thin films consist of insulating and metallic phase domains near the critical temperature, whose sizes depend on the crystallinity determined by the growth substrates. Recently, we have demonstrated the growth of high-quality polycrystalline VO₂ thin films on hexagonal boron nitride (hBN) that is an insulating layered material. However, the phase domain sizes of VO₂/hBN have yet to be characterized.

Here, we investigate the phase domain sizes and the scaling behavior of the resistance-temperature characteristics of VO₂/hBN. VO₂ thin films were grown on mechanically-exfoliated thin flakes of hBN by pulsed laser deposition. First, we employed temperature-dependent optical microscopy to characterize the domain sizes of VO₂/hBN, since insulating and metallic VO₂ are known to show different optical contrasts under visible light illumination [Fig. a]. By optical microscopy, we found that the metallic phase domains were emerged near the critical temperature. The sizes of metallic domains were observed to range from several hundreds of nanometers up to a few micrometers, which are comparable to the grain sizes of VO₂/hBN measured by atomic force microscopy.

Next, we measured the temperature-dependent resistances of VO₂/hBN of various sizes. We found that micrometer-scale VO₂/hBN showed a step-like behavior in the resistance-temperature characteristic, which reflects the MIT of individual domains in the thin film [Fig. b]. The step-like resistance changes became more marked with scaling down to a few micrometers [Fig. c]. Such step-like resistance changes can never be seen in a similar size of polycrystalline VO₂ on other substrates such as Al₂O₃ and is a unique feature of VO₂/hBN that consists of micrometer-scale domains.

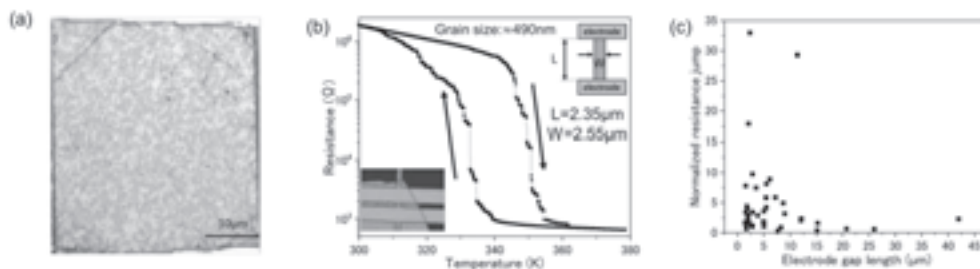


Fig. (a) Optical image of the VO₂/hBN microwire around the transition temperature. (b) Temperature dependence of the resistance of VO₂/hBN. The inset is the optical image of the microwire. (c) Maximum resistance jumps as a function of the electrode gap distance.

Theoretical Study on Intermolecular Magnetic Interaction between Double-Decker Phthalocyaninato Lanthanide(III) Complex

Kazuki Ikenaga,¹ Yasutaka Kitagawa¹, Keiichi Katoh², Masahiro Yamashita²,
Masayoshi Nakano^{1,3}

¹Division of Materials Engineering Science, Graduate School of Engineering Science, Osaka University, Toyonaka, Osaka 560-8531, Japan; ²Graduate School of Science, Tohoku University, Sendai, Miyagi 980-8578, Japan; ³Institute for Molecular Science, Okazaki, Aichi 444-8585

kazuki.ikenaga@cheng.es.osaka-u.ac.jp

In this decade, single-molecule magnets (SMMs) such as double-decker bis(phthalocyaninato) terbium(III) complex, which is abbreviated as [TbPc₂], have been actively studied in order to realize an ultra-high density memory^{1,2}. The SMM behavior has been gradually clarified by experimental and theoretical approaches; however, it has been still unclear about the intermolecular magnetic interactions between those complexes. For example, the neutral [TbPc₂] complex (Fig.1) has a π -radical in the phthalocyanine ring, so that π - π magnetic interactions between adjacent complexes are expected.

In this study, therefore, we aim to elucidate an intermolecular magnetic interaction between adjacent double-decker Ln(III)Pc₂ complexes (Ln = terbium(III) or yttrium(III)). First, we examine [YPc₂](I₃⁻)_{0.57} system, which has the same structure as [TbPc₂] although the metal ion has no *f*-electrons. We construct columnar and planar dimer model structures based on its X-ray crystallographic structure (models **1** and **2**, respectively). In addition, we also examine a modified planar model in which phthalocyanine rings contact more closely with two adjacent complexes (model **3**). We perform density functional theory (DFT) calculations for those models. In order to clarify the influence of *f*-electrons, we further examine similar dimer models that are constructed using the optimized structure of [TbPc₂].

Using the total energies and $\langle \hat{S}^2 \rangle$ values of those models, we calculate the effective exchange integral (J_{ab}) values by Yamaguchi equation³. The obtained J_{ab} values are shown in Table 1. For models **1** and **2**, the J_{ab} values are negative, indicating the antiferromagnetic interaction. It is also found that the magnetic interaction in the columnar model is about 1000 times as strong as that in the planar model. Natural orbital analysis reveals that the overlap between π -radical orbital is quite large along the columnar direction, so that the antiferromagnetic coupling along the direction is found to become strong. As for another planar model **3**, the intermolecular magnetic interaction is shown to be still very weak. The calculated J_{ab} values of [TbPc₂] models exhibit similar tendency to [YPc₂]. These results suggest that a series of those double-decker phthalocyaninato complexes has a strong intermolecular magnetic interaction along the columnar direction, while negligibly small along the planar direction.

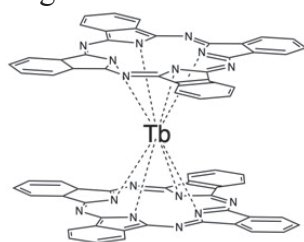


Fig. 1. Double-decker bis(phthalocyaninato) terbium(III) complex

Table 1. J_{ab} value [cm ⁻¹] of each [YPc ₂] model			
Number of I ₃ ⁻	0	1	2
model 1	-730.2	-778.8	-822.4
model 2	-0.7	-0.5	-0.5
model 3	0.04	-	-

(1) N. Ishikawa et al., J. Am. Chem. Soc. **125** (2003) 8694.

(2) K. Katoh, et al., J. Am. Chem. Soc. **131** (2009) 9967.

(3) K. Yamaguchi et al., Chem. Phys. Lett. **15** (1986) 625.

Self-Sensing Cantilever Using Graphene Strain Sensor

Yuto Takeuchi¹, Fujio Wakaya^{1,2}, Satoshi Abo^{1,2},
Katsuhisa Murakami³, Masayoshi Nagao³

¹Department of System Innovation, Graduate School of Engineering Science, Osaka University, Toyonaka, Osaka 560-8531, Japan; ²Center for Science and Technology under Extreme Conditions, Graduate School of Engineering Science, Osaka University, Toyonaka, Osaka 560-8531, Japan; ³National Institute of Advanced Industrial Science and Technology, 1-1-1 Umezono, Tsukuba, Ibaraki 305-8568, Japan
u026242h@ecs.osaka-u.ac.jp

1. Introduction

Self-sensing cantilevers, in which strain sensors detect the displacement, are used in various applications such as gas sensors, atomic force microscopy for photosensitive materials, *etc.* It is reported that graphene shows a large gauge factor¹, suggesting that a highly sensitive self-sensing cantilever can be realized. The gauge factor of graphene in the literature, however, varies considerably from reference to reference^{2,3}, although it should be a material constant. This should be because the adhesion between the graphene, transferred on the cantilever, and the cantilever is poor, and hence the graphene may slip on the cantilever surface when strain is applied. The purpose of this study is to improve the sensitivity of the self-sensing cantilever by using the graphene strain sensor grown directly on the cantilever. In the following, strain sensitivities of graphene with different thickness are discussed.

2. Experimental

Self-sensing cantilevers with graphene strain sensors were fabricated. Fig. 1 shows a photograph of the fabricated cantilever with a length of 100 μm , a width of 40 μm , and a thickness of 800 nm. The length of graphene between the two electrodes is 3 μm and the width is 2 μm . The resistance was measured with applying strain by displacing the free end of the cantilever with a hard cantilever. The measurement setup is schematically shown in Fig. 2.

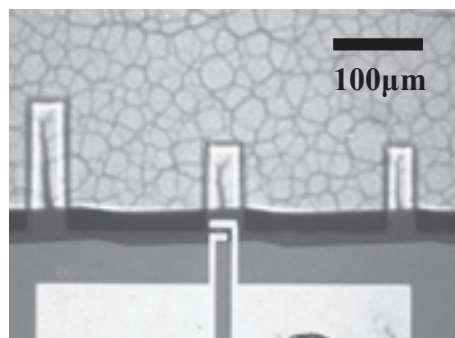


Fig. 1. Optical microscope image of a SiO₂ cantilever.

3. Summary

Strain sensitivities of graphene with thicknesses of 2 nm, 10 nm, and 20 nm were measured. The sensitivities were $6.5 \times 10^{-3} \mu\text{m}^{-1}$, $5.7 \times 10^{-4} \mu\text{m}^{-1}$ and $4.2 \times 10^{-4} \mu\text{m}^{-1}$, respectively. The dependence of the strain sensitivity on the graphene thickness will be discussed, since it is reported that there is the optimum thickness for the strain sensitivity in the case of the other material⁴.

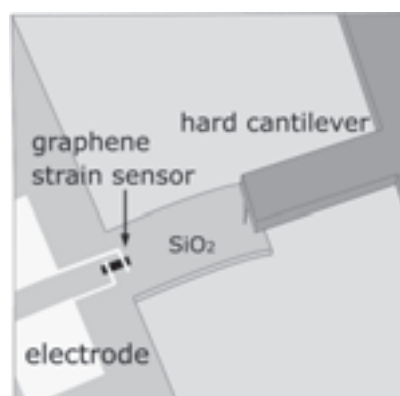


Fig. 2. Schematic of measurement setup.

(1) X. Chen *et al.*, J. Vac. Sci. Technol. B **29** (2011) 06FE01.

(2) Y. Kim *et al.*, Curr. Appl. Phys. **11** (2011) S350.

(3) Y. Lee *et al.*, Nano Lett. **10** (2010) 490.

(4) K. Kashida *et al.*, Abstract of the 65th JSAP Spring Meeting (2018) p.06-046.

Light assisted synchronization of mechanical vibration in arrayed optomechanical system

Sho Tamaki,¹ Tomohiro Yokoyama¹ and Hajime Ishihara^{1,2}

¹Dept. of Material Engineering Science, Grad. Sch. of Engineering and Science, Osaka University, Toyonaka, Osaka, 560-8531, Japan; ²Dept. of Physics and Electronics, Grad. Sch. of Engineering, Osaka Prefecture University, Sakai, Osaka, 599-8531, Japan

tamaki.s@opt.mp.es.osaka-u.ac.jp

In an optical cavity, photons are confined resonantly according to the cavity size. The confined photons exert an enhanced optical force on the cavity. This force slightly modulates the resonant condition. Then, the number of photons and the optical force change. This intrinsic coupling between the photons and phonons (mechanical motion) causes the optomechanics¹.

We examine a sensitive detection of molecules or small objects and optical control of mechanical motion based on the optomechanical systems. When the molecule is not directly coupled with the photon but modulates the mechanical oscillation of cavity, the molecules might be detected optically via the optomechanical systems. On the other hand, if one can control a mechanical motion by completely optical methods, the motion could be used for computational devices.

In this study, we consider a one-dimensional array of the optomechanical cavities. In such optomechanical systems, both the photon and phonon transportations to neighboring cavities can take place like a tight-binding model². Although the photon-phonon interaction is localized in each cavity, the hopping of photon and phonon between the cavities induce “many body” optomechanical phenomena that all cavities contribute to, e.g., synchronization. A synchronization of mechanical oscillations is obviously found when the frequencies of mechanical oscillation are not uniform. Fig. 1 exhibits the spectrum of mechanical oscillation strength in each cavity without (upper) and with (lower panel) the phonon hopping. As the photons are injected to the system by a uniform laser, the cavities reach quasi-steady states being accompanied by the fluctuations of photon and phonon numbers, where the averages of numbers are constant. A spectrum of the fluctuation indicates a single peak for each cavity in the upper panel of Fig. 1. This is reasonable since the phonons in cavities are independent from the other cavities. If the phonon-hopping is enough strong, all the cavities are synchronized with the others and show six peaks in the respective spectra, as shown in the lower panel. Therefore, the synchronization makes each cavity sensitive against a modulation of the others. If one can combine an easy-phonon-detection cavity and a molecule-sensitive cavity, the sensitive modulation by a molecule would be easily observed by the synchronization.

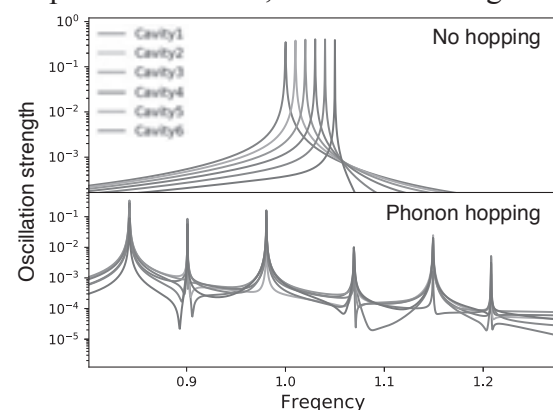


Fig. 1: Spectrum of mechanical oscillation of one-dimensionally arrayed six cavities with different frequencies in the absence (upper) and presence of phonon-hopping (lower panel).

(1)M. Aspelmeyer, T. J. Kippenberg and F. Marquardt, Rev. Mod. Phys. **86** (2014) 1391.

(2)M. Ludwig and F. Marquardt, Phys. Rev. Lett. **111** (2013) 073603.

Theoretical Study on Chain Length Dependence of Electron Conductivity of Polyenes

Naoka Amamizu,¹ Hayato Tada,² Kazuki Ikenaga,² Iori era,² Takuya Fujii,²
Yasutaka Kitagawa² and Masayoshi Nakano^{2,3}

¹Department of Engineering Science, Osaka University, Toyonaka, Osaka 560-8531, Japan;

²Division of Materials Engineering Science, Graduate School of Engineering Science, Osaka University, Toyonaka, Osaka 560-8531, Japan; ³Institute for Molecular Science, Okazaki, Aichi 444-8585

naoka.amamizu@cheng.es.osaka-u.ac.jp

Since Aviram and Ratner have proposed the concept of the molecular diode, a single-molecular electron conductivity has been studied actively by theoretical approaches as well as by experimental ones toward a realization of molecular devices¹. It has been predicted that conventional silicon-based devices reach the limit on miniaturization, so that molecular devices have attracted much attention in the field of molecular nanoelectronics^{2,3}. Usually, electronic devices are composed of elements such as switches, wires, and diodes, while these elements must be substituted by single molecules in the case of molecular devices. In order to design such molecular devices, therefore, it is important to investigate current-voltage characteristics of single-molecules.

The π -conjugated molecules are predicted to show high conductivity, so that they are expected to be one of the promising candidates for the molecular wire. In this study, therefore, we investigate the chain length dependence of electron conductivity of polyenes that are one of the simplest π -conjugated molecules (Fig. 1). We calculated their electronic structures with the density functional theory (DFT) method, and estimated I - V characteristics using the elastic scattering Green's function method. We performed B3LYP calculation using LANL2DZ and 6-31G* basis sets for Au and others, respectively. Fig. 2 shows I - V characteristics of polyenes($n=1-7$), and Fig. 3 describes decay in conductance along the chain length. The results clearly indicate that the transmittance depends on the chain length, and estimated β -decay factor is 0.335 \AA^{-1} .



Fig.1 Model structure of polyene

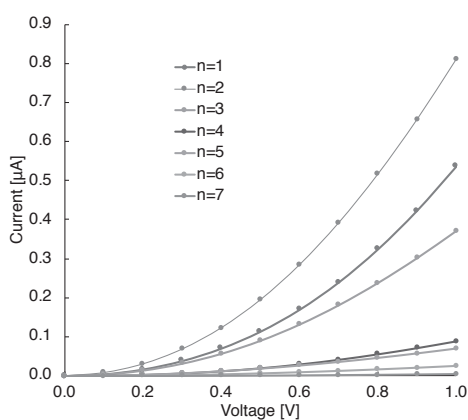


Fig. 2. I - V characteristics of polyenes

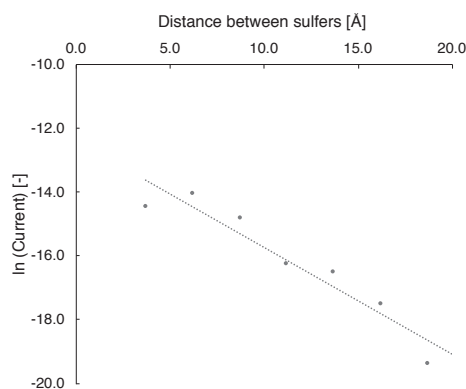


Fig. 3. Decay in conductance along chain length at 1.0 V

(1)A. Aviram, M. A. Ratner, Chem. Phys. Lett. **29** (1974) 277.

(2)M. A. Reed et al., Science. **278** (1997) 252.

(3)C. -K. Wang et al. Phys. Chem. Chem. Phys., **3** (2001) 5017.

Theoretical Study on Substitution Effects on Frontier Orbital Energies of Ru(bpy)₃ by Multivariate Analysis

Hiromasa Sato,¹ Moe Tominaga,¹ Kazuki Ikenaga,² Hayato Tada,² Iori Era,² Takuya Fujii,² Yasutaka Kitagawa² and Masayoshi Nakano^{2,3}

¹Department of Chemical Science and Engineering, School of Engineering Science, Osaka University, Toyonaka, Osaka 560-8531, Japan; ²Division of Materials Engineering Science, Graduate School of Engineering Science, Osaka University, Toyonaka, Osaka 560-8531, Japan; ³Institute for Molecular Science, 38 Nishigo-Naka, Myodaiji, Okazaki, Aichi, 444-8585, Japan

hiromasa.sato@cheng.es.osaka-u.ac.jp

Tris(2,2'-bipyridine) ruthenium(II) (Ru[(bpy)₃]²⁺) complex (Fig.1. (a)) is widely used in the colorimetric determination of metals, photosensitizer and so on. It is well known that the frontier orbital energies and chemical properties of [Ru(bpy)₃]²⁺ can be controlled by introducing substituents. However, the substitution effects on the electronic structure of the complex have not been elucidated well^{1,2}.

In this study, therefore, we clarify the effects of substituents on the frontier orbital energies of the Ru(II) complex. First, we performed density functional theory (DFT) calculations for bpy (Fig.1. (b)) and substituted bpy derivatives (bpy'). Then, the HOMO–LUMO energy gap for the [Ru(bpy)₃]²⁺ and substituted [Ru(bpy')₃]²⁺ are examined. We, next, performed a multiple regression analysis using the DFT results. We focus on the substitution position, substituent species etc., as descriptors, while the HOMO–LUMO energy gap of [Ru(bpy)₃]²⁺ is settled on an objective variable.

The results show that the bpy' with electron donation groups at 5 and 5' positions effectively contributes to increasing the LUMO energy of the complex. This is predicted to originate in the frontier orbitals of the bpy that have a large population at 5 and 5' positions in the LUMO, while there is a node in the HOMO as illustrated in Fig. 2.

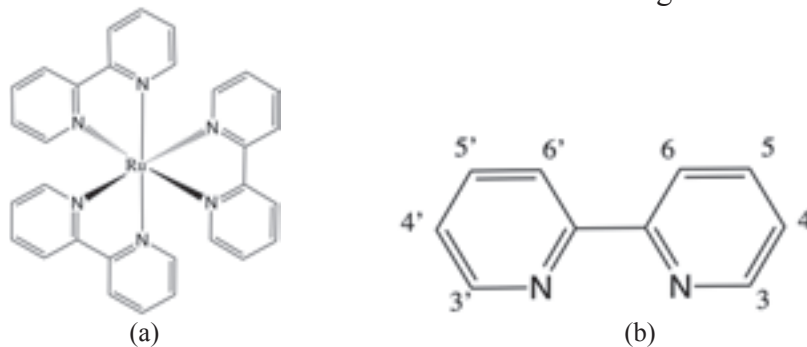


Fig.1. Illustration of (a) Ru[(bpy)₃]²⁺ and (b) bpy



Fig.2. (a) LUMO and (b) HOMO of bpy

(1) K. Araki, S. Shiraishi, J. Synth. Org. Chem. Jpn. **18** (1987) 462.

(2) K. Hasan et al., Scientific Reports. **5** (2015) 12325.

Ultrafast electron diffraction using relativistic femtosecond electron pulses

Kazuki Gen, Jinfeng Yang, Koichi Kan, Youichi Yoshida

*Department of, the Institute of Scientific and Industrial Research, Osaka University, Suita,
Osaka 567-0047, Japan;
gen-kazuki81@sanken.osaka-u.ac.jp*

[Abstract]

Ultrafast electron diffraction (UED) is a very promising technique for studying ultrafast structural dynamics in materials. We have developed a relativistic UED with relativistic femtosecond electron pulses. The spatial resolution was obtained to $0.026 \pm 0.002 \text{ \AA}^{-1}$. The relativistic UED is expected for the structural dynamics study of protein crystals.

[Introduction]

Ultrafast dynamics of biomaterials i.e. protein crystals are studied recently by a time-resolved diffraction method using femtosecond X-ray pulses. Electrons have a large elastic scattering cross section comparing with X-rays and easily be focused. UED is expected to be used for the study of the structural dynamics in biology. However, a high spatial resolution(σ) is required because of the high lattice constants in biomaterials; for example, $\sigma = 0.02 \text{ \AA}^{-1}$ for catalase crystals. In this study, we developed a relativistic UED with femtosecond electron pulses. The spatial resolution was improved using a low emittance electron beam.

[Experimental result]

Our relativistic UED consists of a photocathode RF electron gun, electron lens system, electron diffraction pattern imaging system, and a detector as shown in Fig.1(a). To generate a low-emittance electron beam, first, we reduced the initial emittance by focusing laser on the cathode (oxygen-free copper). Next, we reduced furthermore the beam emittance by collimating the electron beam after RF gun with a 0.3mm-diameter condenser aperture. Figure 1(b) shows the UED image of single crystal of Si observed with single shot. The beam energy was 2.5 MeV and pulse duration was 90 fs. The spatial resolution of electron diffraction was obtained as $0.026 \pm 0.002 \text{ \AA}^{-1}$ from widths of (000) spot and diffraction spots. This value is close to the required resolution for the diffraction measurement of protein crystals.

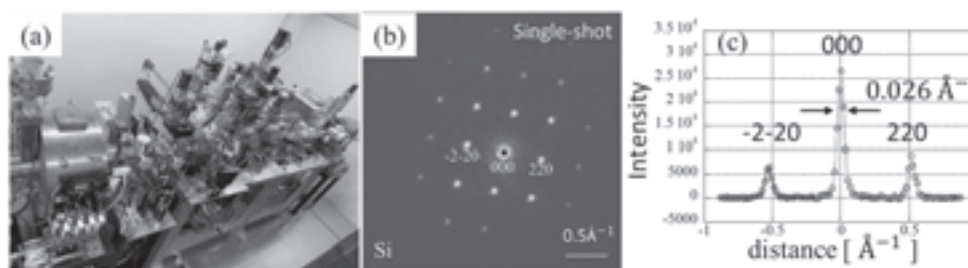


Fig.1 (a) Our relativistic UED instrument, (b) diffraction image of single-crystal Si, and (c) intensity distribution along the direction of (-2-20) and (220) spots

[Conclusion]

We succeeded to develop an UED with relativistic femtosecond electron pulses. The spatial resolution was obtained to 0.026 \AA^{-1} in the UED measurement of single-crystal Si. The relativistic UED is expected to be used for the study of structural dynamics of biomaterials.

Local Analysis of Interfacial Structure at Mg²⁺-containing Ionic Liquid / Au(111) using Frequency Modulation Atomic Force Microscopy

Yuki Hirota¹, Ichiro Tanabe¹, Ken-ichi Fukui^{1,2}

¹Department of Material Engineering Science, Graduate School of Engineering Science, Osaka University, Toyonaka, Osaka 560-8531, Japan; ²Institute for Molecular Science (IMS), Myodaiji, Okazaki 444-8585, Japan
hirota@surf.chem.es.osaka-u.ac.jp

In recent years, ionic liquids (ILs) have attracted considerable interests as electrolytes for efficient and safe electrochemical devices such as batteries owing to their unique properties e.g., negligible vapor pressure, non-flammability, high ion-conductivity and electrochemical stability. However, experimental and theoretical works have recently revealed that ILs form uniform layer structures on the electrode surface [1-3]. Conventional electric double layer (EDL) model is not applied to the ILs/electrode interface. The EDL composed of ILs on the electrode affects on charge transfer processes at the interface and the device performance. In particular, the behavior of metal ions that work as energy carrier is important but the effect of metal ions for the layer structures is not evident.

In this study, we investigated the IL (BMIM-TFSI) layer structures on the electrode surface (Au(111)) with various concentration of metal ions (Mg²⁺). We directly probed the layer structures by force curve measurements using frequency modulation AFM (FM-AFM) that can detect the number, thickness and structural force of the layer structures. Furthermore, we detected not only frequency shift but also deflection of the cantilever to estimate the width of the solid-like layer structure that may exist nearest the interface and is hard to be detected by normal FM-AFM. Fig. 1 (a) shows the representative data of the interface of BMIM-TFSI / Au(111). Three oscillations can be found and the width of them corresponds to the BMIM-TFSI ion pair size. The curve indicates three layer structures composed of ion pairs outside of the solid-like structure. Addition of Mg²⁺ strengthened the IL layer structures at the interface of BMIM-TFSI / Au(111) as shown Fig. 1 (b).

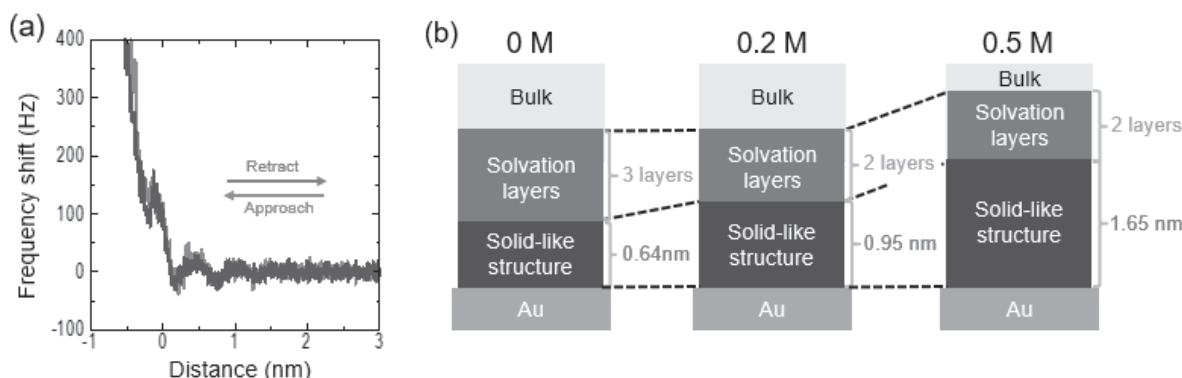


Figure 1 (a) A force curves at an interface of BMIM-TFSI / Au(111) by FM-AFM. (b) The change of BMIM-TFSI layer structures on Au(111) by addition of Mg²⁺.

[1]M. Mezger, H. Schröder, H. Reichert, S. Schramm, *et.al.*, *Science*, **322**, 424 (2008).

[2]F. Endres, O. Höfft, N. Borisenko, L. H. Gasparotto, *et.al.*, *Phys. Chem. Chem. Phys.*, **12**, 1724 (2010).

[3]K. Fukui, *et.al.*, *Chem. Soc. Jpn.*, **91** 1210 (2018)

Behavior of Solute Metal Ions at Ionic Liquid/Electrode Interface Studied by Electrochemical Impedance Spectroscopy

Yoshinobu Fujihira¹, Ken-ichi Fukui^{1,2}, and Akihito Imanishi¹

¹Department of Materials Engineering Science, Graduate school of Engineering Science, Osaka University, Toyonaka, Osaka, 560-8531, Japan, ²Institute of Molecular Science Myodaiji, Okazaki, Aichi, 444-8585, Japan
fujihira@surf.chem.es.osaka-u.ac.jp

Ionic liquids (ILs) have attracted keen attention due to their applicability to various kinds of electrochemical devices such as Li-ion battery, wet-type solar cell, etc. However, we still lack enough knowledge on the behavior of ILs and solute molecules at the interface during the electrochemical processes.

In this study, we investigated the behavior of metal ions (Au^{3+} and Ag^+) at an ionic liquid (BMI-TFSA) carbon (GC) electrode interface by using electrochemical impedance spectroscopy (EIS). Fig. 1 shows the capacitance C and a kD value plotted against applied electrode potential in 1.0 mM Ag^+ /BMI-TFSA (a) and 2.3 mM Au^{3+} /BMI-TFSA (b) solutions under the cathodic reaction ($\text{M}^{n+} + n\text{e}^- \Rightarrow \text{M}$). Impedance spectra (Nyquist plots) used for the analysis were also shown in the insets. In the case of Ag^+ solution, the capacitance increased by decreasing the applied potential. It indicates that the structure of the solvation layer of BMI-TFSA at the interface was changed depending on the local concentration of metal ions and/or the change of the electric field. Decrease of the diffusion coefficient is probably due to the structural change of the solvation layer. On the other hand, in the case of the Au^{3+} solution, obvious potential dependences were not observed for the capacitance and the kD value. These results suggest that the structural change of the solvation layer induced by the applied potential is influenced by the metal ion species contained in the IL solution.

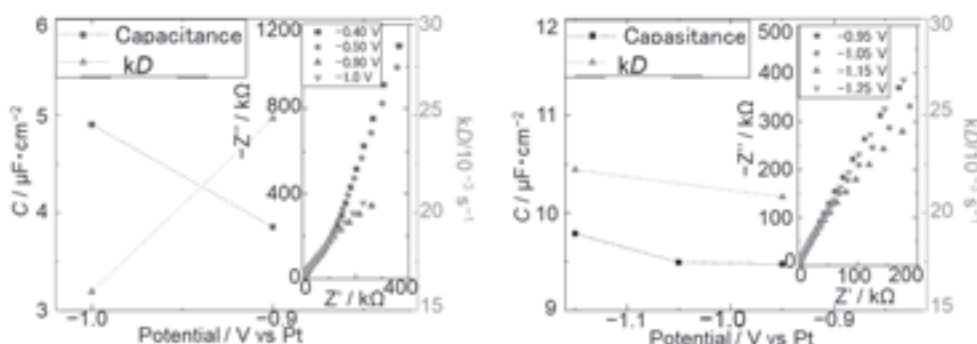


Fig.1. Applied potential dependence of C (capacitance) and kD (D : diffusion coefficient of metal ion, k : constant value related to the width of a diffusion layer) of metal ions in 1.0 mM Ag^+ /BMI-TFSA (a) and 2.3 mM Au^{3+} /BMI-TFSA (b) solutions under the cathodic reaction.

Potential dependent compositional change of Mg^{2+} -containing ionic liquid solutions at the interface on Au(111) electrode for different Mg^{2+} concentrations analyzed by XPS

Hiroki Ueda,¹ Akihiro Takahashi,¹ Ichiro Tanabe,¹ Akihito Imanishi,¹ Ken-ichi Fukui^{1,2}

¹Department of Materials Engineering Science, Graduate School of Engineering Science, Osaka University, Toyonaka, Osaka 560-8531, Japan; ²Institute for Molecular Science (IMS), Myodaiji, Okazaki, Aichi 444-8585, Japan
ueda@surf.chem.es.osaka-u.ac.jp

Ionic liquids (ILs) attracts much attention owing to their unique functional properties including large electrochemical stability window, low vapor pressure, high ion conductivity, etc. Furthermore ILs are nonflammable, so that they are expected as new “green” electrolytes for batteries, solar cells and supercapacitors. To design such efficient devices, it is important to clarify the interfacial behavior at the IL / electrode interfaces. Also, understanding of the behavior of solute metal ions is essential. However, the lack of knowledge about the IL / electrode interface under working conditions renders widespread use of ILs questionable. In this work, we used XPS to study the compositional change of IL at the interface on an Au electrode. We used a new experimental setup that allowed us to perform in situ electrochemical XPS measurement at various potentials (**Fig. 1**).

Mg^{2+} containing IL solutions were prepared by dissolving $\text{Mg}(\text{TFSI})_2$ to 1-butyl-3-methylimidazolium bis(trifluoromethylsulfonyl)imide (BMIM-TFSI). Au wires were used for a reference electrode and a counter electrode, respectively. A few micro-liters of prepared solution was dropped on an Au / mica working electrode and three electrodes system was set for in the XPS measurement chamber (**Fig. 1**). Thin precursor film region is spread

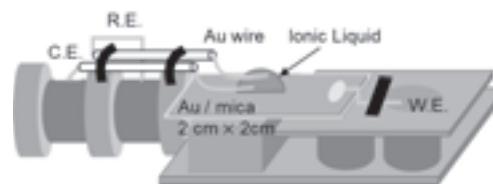


Fig. 1 Schematic of the three electrode system

surrounding droplet edge and the XPS was measured for the region. It was confirmed that the film had several nm-thick by attenuation of Au 4f intensity from the Au electrode. Besides, the liquid potential was successfully controlled by the electrode potential.

Fig. 2 show the peak intensity ratio of N 1s derived from BMIM cation to that from TFSI anion. It was suggested that the anion is abundant at the interface by larger ratio for thinner region. Reversible response was found depending on an applied voltage. From these results, interfacial behavior will be discussed.

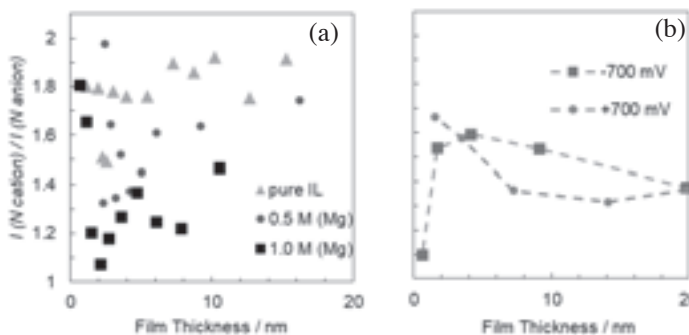


Fig. 2 Film thickness dependence of peak intensity ratio derived from N 1s depending on the Mg^{2+} concentration (a) and the electrode potential (b).

Local Operational Mechanism of Electric Double Layer OFET at the Ionic liquid/Organic Semiconductor Interface revealed by Electrochemical Frequency Modulation AFM Analyses

Takahiro Koyake,¹ Kota Sakamoto,¹ Akihito Imanishi,¹ Ichiro Tanabe,¹ Jun Takeya² and Ken-ichi Fukui^{1,3}

¹Department of Materials Engineering Science, Graduate School of Engineering Science, Osaka University, Toyonaka, Osaka 560-8531, Japan, ²Department of Advanced Materials Science, Graduate School of Frontier Sciences, The University of Tokyo, Kashiwa, Chiba, 277-8561, Japan, ³Institute for Molecular Science (IMS), Myodaiji, Okazaki 444-8585, Japan
koyake@surf.chem.es.osaka-u.ac.jp

In organic field effect transistor (OFET) using an ionic liquid (IL) as a gate dielectric, an electric double layer (EDL) forms at the IL/organic semiconductor (OSC) interface (EDL-OFET). EDL's large capacitance enables efficient carrier accumulation at the interface. This results in extremely low operation voltage of OFET.^[1] Recently, C₁₀-DNBDT-NW (**Fig.1**) has attracted attention as an OSC of OFET. Single crystal-like C₁₀-DNBDT-NW can be easily fabricated by all-solution process with a few-monolayer thickness. EDL-OFET combined with C₁₀-DNBDT-NW and IL will achieve extremely low operational voltage and at low fabrication cost. EDL formed within a few nm is the key of the operational mechanism of EDL-OFET.^[2] However, detailed operational mechanism on nm-scale of EDL-OFET is not clearly understood. Operando observation of the interfacial local structure in EDL-OFET is required.

In this study, we use electrochemical frequency modulation atomic force microscopy (EC-FM-AFM, **Fig.2**) to observe IL/C₁₀-DNBDT-NW interfaces under device operation. EC-FM-AFM can observe interface within a few nm directly under electrochemical environment.^[3]

To understand the operational mechanism, we have to know how hole carriers move in the OSC and how it affects to the local structure of the IL (**Fig.2b**). We succeeded in fabricating EDL-OFET with a step different layer thickness between the source and drain electrode, which may affect the mobility and threshold voltage of the EDL-OFET. EC-AFM operando measurements for the sample are in progress.

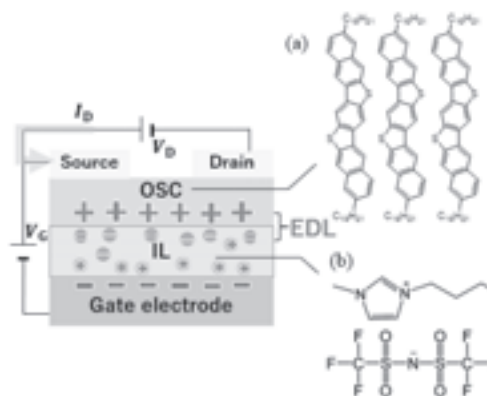


Fig.1 Schematic of EDL-OFET and chemical structures of (a)C₁₀-DNBDT-NW and (b)BMIM-TFSI.

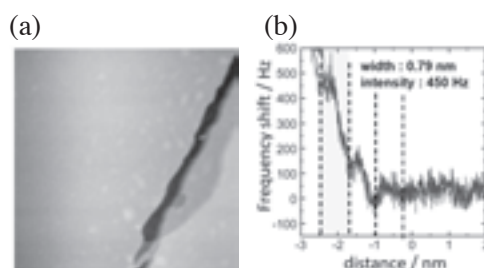


Fig.2 (a)EC-FM-AFM image of C₁₀-DNBDT-NW (b) Frequency shift vs. tip-sample distance curve. W1/W2 : 0.4 V / 0.7 V vs. Au/AuOx. $A_{pp} = 0.8$ nm, $f_0 = 99.5$ kHz, $\Delta f = 100$ Hz.

[1] S. Ono, K. Miwa, S. Seki, J. Takeya., *Appl. Phys. Lett.*, **94**, (2009) 063301.

[2] S. H. Kim *et al.*, *Adv. Mater.*, **25** (2013) 1822.

[3] K. Fukui, *Bull. Chem. Soc. Jpn.*, **91**, (2018) 1210.

Numerical estimation of the viscosity distribution in a gas-liquid interface

Kyoichiro Urano,¹ Atsushi Sekimoto,¹ Yasunori Okano,¹

¹ Department of Materials Engineering Science, Osaka University, Machikaneyama 1-3, Osaka 563-8531, Japan;
okano@cheng.es.osaka-u.ac.jp

In recent years, fluid phenomena in the mesoscale, such as a flow in a micro fuel cell, have gained attention. It is important to reveal the fluid behavior in such a small scale by numerical simulations because an experimental observation is difficult. However, Computational Fluid Dynamics (CFD), used for the analysis in the macroscale, cannot be applied in the mesoscale because the intermolecular interactions break the continuum approximation. Molecular dynamics (MD), used in the nanoscale, also cannot be applied because of the high cost. In order to analyze the fluid behavior in the mesoscale, it is necessary to implement nano-level fluid effects into CFD. In nano-level scale, a flow driven by surface force such as Marangoni convection is dominant, so the present research applies a nano-order liquid film with a free surface as shown in **Fig.1**. Liquid water is placed between solutes. The previous study considered the same liquid film and revealed that the effect of a gas-liquid interface decreases the viscosity in it [1]. The present research focuses of Marangoni convection, and develops of the CFD simulation method which express the reduction of the viscosity in a gas-liquid interface in nanoscale.

The viscosity of the solutes, Methanol(MeOH), Ethanol(EtOH), Propanol(PrOH) and Butanol(BuOH), is calculated by using the Green-Kubo formula.

Fig. 2 shows the relationship between the number density of each solute and its viscosity. **Fig. 3** shows the viscosity distribution at 10 ps in a gas-liquid interface in the nanoscale by using an approximation function of **Fig. 2**. It is revealed that the viscosity distribution in the gas-liquid interface in the nanoscale has an exponential relationship. And then, we have implemented the viscosity distribution in a gas-liquid interface in nanoscale into CFD.

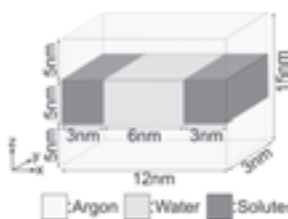


Fig. 1 Numerical domain for calculation of Marangoni convection. Red, blue and yellow regions express solute, water and argon, respectively.

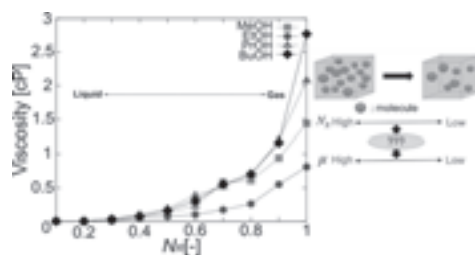


Fig. 2 Relationship between the viscosity and the number density of the fluid. The red, blue, purple and black lines correspond to Methanol, Ethanol, Propanol and Butanol, respectively. N_R is a non-dimension number of the number density of solute molecules.

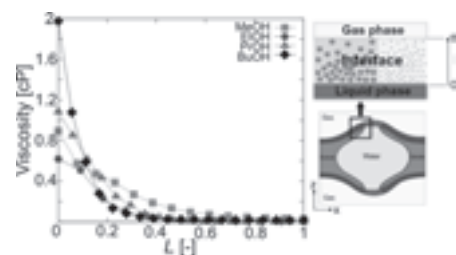


Fig. 3 Viscosity distribution at 10 ps in a gas-liquid interface in nanoscale. Lines are the same as Fig. 2. L is the ratio of the height from the liquid phase in the interface to the interface thickness. Right figures explain L .

[1] Y. Imai *et. al.*, J. Taiwan Inst. Chem. Engineers, 98, 20-26 (2019).

Human Resource Development Program in Computational Science, Advanced Computational Science A & B

Masaaki Geshi^{1,2}

¹*Institute for NanoScience Design (INSD), Osaka University, Toyonaka, Osaka 560-0043*

²*RIKEN Center for Computational Science (R-CCS), RIKEN, Japan
geshi@insd.osaka-u.ac.jp*

Two lectures (Advanced Computational Sciences A and B) that provide advanced knowledge and technology in advanced computational science and high performance computing (HPC) were offered every other year from 2013. After finishing the project of K-computer, the host organization is INSD, Osaka University, and the co-host organizations are ISSP, the University of Tokyo and R-CCS, RIKEN and the supported organizations are Professional development Consortium for Computational Materials Scientists (PCoMS), Tohoku University, and Challenge of Basic Science – Exploring Extremes through Multi-Physics and Multi-Scale Simulations. These are provided at Thursday 13:00-14:30 from April to July. This year we used cloud-based video conferencing service that connects participants across a wide range of devices and conferencing platforms. This made it easier for participants to participate in the lecture and we obtained new participants. The texts and videos are open for all people who are interested in computational science and HPC on the Web site in Japanese¹. The textbooks of these lectures of Japanese version were published in 2017² and the English version were also published this year³.

We aim to produce many computational scientists to be able to develop scientific codes and to achieve significant results in science, engineering, and technology. We will continue to these lectures to realize this purpose and to build out the community-based educational or human resource development system of computational science.



- (1) https://www.r-ccs.riken.jp/library/event/tokuronA_2019.html .
- (2) <http://www.osaka-up.or.jp/books/ISBN978-4-87259-586-4.html>
<http://www.osaka-up.or.jp/books/ISBN978-4-87259-587-1.html> .
- (3) <https://www.springer.com/gp/book/9789811361937>
<https://www.springer.com/gp/book/9789811398018> .

Computational Materials Design (CMD®) workshop

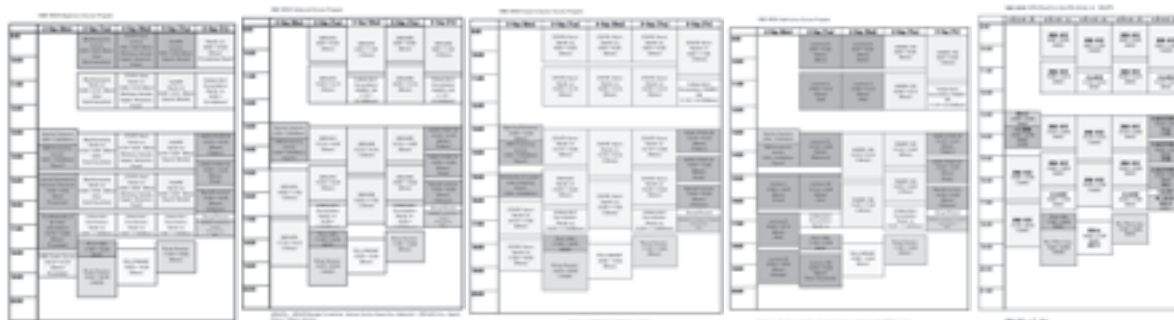
Masaaki Geshi¹

¹*Institute for NanoScience Design (INSD), Osaka University, Toyonaka, Osaka 560-0043
geshi@insd.osaka-u.ac.jp*

With the aim of publicizing and disseminating the first-principles calculation method, the first-principles calculation group centered on Osaka University started a computer material design (CMD®) workshop in 2002. Completed the 35th workshop in September 2019 and we have continued for over 17 years. We hold each year in September and February, and in recent years we have accepted more than 100 participants every year. This workshop is a 5-day, tutorial-based program that offers Beginner courses, Advanced courses, Supercomputer courses, Expert courses, and Spintronics design courses, depending on the level and purpose of the participants. Materials Informatics course was newly set up this time. Introducing the current new trend, we are preparing practical training from various aspects of material design. To date, there have been more than 1,600 participants, of which about 20% are repeaters. There are participants for various purposes such as those who want to learn first-principles calculations, those who are aiming for full-scale introduction, people who want to make connections, etc., but the questionnaire results answered that more than 95% were satisfied each time. In the future, we will continue to study to be able to provide content that fits the times flexibly.

This workshop has greatly contributed to the basic and intermediate levels of human resource development in the field of DFT computation in computational science. This workshop is also recognized as Osaka University Trans-disciplinary Graduate and Refresher Programs for Education, Research and Training in the Fields of Nanoscience and Nanotechnology (OU-NANOPROGRAM)².

This workshop has pioneered achievements in human resource development related to computational science. This workshop has a big feature in the point that it is centered on the tutorial and that it is held in the relatively long period of 5 days, and it is different from the workshop of only half day or one day. PCs are also available here, so "empty-handed" is also possible. Furthermore, PC clusters are provided for those who do not have a computing environment so that calculations can continue after the workshop. Although the impression that it can be used easily is spreading due to the development of computers and the progress of software packages, practical training is necessary. In order to continue to develop human resources who can understand correctly and calculate correctly, efforts by the entire community are necessary. I would like to discuss such a vision in the presentation.



- (1) <http://phoenix.mp.es.osaka-u.ac.jp/CMD/index.html> .
 (2) [http://www.insd.osaka-u.ac.jp/nano/Homepage\(Eng\)/index.htm](http://www.insd.osaka-u.ac.jp/nano/Homepage(Eng)/index.htm) .

Temperature, Concentration and Solvent Dependence in Chromic Behaviors of Diflavinylethenes Induced by Aggregation Based Control of π -Conjugated Platform

Zimeng Li, Soichiro Kawamorita, Takeshi Naota

Division of Materials Engineering Science, Graduate School of Engineering Science, Osaka University, Toyonaka, Osaka 560-8531, Japan
zimengli@soc.chem.es.osaka-u.ac.jp

Flavins, simple model compounds of various flavoenzymes attract much attention as organocatalysts for molecular transformation¹ and functional materials with intense emission properties² As part of our program aimed at developing a new strategy for creation of functional luminescent materials based on synthetic alternation on potentially emissive isoalloxazine skeletons,³ we studied the photophysical properties of newly synthesized diflavinylethenes **1** and **2**, where two riboflavin moieties are linked to ethylene moiety at C8 position (Figure 1a). In contrast to **2** (R= CH₃), **1** (R= H) exhibits remarkable chromic behaviors dependent on concentration, temperature and solvent due to the formation of supramolecular aggregates.

Diflavinylethenes **1** and **2** were synthesized by base-mediated dimerization reaction⁴ and characterized by spectroscopic methods such as NMR, MS. A solution of **1** shows drastic concentration-dependent chromism in fluorescence. **1** emits an intense yellow emission at ambient temperature under UV irradiation at a concentration of 0.2 mM in CHCl₃. While with the concentration increased to 3.2 mM, the emission color is changed to orange-red. Meanwhile, the emission peaks of **1** (λ_{\max} =548 nm) decreases sharply and a new emission band appears with a maximum wavelength at 604 nm (Figure 1b). **1** also exhibits remarkable thermochromism in fluorescence emission, where the forgoing yellow emission (λ_{\max} =548 nm) observed in CHCl₃ at 298 K is drastically changed to red one (in CHCl₃ at 77 K. Solvatochromic behaviors can be observed on **1** as well.

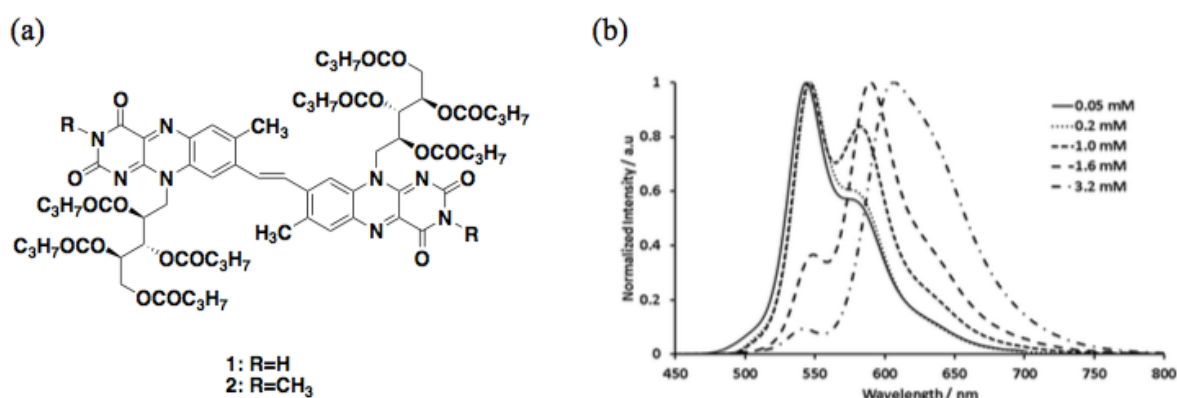


Figure 1. (a) The structures of diflavinylethenes **1** and **2**; (b) Concentration-dependent emission spectra of **1** in CHCl₃ at 298 K (λ_{exc} =400 nm).

(1) Y. Imada, T. Naota, Chem. Rec. **7** (2007) 354.

(2) P. F. Heelis, Chem. Soc. Rev. **11** (1982) 15.

(3) H. Suzuki, R. Inoue, S. Kawamorita, N. Komiyama, Y. Imada, T. Naota, Chem. Eur. J. **21** (2015) 9171.

(4) V. M. Berezovskii, R. V. Artemkina, E. D. Khomutova. Zh. Obshch. Khim. **34** (1964) 2791.

Venue

Σ Hall (International Hall), Osaka Univ., Toyonaka Campus

Address

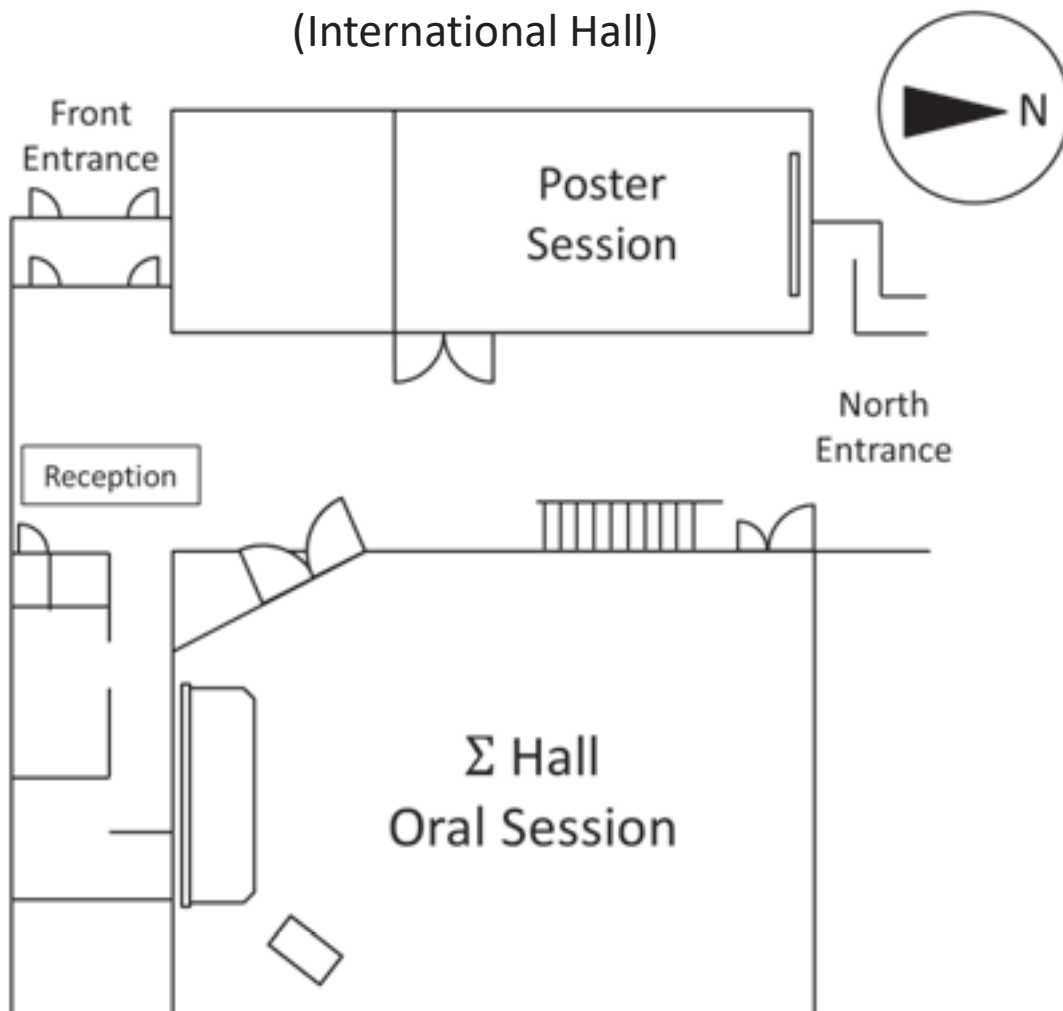
1-3 Machikaneyama-cho, Toyonaka, Osaka 560-0043, Japan

TEL: +81-6-6850-5977

FAX: +81-6-6850-5979

e-mail: ouhalloffice-gea@ml.office.osaka-u.ac.jp

Σ Hall 1st floor (International Hall)



Sponsors



HITACHI
Inspire the Next¹

Innovating Healthcare, Embracing the Future

For a society where all can enjoy a secure, safe, healthy way of life, Hitachi delivers innovation for implementing healthcare services tailored to individuals.

 Hitachi, Ltd. Healthcare Business Unit www.hitachi.com/healthcare

KANEKA

カガクでネガイをカナエル会社



たとえば、医療用製品も、カネカ。

再生・細胞医療における研究開発や心臓や脳の治療用カテーテルなどの製品で、
医療現場を支えています。

製造販売元 **株式会社 カネカ**
www.kaneka.co.jp

Company That Provides Affluence and Comfort to People and Society by Creating “Amazing Materials”



Nippon Shokubai materials are used in
one quarter of the world's disposable diapers

Even though they're made of such thin materials, these disposable diapers are so absorbent they don't leak.

Having replaced cloth diapers, disposables are now worn by babies around the world, saving mothers and fathers everywhere a great deal of time and hassle.

It is Nippon Shokubai that pioneered the superabsorbent polymers (SAP) that are used in disposable diapers today. Polymers created with our unique technology are now used in approximately one-quarter of the disposable diapers in the world, earning Nippon Shokubai top-level share of this global market.

TechnoAmenity

Providing affluence and comfort to people and society with our unique technology.

**NIPPON
SHOKUBAI** 



大学ゼミ・研究室のためのホームページ作成システム

LABORATORIES

【ラボラトリーズ】



- 研究室のウェブサイトをまだ持っていない
- ウェブサイトは持ちたいと思っているが、まとまった予算が確保できない、作るスタッフがない
- 何年前かに学生に作ってもらったが、いまは卒業してしまって更新できない、何年も放置されたままになっている
- いまはホームページビルダーなどのソフトウェアを使って更新しているが、面倒くさいので滞りがちになっている

自分で更新できるホームページがこの価格で

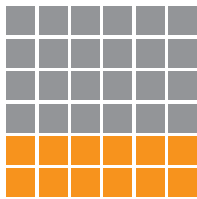
110,000[※]円(税別)

ラボラトリーズ商品サイト

<http://sales.laboratories.ac>

30日間無料お試し登録で使い勝手をご確認ください

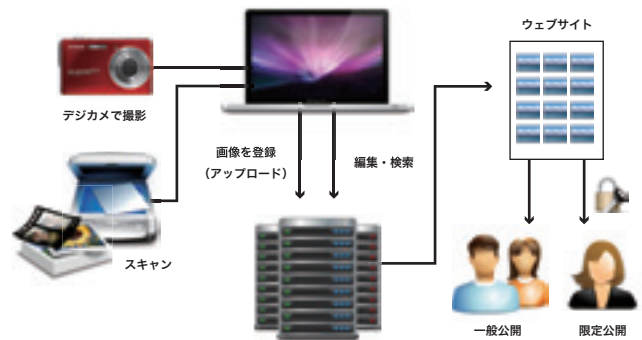
※上記価格は初期登録料と年間ライセンス料を合計した初年度にかかる金額です。次年度以降は年間ライセンス料(50,000円)がかかります。
※大学や学部単位で導入する場合のライセンス料はユーザー数に応じて変わります。 ※ドメイン取得代行(5,000円)や入力代行(20,000円)も承ります。



写真データの登録から編集・検索
ダウンロード用パスワードの発行
ウェブサイトでの公開まで一元管理

PhotoServ

【フォトサーヴ】



フォトサーヴはすべての写真をストックするためのオンラインストレージではありません。パンフレットやウェブなどで利用する重要な写真だけをアップロードし、管理するためのものです。

お試し	エントリープラン	スタンダードプラン	プレミアムプラン
30日間 無料	月額 4,000 円(税別)	月額 6,000 円(税別)	月額 8,000 円(税別)
初期費用 0円	初期費用 0円	初期費用 0円	初期費用 0円
アップロード数上限 99枚	アップロード数上限 100枚	アップロード数上限 1,000枚	アップロード数上限 5,000枚

※価格はすべて税別です。 ※アップロードできるファイルは画像(JPGデータ)のみです。 ※サーバー利用料を含んだ料金です。
※最低契約期間は6カ月です。 ※一般公開機能はオプションです(税別20万円)。

製品・サービスに関するお問い合わせ

【電話】 **076-274-0084**

担当: 吉田 受付時間: 9時~18時(土日・祝日を除く)

【メール】 info@laboratories.ac

NOTOINSATU 熊登印刷株式会社 <http://www.notoinsatu.co.jp>

【本社】 〒920-0855 石川県金沢市武蔵町7-10 TEL 076-233-2550

【印刷事業部】 〒924-0013 石川県白山市番匠町293 TEL 076-274-0084

【東京営業所】 〒101-0024 東京都千代田区神田和泉町1-7-1 TEL 03-5822-2772

【関西営業所】 〒563-0032 大阪府池田市石橋2-14-1 TEL 072-760-3155

【富山営業所】 〒939-8064 富山県富山市赤田761-1 TEL 076-420-7030

Dedicated to the Quest for a New Tomorrow



SUMITOMO CHEMICAL GROUP



Attractive IoT



Attractive Connections



Attractive Mobility



Attractive Wellness



Attractive Energy



Attractive Robotics



Attractive Experience

あす、また世界をあたらしく。

IoTに5G通信、自動運転やロボットも私たちのフィールド。
世界のあらゆる領域で未来をひきよせるテクノロジーのTDK。

Attracting Tomorrow  **TDK**

マイクロンは優秀な 人材を求めています

半導体リーディングカンパニー
マイクロンメモリジャパン

jp.micron.com

Sparking next-
generation discovery
in science and AI.

**Micron**[®]
Intelligence
Accelerated[™]

© 2019 Micron Technology, Inc. All rights reserved. Micron, the Micron logo, and Intelligence Accelerated are trademarks of Micron Technology, Inc. All other trademarks are the property of their respective owners.

Agenda

Day 1 (Wed, 27 th , Nov.)	
9:00 - 9:30	Registration
9:30 - 9:45	Opening Remarks
9:45 - 10:55	IT1: Yousoo Kim
10:55 - 11:10	CT1: Koki Sasaki
11:10 - 11:15	Short Break
11:15 - 12:15	Poster Session (odd numbers)
12:15 - 13:45	Lunch Break
13:45 - 14:55	IT2: Makoto Fujita
14:55 - 15:10	CT2: Yasutaka Kitagawa
15:10 - 15:30	Coffee Break
15:30 - 16:40	IT3: Yoshiya Inokuchi
16:40 - 16:55	CT3: Satoshi Yamashita
16:55 - 17:30	Group Photo & Free Time
17:30-	Banquet

Day 2 (Thu, 28 th , Nov.)	
9:30 - 9:45	Registration
9:45 - 10:55	IT4: Tongcang Li
10:55 - 11:10	CT4: Ryutaro Ohira
11:10 - 11:15	Short Break
11:15 - 12:15	Poster Session (even numbers)
12:15 - 13:45	Lunch Break
13:45 - 14:55	IT5: Ken-ichi Uchida
14:55 - 15:10	CT5: Halimah Harfah
15:10 - 15:30	Coffee Break
15:30 - 16:40	IT6: Nobuyuki Matsuda
16:40 - 16:55	CT6: Tomohiro Yamazaki
16:55 - 17:10	Closing

- ◆ Invited talk: 70 min (60 min talk + 10 min discussion)
- ◆ Contributed Talk: 15 min (12 min talk + 3 min discussion)